LNG Plume Interaction
with Surface Obstacles

FINAL REPORT
(September 1980 - September 1981)

prepared by

K. M. Kothari, R. N. Meroney, and D. E. Neff

Fluid Mechanics and Wind Engineering Program
Department of Civil Engineering
Colorado State University
Fort Collins, Colorado   80523

CER81-82KMK-RNM-DEN22

for

GAS RESEARCH INSTITUTE

Contract No. 5014-352-0203

GRI Project Manager

Steve J. Wiersma

Environment, Safety, and Distribution Division

September 1981

~277-101

REPORT DOCUMENTATION PAGE	1. REPORT NO. GRI 80/0095	2.	3. Recipient's Accession No.
4. Title and Subtitle LNG PLUME INTERACTION WITH SURFACE OBSTACLES			5. Report Date September 1981
			6.
7. Author(s) K. M. Kothari, R. N. Meroney, and D. E. Neff			8. Performing Organization Rept. No. CER81-82KMK-RNM-DEN22
9. Performing Organization Name and Address Civil Engineering Department Colorado State University Fort Collins, CO 80523			10. Project/Task/Work Unit No. 5014-352-0203
			11. Contract(C) or Grant(G) No. (C) 5014-352-0203 (G)
12. Sponsoring Organization Name and Address Gas Research Institute 8600 West Bryn Mawr Avenue Chicago, Illinois 60613			13. Type of Report & Period Covered Final (September 1980 September 1981)
			14.

15. Supplementary Notes

16. Abstract (Limit: 200 words) A wind-tunnel test program was conducted on a 1:250 scale model to determine the effects of surface obstacles on the dispersion of LNG and neutral density plumes. The tests were conducted with continuous LNG boiloff rate of 30 m^3/min, 4 and 7 m/sec wind speeds and 21 different sets of surface obstacle configurations. Plots of ground-level concentration (mean and peak) contours were constructed. The highest concentrations were observed without any surface obstacles. In general, the lower speed resulted in higher ground-level concentration when the surface obstacle interacted with the plume. The mean concentration measured with neutral density plume was about three to five times smaller in magnitude than those observed with the LNG plume. The measured concentration for LNG plumes tended to have its maximum off the centerline. The addition of smaller buildings gave only slight reduction in the LFL distances. The simulated tree line resulted in approximately the same concentration parallel to the tree line.

17. Document Analysis a. Descriptors

Liquefied Natural Gas, Wind tunnel, Dispersion of heavy plume, Surface obstacle, Turbulent boundary layer.

b. Identifiers/Open-Ended Terms

c. COSATI Field/Group

18. Availability Statement	19. Security Class (This Report)	21. No. of Pages 140
	20. Security Class (This Page)	22. Price

(See ANSI-Z39.18) See Instructions on Reverse

OPTIONAL FORM 272 (4-77)
(Formerly NTIS-35)
Department of Commerce

GRI DISCLAIMER

LEGAL NOTICE This report was prepared by Colorado State University as an account of work sponsored by the Gas Research Institute (GRI). Neither GRI, members of GRI, not any person acting on behalf of either:

    a.   Makes any warranty or representation, expressed or implied with respect to the accuracy, completeness, or usefulness of the information contained in this report, or that the use of any information, apparatus, method or process disclosed in this report may not infringe privately owned rights; or

    b.   Assumes any liability with respect to the use of, or for damages resulting from the use of, any information, apparatus, method, or process disclosed in this report.

RESEARCH SUMMARY

Title	LNG Plume Interaction with Surface Obstacles
Contractor	Civil Engineering Department Colorado State University Fort Collins, Colorado 80523
Principal Investigators	K. M. Kothari, R. N. Meroney, and D. E. Neff
Time Span	September 1980 - September 1981 Final Report

Major Achievements

A wind-tunnel test program was conducted to determine the effects of selected obstructions, such as tanks, buildings and vegetation upwind and downwind from an LNG release point, on the extent of the hazardous cloud. The experimental measurements led to the following conclusions: 1) Surface obstacles enhance LNG vapor dispersion resulting in a reduction of lower flammability limit (LFL) distances. 2) The surface obstacles appeared to have a greater enhancement effect at the higher wind speeds. 3) Mean gas concentrations for dispersing neutral-density (i.e., having no buoyancy in air) plumes were only 1/3 to 1/5 the magnitude of those observed for the simulated LNG plume indicating the importance of the buoyancy effect. 4) Surface obstacles in general shift the maximum concentrations to locations off the centerline. 5) The obstructions representing small buildings gave only slight reductions in LFL distances. It appears that the obstruction must be of at least the same characteristic size as the spill to reduce the LFL distance significantly. 6) The simulated tree line obstructions significantly changed the hazardous vapor cloud area, producing a wider, but shorter, hazardous cloud.

Project Implications

This task of the wind-tunnel test program has shown that surface obstacles have a significant effect on vapor cloud dispersion. Another task has already been initiated at Colorado State University to evaluate the use of intentionally placed obstacles to accelerate dilution of LNG plumes. The objective is to be able to design vortex generators and/or vapor fences for LNG facilities which will ensure the necessary dilutions in most wind conditions in the event of an accidental spill.

This task has also shown the importance of gas density on dilution through the comparison of plumes having neutral density and plumes having the same density as LNG vapor. Further research in the effects of surface heating and the resulting change in density of a vapor on plume dispersion will be initiated in 1982.

GRI Project Manager
Steve J. Wiersma
Manager, Safety Research

TABLE OF CONTENTS

LIST OF TABLES

LIST OF FIGURES

LIST OF SYMBOLS

Dimensions are given in terms of mass (m), length (L), time (t), moles (n), and temperature (T).

Symbol	Definition	
A	Area	$[L^2]$
C_p	Specific heat capacity at constant pressure	$[L^2t^{-2}T^{-1}]$
C_p^*	Molar specific heat capacity at constant pressure	$[L^2mt^{-2}T^{-1}n^{-1}]$
D	Source diameter	$[L]$
g	Gravitational acceleration	$[Lt^{-2}]$
h	Local plume depth	$[L]$
k	Thermal conductivity	$[mLT^{-1}t^{-3}]$
L	Length	$[L]$
M	Molecular weight	$[mn^{-1}]$
Ma	Mach number	
n	Mole	$[n]$
p	Velocity power law exponent	
Q	Volumetric rate of gas flow	$[L^3t^{-1}]$
T	Temperature	$[T]$
ΔT	Temperature difference across some reference layer	$[T]$
t	Time	$[t]$
u_*	Friction velocity	$[Lt^{-1}]$
U	Velocity	$[Lt^{-1}]$
V	Volume	$[L^3]$
W	Plume vertical velocity	$[Lt^{-1}]$
x	General downwind coordinate	$[L]$
y	General lateral coordinate	$[L]$
z	General vertical coordinate	$[L]$

Symbol	Definition	
z_o	Surface roughness parameter	[L]
δ	Boundary layer thickness	[L]
Λ	Integral length scale of turbulence	[L]
$\Delta\rho$	Density difference between source gas and air	$[mL^{-3}]$
ρ	Density	$[mL^{-3}]$
σ	Standard deviation	
χ	Mole fraction of gas component	
Ω	Angular velocity of earth = 0.726×10^{-4} (radians/sec)	$[t^{-1}]$
λ_p	Peak wavelength	[L]
ν	Kinematic viscosity	$[L^2 t^{-1}]$

Subscripts and Abbreviations

a	Air
Ar	Argon
b.o.	Boiloff
g	Gas
i	Cartesian index
LNG	Liquefied Natural Gas
m	Model
NG	Natural gas
o	Reference conditions
p	Prototype
s	Source gas

1.0 INTRODUCTION

Natural gas is a highly desirable form of energy for consumption in the United States. Its conversion to heat energy for home and industrial use is achieved with very little environmental impact, and a sophisticated distribution network already services a major part of the country. Recent efforts to expand this nation's natural gas supply include the transport of natural gas in a liquid state from distant gas fields. Unfortunately storage and transport of liquid natural gas may include a relatively large environmental risk [1,2]. Liquefied Natural Gas (LNG) is transported and stored at about -162°C. At this temperature if a storage tank on a ship or land were to rupture and the contents spill out, rapid boiling of the LNG would ensue and the liberation of a potentially flammable vapor would result. It is envisioned that if the flow from a rupture in a typical full LNG storage tank could not be constrained, 28 million cubic meters of LNG would be released in 80 minutes [3]. Past studies [3,4] have demonstrated that the cold LNG vapor plume will remain negatively buoyant for a majority of its lifetime; thus, it represents a ground-level hazard. This hazard will extend downwind until the atmosphere has diluted the LNG vapor below the lower flammability limit (a local concentration for methane below 5 percent by volume).

It is important that accurate predictive models for LNG vapor cloud physics be developed, so that the associated hazards of transportation and storage may be evaluated. Various industrial and governmental agencies have sponsored a combination of analytical, empirical, and physical modeling studies to analyze problems associated with the transportation and storage of LNG. Since these models require assumptions to

permit tractable solution, one must perform atmospheric scale tests to verify the accuracy of these models.

A multitask research program has been designed by a combined Gas Research Institute (GRI)/Department of Energy (DOE) effort to address the problem of preditive methods in LNG hazard analysis. One aspect of this program is the physical simulation of LNG vapor dispersion in a meteorological wind tunnel. The complete sub-program research contract, GRI contract number 5014-352-0203 consists of four tasks.

Task 1:   Laboratory Support Tests for the Forty Cubic Meter LNG Spill Series at China Lake, California.

Task 2:   Physical Simulation in Laboratory Wind Tunnels of the 1981 LNG Spill Tests performed at China Lake, California.

Task 3:   Laboratory Simulation of Idealized Spills on Land and Water.

Task 4:   Laboratory Tests Defining LNG Plume Interaction with Surface Obstacles.

Tasks 1 and 2 were presented in the July 1980 and July 1981 annual reports, respectively. Task 2 is also the subject of a full report to GRI by Neff and Meroney (1981) [36]. Task 3 will be presented in a separate report. Task 4, the LNG plume interaction with surface obstacles is the sole subject of this report.

Some experts currently assume that considerable mixing takes place during gravity driven vapor spreading; whereas others assume no dilution of vapors during this stage of dispersion. It is not surprising then that models based on such a wide variation in agreement concerning the kinematics of plume development predict distances to Lower

Flammability Limit (LFL) ranging from fractions to tens of miles for the same spill conditions.

None of these formulations currently incorporate the additional complications of surface obstructions. Such interference may cause additional plume dilution or temporary pooling of higher gas concentrations. The purpose of this study was to develop an empirical appreciation of the physics of LNG plume interaction with surface obstacles using atmospheric boundary layer wind tunnels.

The program consisted of six tasks and the cases included the arrangements most likely to influence plume dispersion. The objectives of the program were to determine:

1. the extent of LNG plume mixing to be expected in a source tank wake,

2. the influence of a large building or tank structure on LNG plume dispersion when the LNG source is located either upwind or downwind of such a structure,

3. the joint influence of a structure or a tank located in the vicinity of a LNG spill together with a downwind structure located at various distances on or off the plume centerline,

4. the influence of a cluster of structures on LNG plume mixing with the source located upwind, within or downwind of the cylinderical tank,

5. the influence of a hypothetical vegetation belt on LNG plume dispersion when the source is located upwind, and

6. the influence of above effects, but with neutrally buoyant plume.

The wind-tunnel test program was conducted on a 1:250 scale model of various configurations. The program consisted of continuous

releases of a negatively buoyant plume (LNG plume) or a neutrally buoyant plume and the subsequent measurement of ground-level concentrations up to 750 m downwind. The tests were conducted with the LNG boiloff rate of 30 m^3/min, two wind speeds; 4 m/sec and 7 m/sec, and 21 different obstacle configurations. The tests were repeated for the neutrally buoyant plume with a flow rate equivalent to 30 m^3/min LNG plume boiloff rate, two wind speeds (4 and 7 m/sec) and 21 different obstacle configurations.

The methods employed in the physical modeling of atmospheric and plume motion are discussed in Chapter 2. The details of model construction and experimental measurements are described in Chapter 3. Chapter 4 discusses the test program and results. Chapter 5 summarizes the conclusions of this study.

2.0 MODELING OF PLUME DISPERSION

To obtain a predictive model for a specific plume dispersion problem one must quantify the pertinent physical variables and parameters into a logical expression that determines their interrelationships. This task is achieved implicitly for processes occurring in the atmospheric boundary layer by the formulation of the equations of conservation of mass, momentum, and energy. These equations with site and source conditions and associated constituitive relations are highly descriptive of the actual physical interrelationship of the various independent (space and time) and dependent (velocity, temperature, pressure, density, etc.) variables.

These generalized conservation statements subjected to the typical boundary conditions of atmospheric flow are too complex to be solved by present analytical or numerical techniques. It is also unlikely that one could create a physical model for which exact similarity exists for all the dependent variables over all the scales of motion present in the atmosphere. Thus, one must resort to various degrees of approximation to obtain a predictive model. At present, purely analytical or numerical solutions of plume dispersion are unavailable because of the classical problem of turbulent closure [5]. Such techniques rely heavily upon empirical input from observed or physically modeled data. The combined empirical-analytical-numerical solutions have been combined into several different predictive approaches by Pasquill [6] and others. The estimates of dispersion by these approaches are often crude; hence, they should only be used when the approach and site terrain are uniform and without obstacles. Boundary layer wind tunnels are capable of physically modeling plume processes in the atmosphere under certain

restrictions. These restrictions are discussed in the next few sections.

2.1 PHYSICAL MODELING OF THE ATMOSPHERIC BOUNDARY LAYER

The atmospheric boundary layer is that portion of the atmosphere extending from ground level to a height of approximately 100 meters within which the major exchanges of mass, momentum, and heat occur. This region of the atmosphere is described mathematically by statements of conservation of mass, momentum, and energy [7]. The general requirements for laboratory-atmospheric-flow similarity may be obtained by fractional analysis of these governing equations [8]. This methodology is accomplished by scaling the pertinent dependent and independent variables and then casting the equations into dimensionless form by dividing through by one of the coefficients (the inertial terms in this case). Performing these operations on such dimensional equations yields dimensionless parameters commonly known as:

Reynolds number $\quad Re = U_0 L_0 / \nu_0 \qquad = \dfrac{\text{Inertial Force}}{\text{Viscous Force}}$

Bulk Richardson number $\quad Ri = [(\Delta T)_0 / T_0]\,(L_0 / U_0^2)\,g_0 = \dfrac{\text{Gravitational Force}}{\text{Inertial Force}}$

Rossby number $\quad Ro = U_0 / L_0 \Omega_0 \qquad = \dfrac{\text{Inertial Force}}{\text{Coriolis Force}}$

Prandtl number $\quad Pr = {}_0/(k_0 / \rho_0 C_{p_0}) \qquad = \dfrac{\text{Viscous Diffusivity}}{\text{Thermal Diffusivity}}$

Eckert number $\quad Ec = U_0^2 / C_{p_0}\,(\Delta \bar{T})_0$

For exact similarity between different flows which are described by the same set of equations, each of these dimensionless parameters must be equal for both flow systems. In addition to this requirement, there must be similarity between the surface-boundary conditions.

Surface-boundary condition similarity requires equivalence of the following features:

a.   Surface-roughness distributions,

b.   topographic relief, and

c.   surface-temperature distribution.

If all the foregoing requirements are met simultaneously, all atmospheric scales of motion ranging from micro to mesoscale could be simulated within the same flow field for a given set of boundary conditions [9]. However, all of the requirements cannot be satisfied simultaneously by existing laboratory facilities; thus, a partial or approximate simulation must be used. This limitation requires that atmospheric simulation for a particular wind-engineering application must be designed to simulate most accurately those scales of motion which are of greatest significance for the given application.

2.1.1   Partial Simulation of the Atmospheric Boundary Layer

A partial simulation is practically realizable only because the kinematics and dynamics of flow systems above a certain minimum Reynolds number are independent of its magnitude [10,11]. The magnitude of the minimum Reynolds number will depend upon the geometry of the flow system being studied. Halitsky [12] reported that for concentration measurements on a cube placed in a near uniform flow field the Reynolds number required for invariance of the concentration distribution over the cube surface and downwind must exceed 11,000. Because of this invariance, exact similarity of Reynolds parameter is neglected when physically modeling the atmosphere.

When the flow scale being modeled is small enough such that the turning of the mean wind directions with height is unimportant,

similarity of the Rossby number may be relaxed. For the case of dispersion of LNG or neutral plume near the ground level the Coriolis effect on the plume motion would be extremely small.

The Eckert number for air is equivalent to $0.4 \, Ma^2 \left(\frac{T_o}{\Delta T_o}\right)$ where Ma is the Mach number [5]. For the wind velocities and temperature differences which occur in either the atmosphere or the laboratory flow the Eckert number is very small; thus, the effects of energy dissipation with respect to the convection of energy is negligible for both model and prototype. Eckert number equality is relaxed.

Prandtl number equality is easily obtained since it is dependent on the molecular properties of the working fluid which is air for both model and prototype.

Bulk Richardson number equality may be obtained in special laboratory facilities such as the Meteorological Wind Tunnel at Colorado State University [13].

Quite often during the modeling of a specific flow phenomenon it is sufficient to model only a portion of a boundary layer or a portion of the spectral energy distribution. This relaxation allows more flexibility in the choice of the length scale that is to be used in a model study. When this technique is employed it is common to scale the flow by any combination of the following length scales, δ, the portion of the boundary layer to be simulated; z_o, the aerodynamic roughness; Λ_i, the integral length scale of the velocity fluctuations, or λ_p, the wavelength at which the peak spectral energy is observed.

Unfortunately many of the scaling parameters and characteristic profiles are difficult to obtain in the atmosphere. They are infrequently known for many of the sites to which a model study is to

be performed. To help alleviate this problem Counihan [14] has summarized measured values of some of these different parametric descriptions for the atmospheric flow at many different sites and flow conditions.

2.2 PHYSICAL MODELING OF LNG PLUME MOTION

In addition to modeling the turbulent structure of the atmosphere in the vicinity of a test site it is necessary to scale the LNG plume source conditions properly. One approach would be to follow the methodology used in Section 2.1, i.e., writing the conservation statements for the combined flow system followed by fractional analysis to find the governing parameters. An alternative approach, the one which will be used here, is that of similitude [8]. The method of similitude obtains scaling parameters by reasoning that the mass ratios, force ratios, energy ratios, and property ratios should be equal for both model and prototype. When one considers the dynamics of gaseous LNG plume behavior the following nondimensional parameters of importance are identified [12,15,16,17].[1,2]

$$\text{Mass Ratio} = \frac{\text{mass flow of LNG plume}}{\text{effective mass flow of air}}$$

$$= \frac{\rho_s W_s A_s}{\rho_a U_a A_a} = \frac{\rho_s Q}{\rho_a U_a L^2}$$

---

[1]It has been assumed that the dominant transfer mechanism is that of turbulent entrainment. Thus the transfer processes of heat conduction, convection, and radiation are negligible.

[2]The scaling of plume Reynolds number is also a significant parameter. Its effects are invariant over a large range thus making it possible to scale the distribution of mean and turbulent velocities and relax exact parameter equality.

Momentum Ratio
$$= \frac{\text{inertia of LNG plume}}{\text{effective inertia of air}}$$

$$= \frac{\rho_s W_s^2 A_s}{\rho_a U_a^2 A_a} = \frac{\rho_s Q^2}{\rho_a U_a^2 L^4}$$

Densimetric Froude
No. (Fr)
$$= \frac{\text{effective inertia of air}}{\text{buoyancy of LNG plume}}$$

$$= \frac{\rho_a U_a^2 A_a}{g(\rho_g - \rho_a) V_s} = \frac{U_a^2}{g\left(\dfrac{\rho_s - \rho_a}{\rho_a}\right) L}$$

Volume Flux Ratio
$$= \frac{\text{Volume flow of LNG plume}}{\text{effective volume flow of air}}$$

$$= \frac{Q}{UL^2}$$

To obtain simulataneous simulation of these four parameters at a reduced geometric scale it is necessary to maintain equality of the LNG plume's specific gravity ρ_s/ρ_a.

2.2.1 Partial Simulation of LNG Plume Motion

The restriction to an exact variation of the density ratio for the entire life of a plume is difficult to meet for LNG plumes which simultaneously vary in molecular weight and temperature. To emphasize this point more clearly, consider the mixing of two volumes of gas, one being the source gas, V_s, the other being ambient air, V_a. Consideration of the conservation of mass and energy for this system yields [16][1]:

$$\frac{\rho_g}{\rho_a} = \frac{\dfrac{\rho_s}{\rho_a} V_s + V_s}{\left(\dfrac{T_a}{T_s} V_s + V_a\right)\left(\dfrac{C_{p_s} M_s}{C_{p_a} M_a} V_s + V_a\right) \Big/ \left(\dfrac{C_{p_s} M_s}{C_{p_a} M_a} \dfrac{T_a}{T_s} V_s + V_a\right)}$$

---

[1]The pertinent assumption in this derivation is that the gases are ideal and properties are constant.

If the temperature of the air, T_a, equals the temperature of the source gases, T_s, or if the product, $C_p M$, is equal for both source gas and air then the equation reduces to:

$$\frac{\rho_g}{\rho_a} = \frac{\dfrac{\rho_s}{\rho_a} V_s + V_a}{V_s + V_a} \qquad (2\text{-}8)$$

Thus for two prototype cases: 1) an isothermal plume and 2) a thermal plume which is mostly composed of air, it does not matter how one models the density ratio as long as the initial density ratio value is equal for both model and prototype.

For a plume whose temperature, molecular weight, and specific heat are all different from that of the ambient air, i.e., a cold natural gas plume, equality in the variation of the density ratio upon mixing must be relaxed slightly if one is to model utilizing a gas different from that of the prototype.[1] In most situations this deviation from exact similarity is small (see discussion Section 2.3.2).

Scaling of the effects of heat transfer by conduction, convection, or radiation cannot be reproduced when the model source gas and environment are isothermal. Fortunately in a large majority of industrial plumes the effects of heat transfer by conduction, convection, and radiation from the environment are small enough that the plume buoyancy essentially remains unchanged. In the specific case of a cryogenic liquid spill the influence of heat transfer on cold dense gas dispersion can be divided into two phases. First, the temperature (and hence specific gravity) of the plume at exit from a containment tank and

---

[1] If one were to use a gas whose temperature is different from that of the ambient air then consideration of similarity in the scaling of the energy ratios must be considered.

surrounding dike area is dependent on the thermal diffusivity of the tank-dike-spill surface materials, the volume of the tank-dike structure, the actual boiloff rate, and details of the spill surface geometry. A second plume phase involves the heat transfer from the ground surface beyond the spill area which lowers plume density.

It is tempting to try to simulate the entire transient spill phenomenon in the laboratory including spill of cryogenic fluid into the dike, heat transfer from the tank and dike materials to the cryogenic fluid, phase change of the liquid and subsequent dispersal of cold gas downwind. Unfortunately, the different scaling laws for the conduction and convection suggest that markedly different time scales occur for these various processes as the length scale changes. Since the volume of dike material storing sensible heat scales versus the cube of the length scale whereas the pertinent surface area scales as the square of the length scale one perceives that heat is transferred to a model cold plume much too rapidly within the model containment structures. This effect is apparently unavoidable since a material having a thermal diffusivity low enough to compensate for this effect does not appear to exist. Calculations for the full-scale situation suggest minimal heating of a cold gas plume by the tank-dike structure thus it may suffice to cool the model tank-dike walls to reduce the heat transfer to a cold model vapor and study the resultant cold plume.

Boyle and Kneebone [18] released under equivalent conditions room temperature propane and LNG onto a water surface. The density of propane at ambient temperatures and methane at $-161^{\circ}C$ relative to air are the same. Using the modified Froude number as a model law they

concluded dispersion characteristics were equivalent within experimental error.

A mixture of 50% helium and 50% nitrogen pre-cooled to 115°K was released from model tank-dike systems by Meroney et al. [19], to simulate equivalent LNG spill behavior. There was no guarantee that these experiments reproduced quantitatively similar situations in the field. Rather it was expected the gross influences of different heat transfer conditions could be determined. Since the turbulence characteristics of the flow are dominated by roughness, upstream wind profile shape, and stratification one expects the Stanton number in the field will equal that in the model, and heat transfer rates in the two cases should be in proper relation to plume entrainment rates. On the other hand, if temperature differences are such that free convection heat transfer conditions dominate, scaling inequalities may exist; nonetheless, model dispersion rates would be conservative.

Visualization experiments performed with equivalent dense isothermal and dense cold plumes revealed no apparent change in plume geometry. Concentration data followed similar trends in both situations. No significant differentiation appeared between insulated versus heat conducting ground surfaces or neutral versus stratified approach flows.

The influence of latent heat release by moisture upon the buoyancy of a plume is a function of the quantity of water vapor present in the plume and the humidity of the ambient atmosphere. Such phase change effects on plume buoyancy can be very pronounced in some prototype situations. Figure 1 displays the variation of specific gravity from a spill of liquefied natural gas in atmospheres of different humidities.
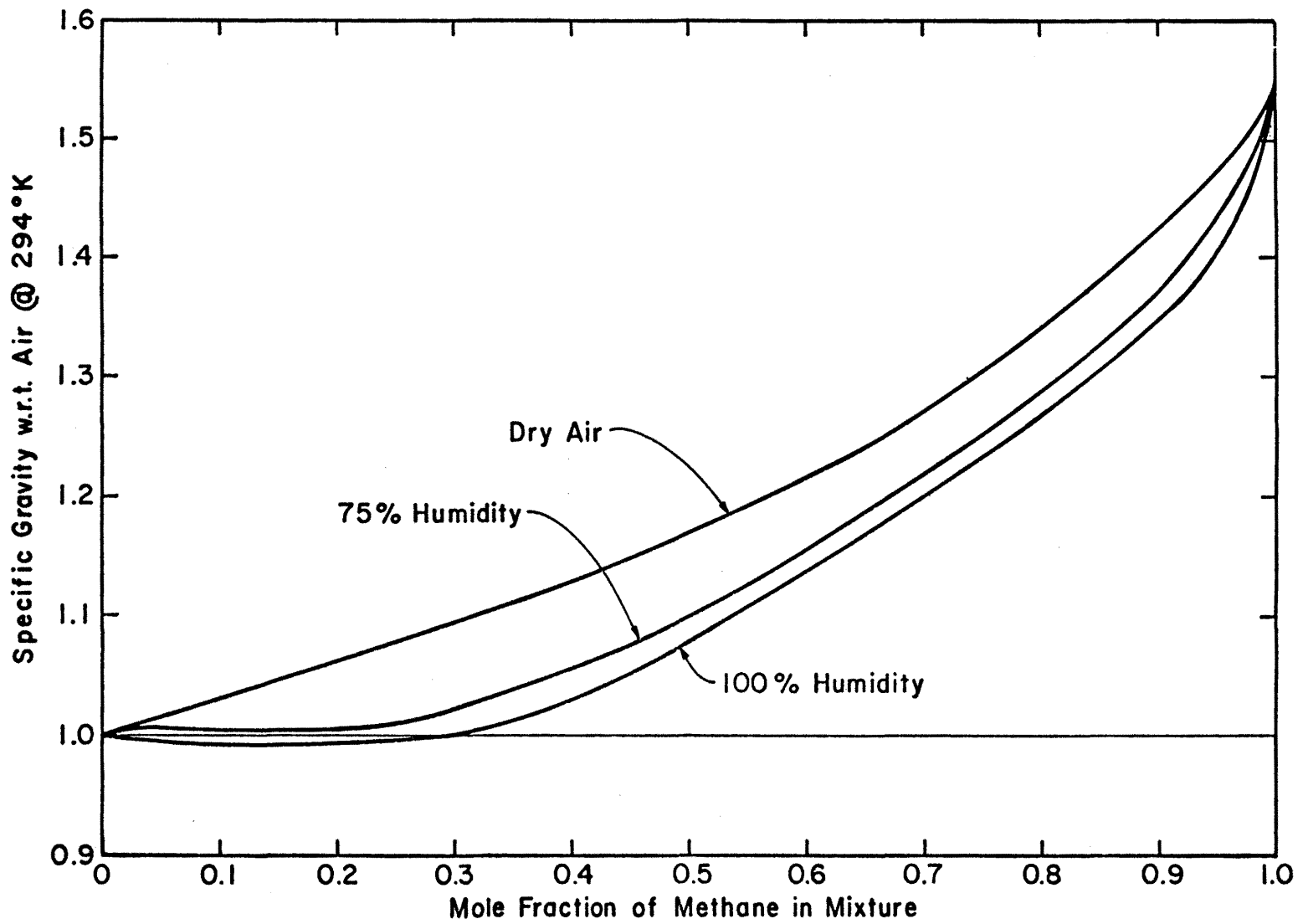
Figure 1. Specific Gravity of LNG Vapor - Humid Atmospheric Mixtures

14

For a LNG vapor plume, humidity effects are thus shown to reduce the extent in space and time of plume buoyancy dominance on plume motion. Hence a dry adiabatic model condition should be conservative.

A reasonably complete simulation may be obtained in some situations even when a modified density ratio ρ_s/ρ_a is stipulated. The advantage of such a procedure is demonstrated most clearly by the statement of equality of Froude Numbers.

$$\left(\frac{U_a^2}{(\frac{\rho_s}{\rho_a} - 1)Lg}\right)_m = \left(\frac{U_a^2}{(\frac{\rho_s}{\rho_a} - 1)Lg}\right)_p$$

Solving this equation to find the relationship between model velocity and prototype velocity yields:

$$(U_a)_m = \left(\frac{S.G._m - 1}{S.G._p - 1}\right)^{\frac{1}{2}}\left(\frac{1}{L.S.}\right)^{\frac{1}{2}} (U_a)_p$$

where S.G. is the specific gravity, (ρ_s/ρ_a), and L.S. is the length scale, (L_p/L_m). By increasing the specific gravity of the model gas compared to that of the prototype gas, for a given length scale, one increases the reference velocity used in the model. It is difficult to generate a flow which is similar to that of the atmospheric boundary layer in a wind tunnel run at very low wind speeds. Thus the effect of modifying the model specific gravity extends the range of flow situations which can be modeled accurately. But unfortunately during such adjustment of the model gases specific gravity at least two of the four similarity parameters listed must be neglected. The options as to which two of these parameters to retain, if any, depends upon the physical situation being modeled. Two of the three possible options are listed below.

(1) Froude No. Equality
     Momentum Ratio Equality
     Mass Ratio Inequality
     Velocity Ratio Inequality[1]

(2) Froude No. Equality
     Momentum Ratio Inequality
     Mass Ratio Inequality
     Velocity Ratio Equality

Both of these schemes have been used to model plume dispersion downwind of an electric power plant complex by Skinner [16] and Meroney [20] respectively.

The modeling of the plume Reynolds number is relaxed in all physical model studies. This parameter is thought to be of small importance since the plume character will be dominated by background atmospheric turbulence soon after its emission. But, if one was interested in plume behavior near the source, then steps should be taken to assure that the model plume is fully turbulent.

2.3 PHYSICAL MODELING OF NEUTRAL DENSITY PLUME MOTION

Once geometric and kinematic similarity for the simulated atmospheric boundary layer are achieved, additional modeling require- ments for similar plume behavior can be stipulated as follows:

1.   Equality of density ratio ρ_s/ρ_a,

2.   consistent scaling of all velocities W_s/U, and

3.   equality of Froude number W_s^2/gD,

where ρ_s and ρ_a are gas density and atmospheric air density respectively, W_s and U are the exit velocity and reference velocity in the approach flow (10 m prototype) respectively. The Froude number equality was utilized with the assumption that the momentum of the area source plume is important. However, if the momentum of the area source

---

[1]When this technique is employed, distortion in velocity scales or similarly volume flow rates requires that a correction be applied to the measured concentration field.

plume is not important, then it would have been possible to run the neutral plume data with the same wind speed and flow rates as utilized in the LNG plume test sequences.

The goal of this experimental measurement was to determine the difference in dispersion behavior between a LNG and a neutral density plume. The actual LNG evaporation for 30 m^3/min spill rate was calculated and during the neutral density plume study, this same evaporation rate was utilized but neglecting the density of plume. With this assumption, ρ_s is equal to ρ_a. Equality of all velocities and equality of the Froude number then would give equivalent model flow rate, Q, of the same gas and a model wind speed at reference height. This similarity criterion has been utilized successfully by Kothari and Meroney [21] for model stack gas dispersion.

2.4 MODELING OF PLUME DISPERSION FOR PRESENT STUDY

In the sections above a review of the extent to which wind tunnels can model plume dispersion (LNG or neutral density) in the atmospheric boundary layer has been presented. In this section these arguments will be applied to the case of an LNG spill or neutral density gas spill for the present study.

2.4.1 Physical Modeling of the Atmospheric Surface Layer

The neutral boundary layer was generated in the Environmental Wind Tunnel using spires and trip at the entrance of the tunnel. The wind speeds were referenced to a 10 m (prototype) height. The aerodynamic roughness, z_o, and power law exponent, α, were specified such that the boundary layer profile was similar to that expected for a flat suburban terrain area.

2.4.2 Physical Modeling of the LNG Spill Plume

The buoyancy of a plume resulting from an LNG spill is a function of both the mole fraction of methane and temperature. If the plume entrains air adiabatically, then the plume would remain negatively buoyant for its entire lifetime. If the humidity of the atmosphere were high then the state of buoyancy of the plume will vary from negative to weakly positive. These conclusions are born out in Figure 1, which illustrates the specific gravity of a mixture of methane at boiloff temperature with ambient air and water vapor.

Since the adiabatic plume assumption will yield the most conservative downwind dispersion estimates this situation was simulated. (Conservative is defined here to be highest peak concentrations furthest downwind.) Several investigators have confirmed that the Froude number is the parameter which governs plume spread rate, trajectory, plume size, and entrainment during initial dense plume dilution [15,18,22,23]. The modeling of momentum is not of critical importance for a ground source released over a fairly large area. The equality of model and prototype specific gravity was relaxed so that pure Argon gas (specific gravity at 1.38) could be used for the model source gas. The Froude number was maintained at equal values by adjusting reference wind speed.

Argon provides almost eight times the detection sensitivity for instantaneous concentration measurements as the carbon dioxide used in previous studies [19]. The variation of specific gravity with equivalent observed mole fraction of methane for these different gases is plotted in Figure 2. The use of an isothermal dense model gas such as Argon in place of a cold methane vapor also results in a slight distortion of the local dynamic forces acting on equivalent plume volumes as the gas mixes. Unfortunately this distortion is not conservative, i.e.,
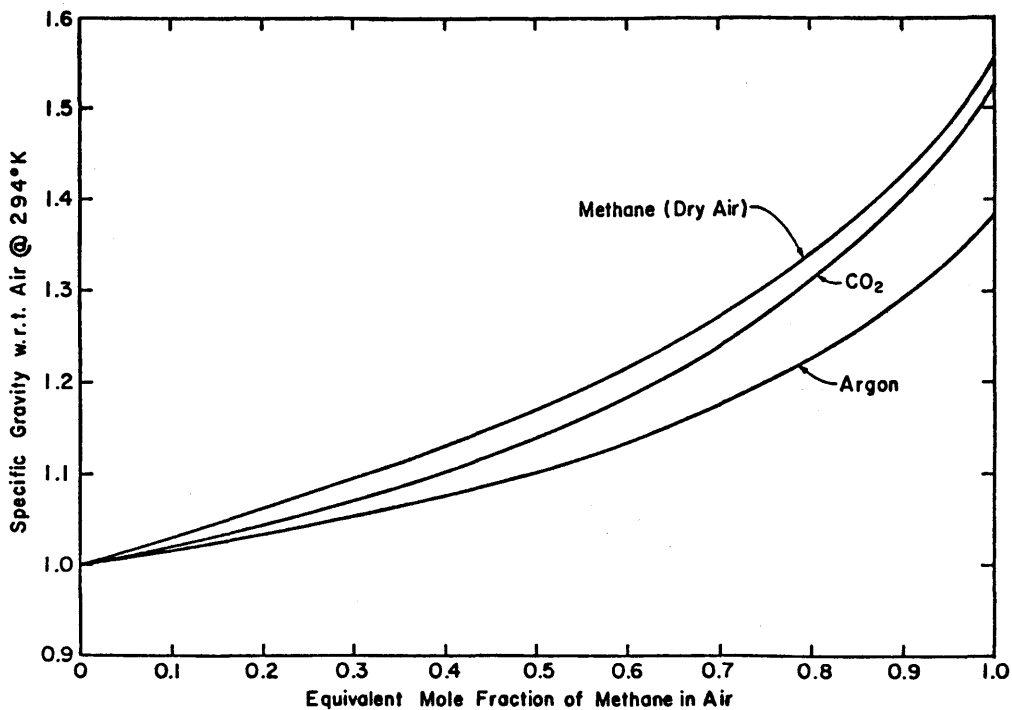
Figure 2.   Specific Gravity of Gas-Air Mixtures
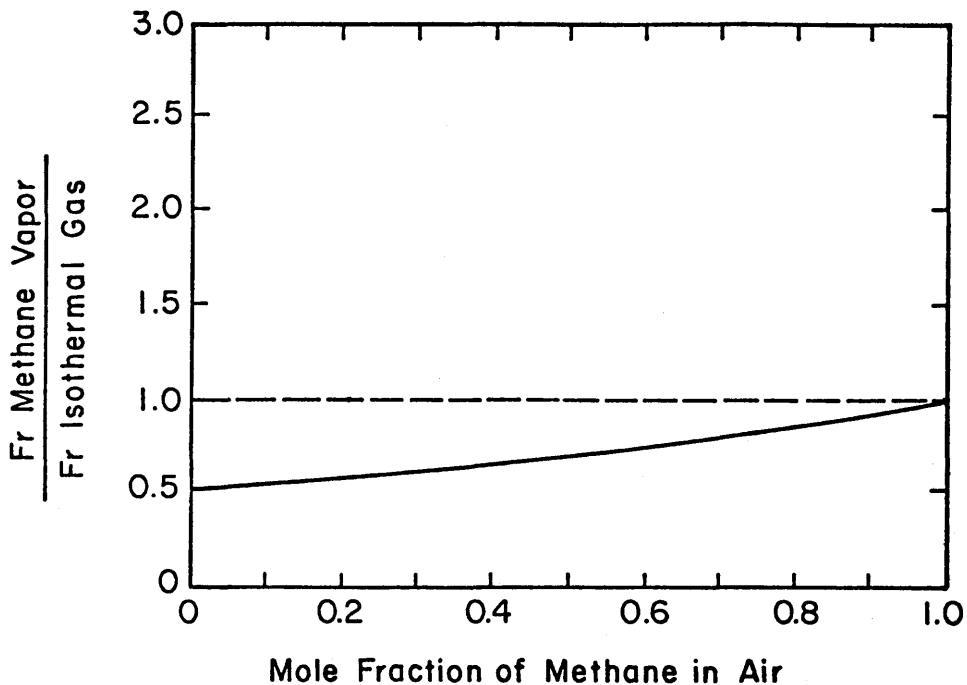
Figure 3.   Variation of Isothermal Plume Behavior from
Equivalent Cold Methane Plume Behavior

the thermal capacitance properties of methane result in plumes which behave more dense than the model equivalent plume. Analytical approximations based on the integral entrainment box model of Fay [24] suggest that buoyancy forces are more at equivalent time and space positions during adiabatic mixing of methane. Let $Fr = \dfrac{U(h)^2}{g \frac{\Delta\rho}{\rho_a} h}$ be a local Froude number, where h is local plume depth, $U(h)$ is wind speed at plume depth, h, and $\Delta\rho/\rho_a$ is a local density difference ratio. Then given a power law wind profile $U(h) \sim h^\alpha$ one finds

$$\frac{Fr_{isothermal\ gas}}{Fr_{LNG\ vapor}} = \frac{(1+\chi S)(\beta+(1-\beta)\theta)}{(\beta(1+\chi S)+(1+S)(1-\beta)\theta)} \left[\frac{(1+\chi S+\chi(1+S)\theta}{(1-\chi\theta)(1+\chi S)} \right]^{2\alpha} \left[\frac{R_{LNG}}{R_{iso}}\right]^{2-4\alpha}$$

where χ = mole fraction methane vapor

R = local plume spread

$\beta = 1 - M_a/M_s \cong -0.81$

$\theta = 1 - T_s/T_a \cong 0.6$

$S = (Cp_s^*/Cp_a^* - 1) \cong 0.22$

α = velocity power law exponent $\cong 0.2$.

The variation of this Froude number ratio with equivalent mole fraction methane is plotted in Figure 3. Nonetheless over most of the concentration range where buoyancy forces are dominant the variation of Froude number is adequately simulated by the isothermal model gas. Indeed, integral-model calculations when corrected for equal mole source strengths predict equal or slightly higher concentration values at equivalent times.

The actual source condition, i.e., the boiloff rate per unit area over the time duration of a spill of LNG on land is highly

unpredictable. The source conditions were approximated by assuming a steady boiloff rate of 30 m^3/min over a constant area.

Since the thermally variable prototype gas was simulated by an isothermal simulation gas, the concentration measurements observed in the model must be adjusted to equivalent concentrations that would be measured in the field. This relationship, which is derived in Appendix A, is:

$$\chi_p = \frac{\chi_m}{\chi_m + (1 - \chi_m) \frac{T_s}{T_a}}$$

where

χ_m = volume or mole fraction measured during the model tests,

T_s = source temperature of LNG during field conditions,

T_a = ambient air temperature during field conditions, and

χ_p = volume or mole fraction in the field.

2.4.3. Physical Modeling of the Neutral Density Plume

The experimental data on the neutrally buoyant plume are presented in two formats: 1) mean concentration at each location with the 100% source gas but neutral buoyancy and 2) nondimensional concentration coefficient,

$$K = \frac{\chi \ U \ D^2}{\chi_s \ V_s} \ ,$$

where

χ = concentration at the sampling point (ppm),

U = reference velocity at 4 cm height (10 m prototype) (m/sec),

D = source diameter (m),

χ_s = source strength (ppm), and

V_s = source flow rate (m^3/sec).

There are two ways of analyzing the neutral density plume data:

1) The neutral density plume source flow rate of the spill area equal to that generated by LNG spill ignoring density and neglecting the equality of the number of moles in both plumes, or

2) The neutral density plume source flow rate at the spill area equal to that generated by LNG spill ignoring density but specifying the equality of the number of moles in both plumes.

If the second method is utilized, the wind tunnel measured concentration has to be corrected by the following formula to derive percentage concentration in field for the neutral density plume data:

$$X_p = \frac{X_m}{X_m + (1 - X_m) \frac{T_p}{T_m} \frac{u_1}{u_2} \frac{Q_2}{Q_1}}$$

where

X_p is the percentage concentration in field for neutral density plume data,

X_m is the measured percentage concentration in the wind tunnel for neutral density plume data,

T_p LNG boiloff temperature,

T_m temperature of neutral density plume,

u_1 model reference velocity during Argon (heavy gas at isothermal temperature) runs,

u_2 model reference velocity during neutral density plume runs,

Q_1 model source strength during Argon (heavy gas at isothermal temperature) runs, and

Q_2 model source strength during neutral density plume runs.

It should be noted that all neutral density data were analyzed according to first method.

3.0 DATA AQUISITION AND ANALYSIS

The methods used to make laboratory measurements and the techniques used to convert these measured quantities to meaningful field-equivalent quantities are discussed in this section. Attention has been drawn to the limitations in the techniques in an attempt to prevent misinterpretation or misunderstanding of the results presented in the next section. Some of the methods used are conventional and need little elaboration.

3.1 WIND-TUNNEL FACILITIES

The Environmental Wind Tunnel (EWT) shown in Figure 4 was used for all tests performed. This wind tunnel, specially designed to study atmospheric flow phenomena, incorporates special features such as adjustable ceiling, rotating turntables, transparent boundary walls, and a long test section to permit reproduction of micrometeorological behavior at larger scales. Mean wind speeds of 0.10 to 12 m/s can be obtained in the EWT. A boundary layer depth of 1 m thickness at 6 m downstream of the test entrance can be obtained with the use of the vortex generators and trip at the test section entrance and surface roughness on the floor. The flexible test section roof on the EWT is adjustable in height to permit the longitudinal pressure gradient to be set to zero. The vortex generators and trip at the tunnel entrance were followed by 8.8 m of smooth floor for the 1:250 scaled area source model.

3.2 MODEL

Based on the previous atmospheric data over sites similar to that of the present idealized site it was decided that the best reproduction of the surface wind characteristics would be at a model scale of 1:250. The area source of diameter 75 m was constructed from Plexiglas.
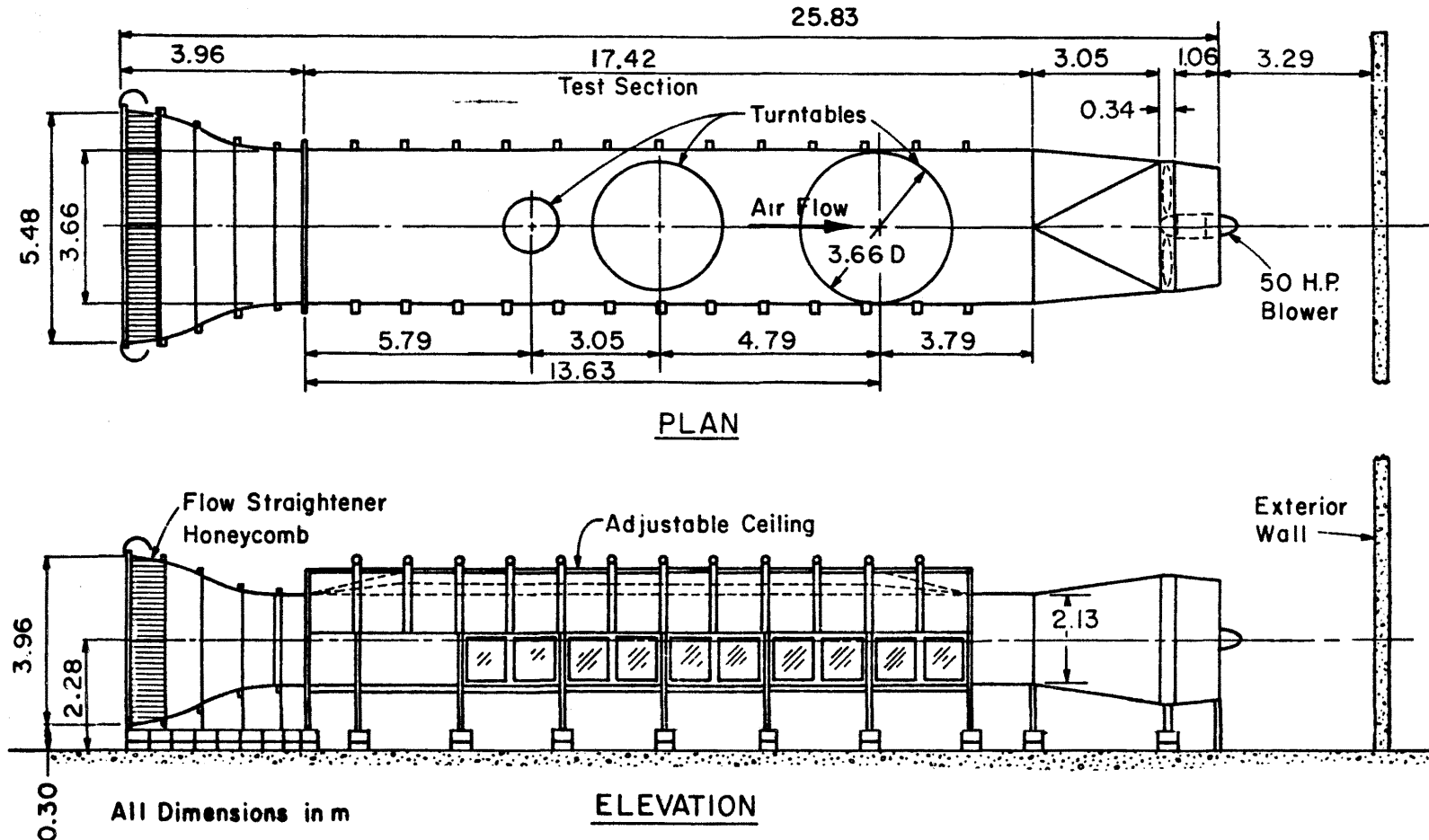
Figure 4. Environmental Wind Tunnel
Fluid Dynamics & Diffusion Laboratory
Colorado State University

The cylindrical tanks having height and diameter equal to 50 m were also constructed from Plexiglas. The cubical buildings 18.75 x 18.75 x 18.75 m were made of styrofoam. The tree line was fabricated with lichen and had an approximate height of 7.5 m and porosity of 30%. The source gases, Argon, or the mixture of 10% Ethane, 4% carbon dioxide, and 86% nitrogen were stored in a high pressured cylinder directed through a flowmeter and into the circular area source mounted in the wind-tunnel floor.

3.3 FLOW VISUALIZATION TECHNIQUES

Smoke was used to define plume behavior during the present study. The smoke was produced by passing the simulation gas through a container of titanium tetrachloride located outside the wind tunnel. The plume was illuminated with arc-lamp beams. A visible record was obtained by means of pictures taken with a Speed Graphic camera utilizing Polaroid film for immediate examination. Additional color slides were obtained with a 35 mm camera and 16 mm silent movie film was taken with a Bolex motion picture camera.

3.4 WIND PROFILE AND TURBULENCE MEASUREMENTS

The velocity profile, reference wind speed conditions, and turbulence were measured with a Thermo-Systems Inc. (TSI) 1050 anemometer and a TSI model 1210 hot-film probe. Since the voltage response of these anemometers is nonlinear with respect to velocity, a multi-point calibration of system response versus velocity was utilized for data reduction.

The velocity standard utilized in the present study was that depicted in Figure 5. This consisted of a Matheson model 8116-0154
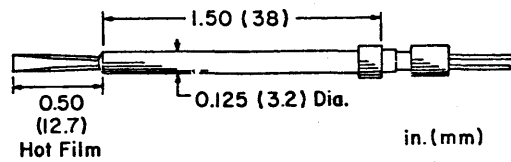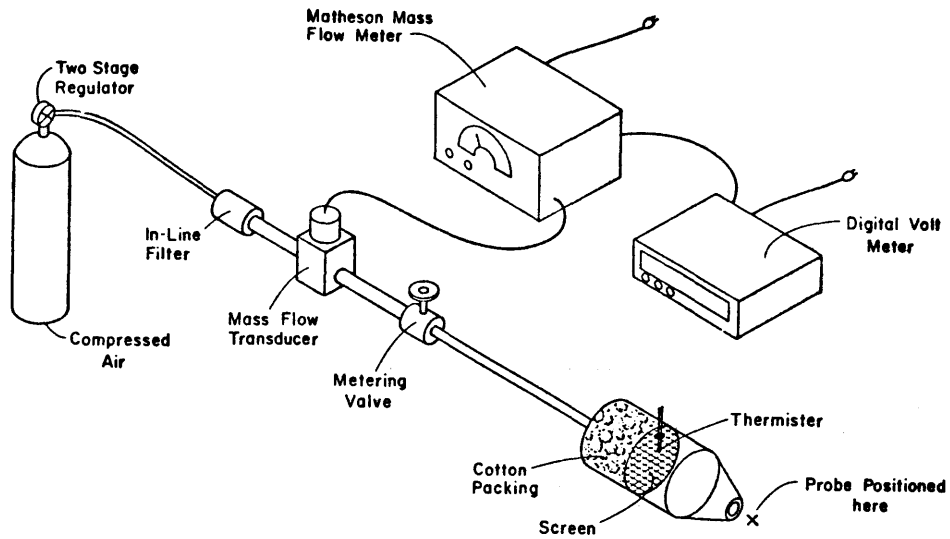
Figure 5. Velocity Probes and Velocity Standard

mass flowmeter, a Yellowsprings thermistor, and a profile conditioning section constructed by the Engineering Research Center shop. The mass flowmeter measures mass flow rate independent of temperature and pressure, the thermistor measures the temperature at the exit conditions. The profile conditioning section forms a flat velocity profile of very low turbulence at the position where the probe is to be located. Incorporating a measurement of the ambient atmospheric pressure and a profile correction factor permits the calibration of velocity at the measurement station from 0.1-2.0 m/s ±5.0 cm/s.

During calibration of the single film anemometer, the anemometer voltage response values over the velocity range of interest were fit to an expression similar to that of King's law [25] but with a variable exponent. The accuracy of this technique is approximately ±2 percent of the actual longitudinal velocity.

The velocity sensors were mounted on a vertical traverse and positioned over the measurement location on the model. The anemometer responses were fed to a Preston analog-to-digital converter and then directly to a HP-1000 minicomputer for immediate interpretation. The HP-1000 computer also controls probe position. A flow chart depicting the control sequence for this process is presented in Figure 6.

3.5 CONCENTRATION MEASUREMENTS (LNG Plume)

To obtain the concentration time histories at points downwind of the spill site a rack of eight hot-wire aspirating probes was designed and constructed. A layout of this design is presented in Figure 7. The films on these probes were replaced with 0.005 in. platinum wire to improve signal-to-noise characteristics. These eight instantaneous concentration sensors were connected to an eight-channel TSI hot-wire
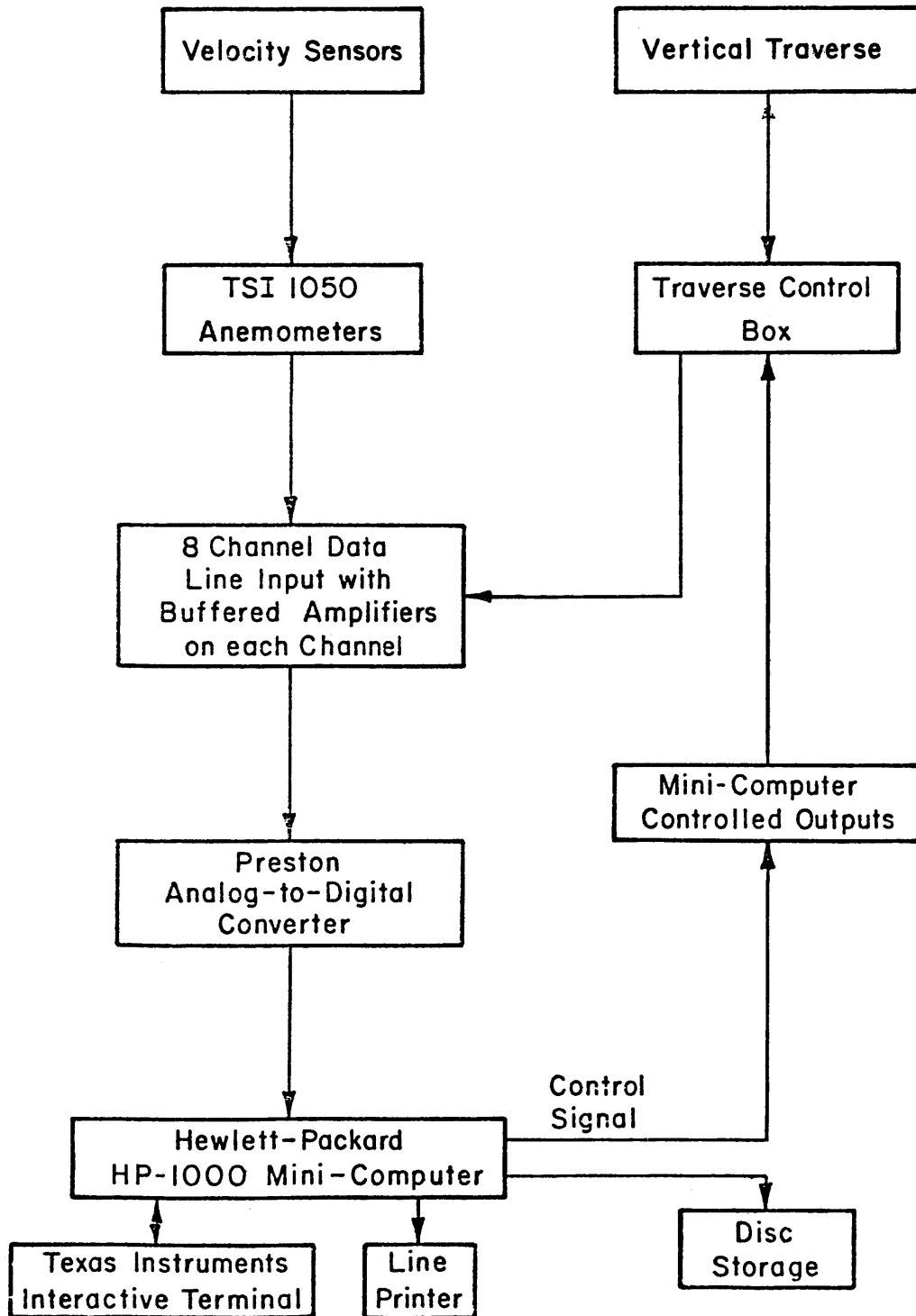
Figure 6. Velocity Data Reduction Flowchart
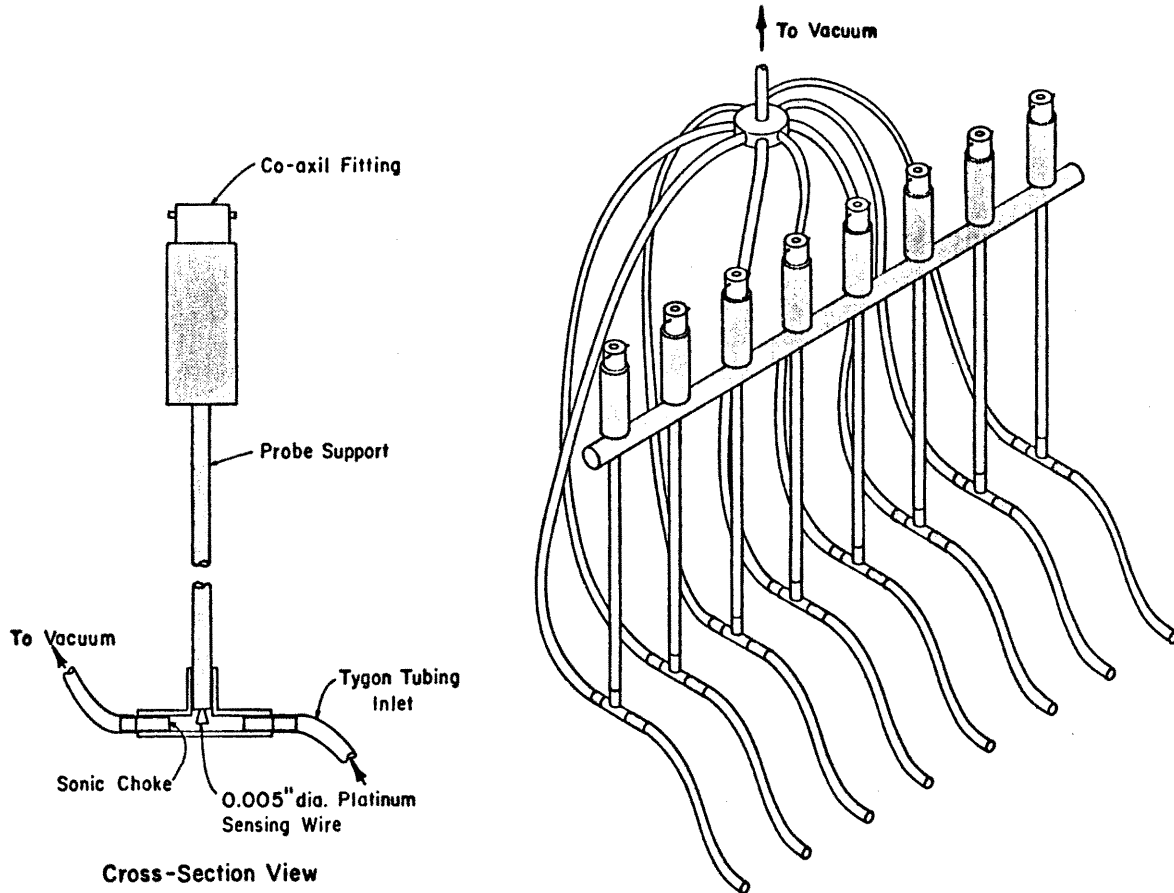
Figure 7. Hot-Wire Katharometer Probes

anemometer system. The output voltages from the TSI unit are conditioned for input to the analog-to-digital converter by a DC-supression circuit, a passive low-pass filter circuit tuned to 100 Hz, and an operational amplifier of gain five. A schedule of this process is shown in Figure 8.

3.5.1 Hot-Film Aspirating Probe

The basic principles governing the behavior of aspirating hot-wire probes have been discussed by Blackshear and Fingerson [26], Brown and Rebollo [27], and Kuretsky [28]. A vacuum source sufficient to choke the flow through the small orifice just downwind of the sensing element was applied. This wire was operated in a constant temperature mode at a temperature above that of the ambient air temperature. A feedback amplifier maintained a constant overheat resistance through adjustment of the heating current. A change in output voltage from this sensor circuit corresponds to a change in heat transfer between the hot wire and the sampling environment.

The heat transfer rate from a hot wire to a gas flowing over it depends primarily upon the wire diameter, the temperature difference between the wire and the gas, the thermal conductivity and viscosity of the gas, and the gas velocity. For a wire in an aspirated probe with a sonic throat, the gas velocity can be expressed as a function of the ratio of the probe cross-sectional area at the wire position to the area at the throat, the specific heat ratio, and the speed of sound in the gas. The latter two parameters, as well as the thermal conductivity and viscosity of the gas mentioned earlier, are determined by the gas composition and temperature. Hence, for a fixed probe geometry and wire temperature, the heat transfer rate, or the related voltage drop across

Sensors

| 1 | 2 | 3 | 4 | 5 | 6 | 7 | 8 |

TSI 8 Channel
Anemometer

DC Suppression

Voltage
Spike
Generator
(To Indicate
Starting Time)

Passive 100 Hz
Low Pass Filters

Operational Amplifiers
with a Gain of Five

Multiplexer and Analog-to-Digital
Converter

HP-1000
Minicomputer
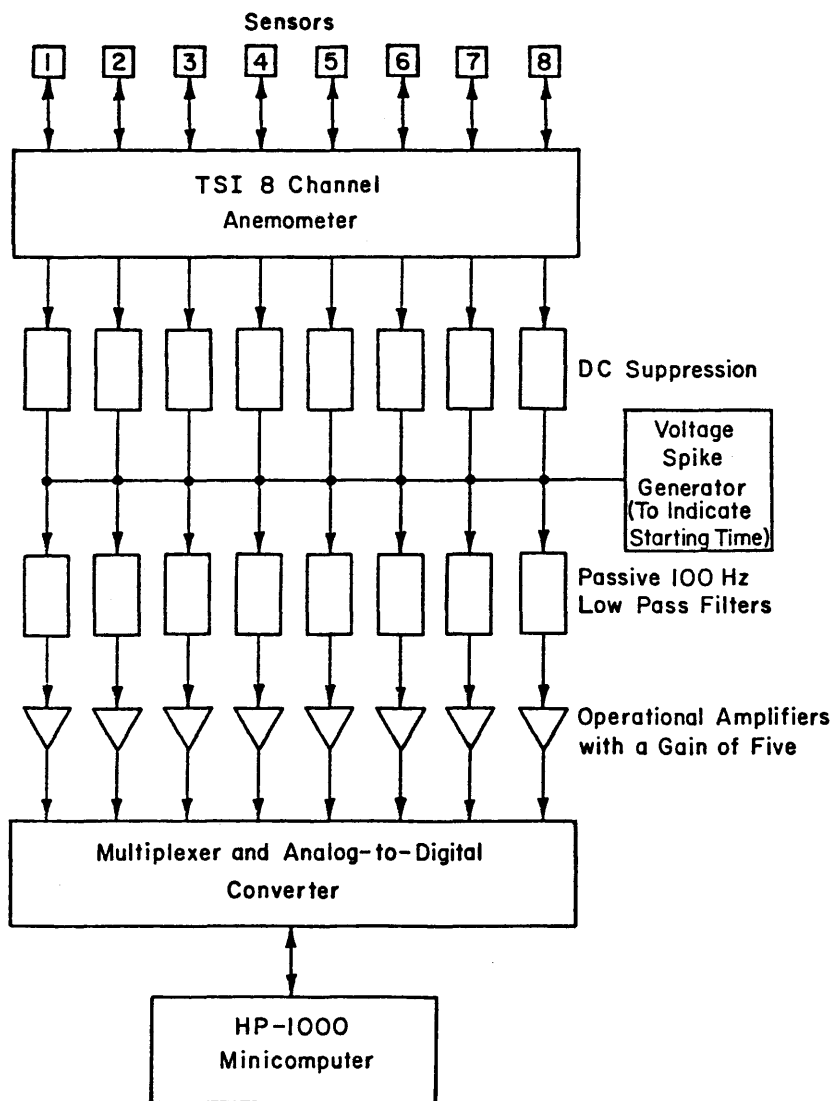
Figure 8. Block Diagram Katharometer Array

the wire is a function of only the gas composition and temperature. Since all tests performed in this study were in an isothermal flow situation the wire's response was only a function of gas composition.

During probe calibration known compositions of Argon-air mixtures were passed through a pre-heat exchanger to condition the gas to the tunnel temperature environment. Known compositions for the Argon-air calibration systems were drawn from bottles of prepared gas compositions provided by Matheson Laboratories. An overheat ratio (temperature of wire/ambient temperature) of 1.65 was used to maximize signal response while maintaining acceptable noise and signal drifting levels.

3.5.2 Errors in Concentration Measurement

The effective sampling area of the probe inlet is a function of the probe aspiration rate and the distribution of approach velocities of the gases to be sampled. A calculation of the effective sampling area during all tests suggests that the effective sampling area was approximately 0.5 cm^2. Thus the resolution of the concentration measurements as applied to the present study is 3.1 m^2 for the 1:250 scaled model.

The travel time from the sensor to the sonic choke limits the upper frequency response of the probe. At high frequencies the correlation between concentration fluctuations and velocity fluctuations (velocity fluctuations are a result of the changes of sonic velocity with concentration) at the sensor begin to decline. The CSU aspirated probe is expected to have a 1000 Hz upper frequency response, but, to improve signal to noise characteristics, the signal was filtered at 100 Hz. This is well above the frequencies of concentration fluctuations that were expected to occur.

The errors caused by a linearity assumption in the reduction of concentration data are approximately the component value (percent Argon) ±0.75 percent. The errors caused by calibration change due to temperature drift are approximately 0.1 percent of the component value per degree centigrade. Since the tunnel temperatures vary at most ±5°C during a given test period the maximum error due to temperature drift would be 0.5 percent of the component value. Finally, peak results were accepted only when they reproduced the same signal output within 10% of component value of the calibration gas (i.e., at 0, 1, 5, 15 and 100%) argon). The accumulative error, due to the combined effect of calibration uncertainties and nonlinear voltage drifting during the testing time, is estimated to be approximately ±20 percent of component value in the range of 5-15 percent equivalent methane concentrations.

Instantaneous concentration fluctuations have been averaged during the continuous spill rate tests to produce the values tabulated as mean (or average) concentrations in Appendix B. These values are equivalent to those obtained during a 10 minute sampling time at full scale. Thus they are suitable for comparison with analytic or numerical models based on 10 minute averaging time statistics. Peak concentrations reported during the continuous spill rate and 10 minute spill duration tests are equivalent to values not expected to be exceeded more than 1% of the time.

3.6 CONCENTRATION MEASUREMENTS (Neutral Density Plume)

The experimental measurements of concentration with neutral density source were performed using gas-chromatograph and sampling systems (Figure 9) designed by Fluid Dynamics and Diffusion Laboratory staff.

3.6.1 Gas Chromatograph

The gas chromatograph with Flame Ionization Detector (FID) operates on the principle that the electrical conductivity of a gas is directly proportional to the concentration of charged particles within the gas. The ions in this case are formed by the effluent gas being mixed in the FID with hydrogen and then burned in air. The ions and electrons formed enter an electrode gap and decrease the gap resistance. The resulting voltage drop is amplified by an electrometer and fed to the HP 3380 integrator. When no effluent gas is flowing, a carrier gas (nitrogen) flows through the FID. Due to certain impurities in the carrier, some ions and electrons are formed creating a background voltage or zero shift. When the effluent gas enters the FID, the voltage increase above this zero shift is proportional to the degree of ionization or correspondingly the amount of tracer gas present. Since the chromatograph[1] used in this study features a temperature control on the flame and electrometer, there is very low zero drift. In case of any zero drift, the HP 3380, which integrates the effluent peak, also subtracts out the zero drift.

The lower limit of measurement is imposed by the instrument sensitivity and the background concentration of tracer within the air in the wind tunnel. Background concentrations were measured and subtracted from all data quoted herein.

3.6.2 Sampling System

The tracer gas sampling system consists of a series of fifty 30 cc syringes mounted between two circular aluminum plates. A variable-speed motor raises a third plate, which in turn raises all 50 syringes simultaneously. A set of check valves and tubing are connected such

---

[1]A Hewlett Packard 5700 gas chromatograph was used in this study (shown in Figure 9).
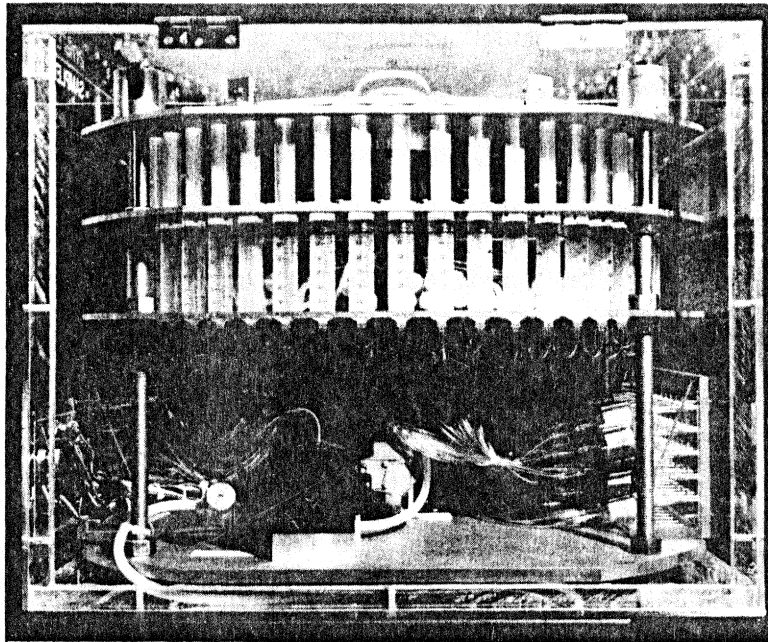
(a)
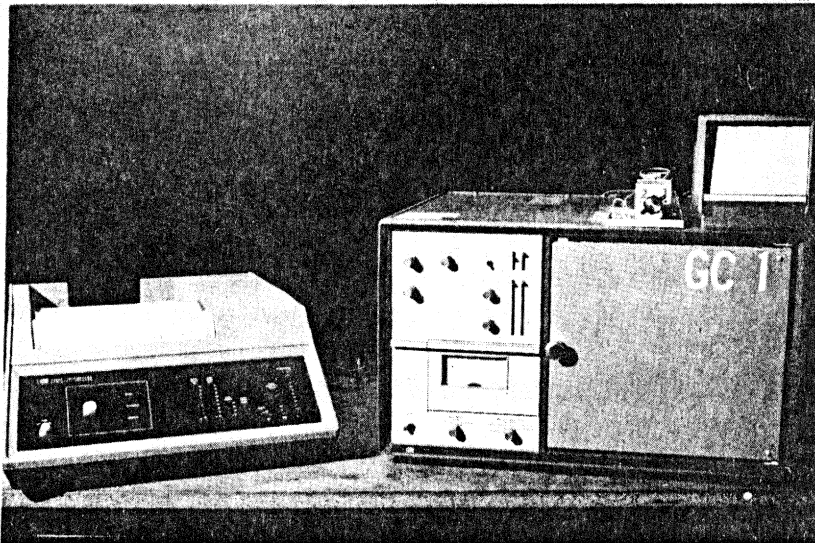
(b)

Figure 9. Photographs of (a) the Gas Sampling System, and
(b) the HP Integrator and Chromatograph

that airflow from each tunnel sampling point passes over the top of each designated syringe. When the syringe plunger is raised, a sample from the tunnel is drawn into the syringe container. The sampling procedure consists of flushing (taking and expending a sample) the syringe three times after which the test sample is taken. The draw rate is variable and generally set to be approximately 6 cc/min.

The sampler was periodically calibrated to insure proper function of each of the check valve and tubing assemblies. The sampler intake was connected to short sections of tygon tubing which led to a sampling manifold. The manifold, in turn, was connected to a gas cylinder having a known concentration of tracer gas. The gas was turned on and a valve on the manifold opened to release the pressure produced in the manifold. The manifold was allowed to flush for about 1 min. Normal sampling procedures were carried out to insure exactly the same procedure as when taking a sample from the tunnel. Each sample was then analyzed for tracer gas concentration. Any sample having an error of greater than ±2 percent indicated a failure in the check valve assembly and the check valve was replaced or the bed syringe was not used for sampling from the tunnel.

3.6.3 Test Procedure

The test procedure consisted of: 1) setting the proper tunnel wind speed, 2) releasing a metered mixture of source gas of the neutral density from the release area source, 3) withdrawing samples of air from the tunnel at the locations designated, and 4) analyzing the samples with a Flame Ionization Gas Chromatograph (FIGC). Photographs of the sampling system and gas chromatograph are shown in Figure 9. The samples were drawn into each syringe over a 300 s (approximate) time period and consecutively injected into the FIGC.

The procedure for analyzing air samples from the tunnel is as follows: 1) a 2 cc sample volume drawn from the wind tunnel is introduced into the Flame Ionization Detector (FID), 2) the output from the electrometer (in microvolts) is sent to the Hewlett-Packard 3380 Integrator, 3) the output signal is analyzed by the HP 3380 to obtain the proportional amount of hydrocarbons present in the sample, 4) the record is integrated, and the ethane concentration is determined by multiplying the integrated signal (μv-s) by a calibration factor (ppm/μv-s), 5) a summary of the integrator analysis (gas retention time and integrated area (μv-s) is printed out on the integrator at the wind tunnel, 6) the integrated values and associated run information were tabulated on a specially designed form, 7) the integrated values for each tracer are entered into a computer along with pertinent run parameters, and 8) the computer program converts the raw data into a normalized prototype concentration K and mean concentration. The calibration factor was obtained by introducing a known quantity, χ_s, of tracer into the FIGC and recording the integrated value, I, in μv-s.

The calibration factor is $\dfrac{\chi_s \text{(ppm)}}{I \text{ (μv-s)}}$

Calibrations were obtained at the beginning and end of each measurement period. The tracer gas mixtures were supplied and certified by Scientific Gas Products.

There are two ways of analyzing the neutral density plume data:

1) The neutral density plume source flow rate of the spill area equal to that generated by LNG spill ignoring density and neglecting the equality of the number of moles in both plumes, or

2) The neutral density plume source flow rate at the spill area equal to that generated by LNG spill ignoring density but specifying the equality of the number of moles in both plumes.

If the second method is utilized, the wind tunnel measured concentration has to be corrected by the following formula to derive percentage concentration in field for the neutral density plume data:

$$X_p = \frac{X_m}{X_m + (1 - X_m)\left(\frac{T_p}{T_m}\right)\left(\frac{u_1}{u_2}\right)\left(\frac{Q_2}{Q_1}\right)}$$

where

X_p is the percentage concentration in field for neutral density plume data,

X_m is the measured percentage concentration in the wind tunnel for neutral density plume data,

T_p LNG boiloff temperature,

T_m temperature of neutral density plume,

u_1 model reference velocity during Argon (heavy gas at isothermal temperature) runs,

u_2 model reference velocity during neutral density plume runs,

Q_1 model source strength during Argon (heavy gas at isothermal temperature) runs, and

Q_2 model source strength during neutral density plume runs.

It should be noted that all neutral density data were analyzed according to first method.

4.0 TEST PROGRAM

The goals of the test series were to determine the effects of surface obstacles on the dispersion of LNG or Neutral Density plumes. It is obvious that if one permits variation in source strength, rate of spill, mean flow velocity, building size, shape and geometry of separation an almost infinite matrix of tests is possible. However, after discussions with GRI personnel the following test matrix was performed:

1. Continuous LNG spill rate of 30 m^3/min to produce a significant density dominated dispersion region, and equivalent spill rate but with neutral density source gas,

2. Two wind speeds, 4 m/sec and 7 m/sec at 10 m equivalent height with neutral atmospheric stability,

3. LNG storage tanks with both diameter and height equal to 50 m,

4. LNG boiloff area with diameter of 75 m,

5. Building with length, height, and width equal to 18.75 m, and

6. Tree line with approximate height of 7.5 m and porosity of 30%.

The coordinate system and sampling point locations used throughout this report are given in Figure 10. It should be noted that all concentration measurements were performed at ground-level. Because of the expected symmetry of the concentration pattern, the sample points were placed only on negative y coordinates. A summary of the test program identifying run numbers, prototype wind speeds, various configuration numbers, and source density is given in Table 1. The configurations 1, 2 to 8, 10 to 12, 13 to 17, and 18 to 22 are described in Figures 10 through 14, respectively. The total program required 84 runs in the Environmental Wind Tunnel. The following formulae were utilized to convert field values to model values,
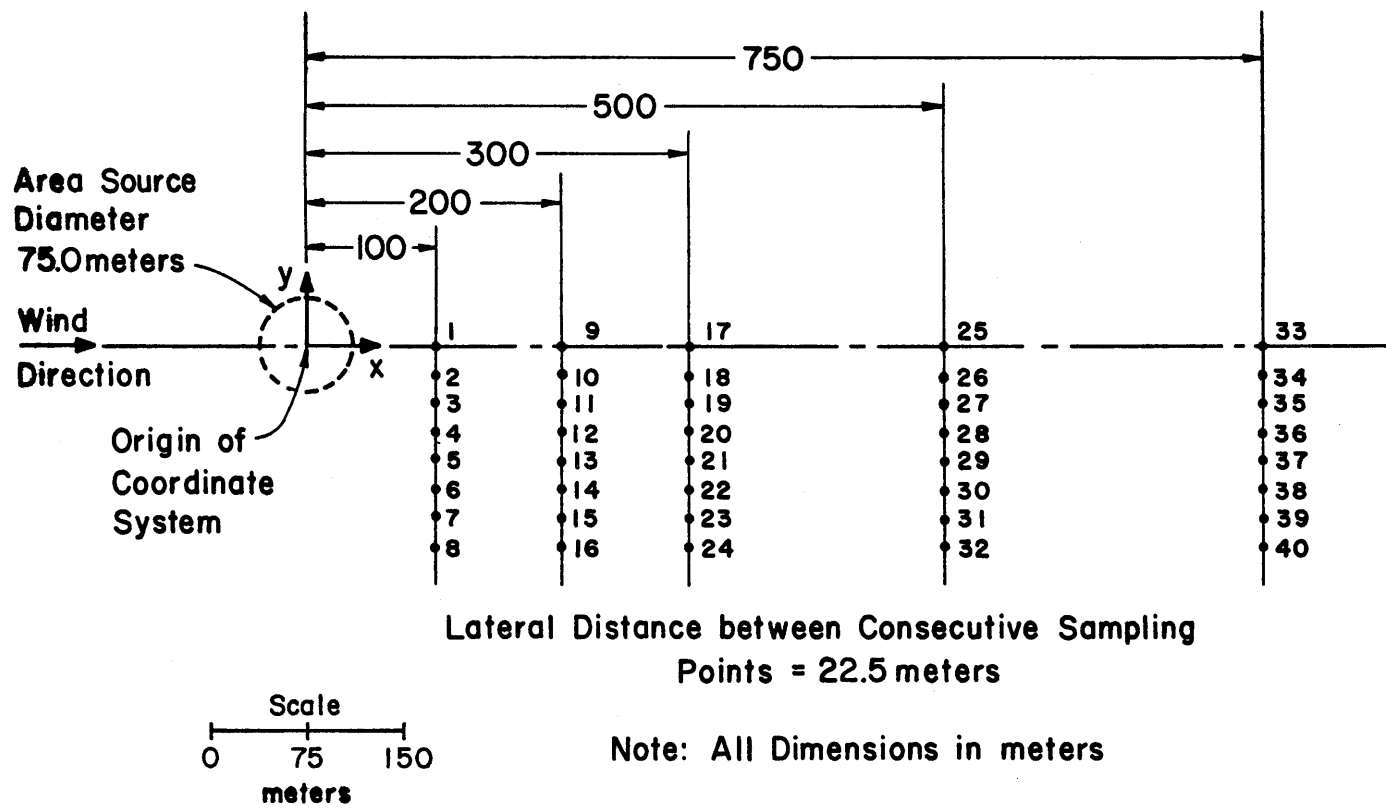
Figure 10. Concentration Measurement Locations and
Configuration 1 Identification
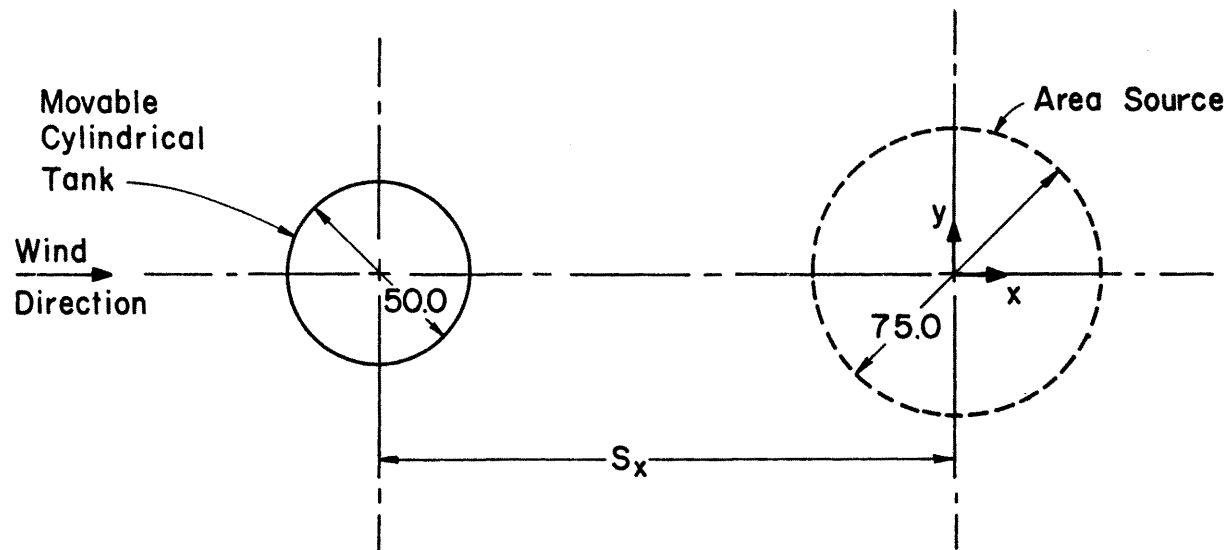
Figure 11. Configurations 2 to 8 Identification
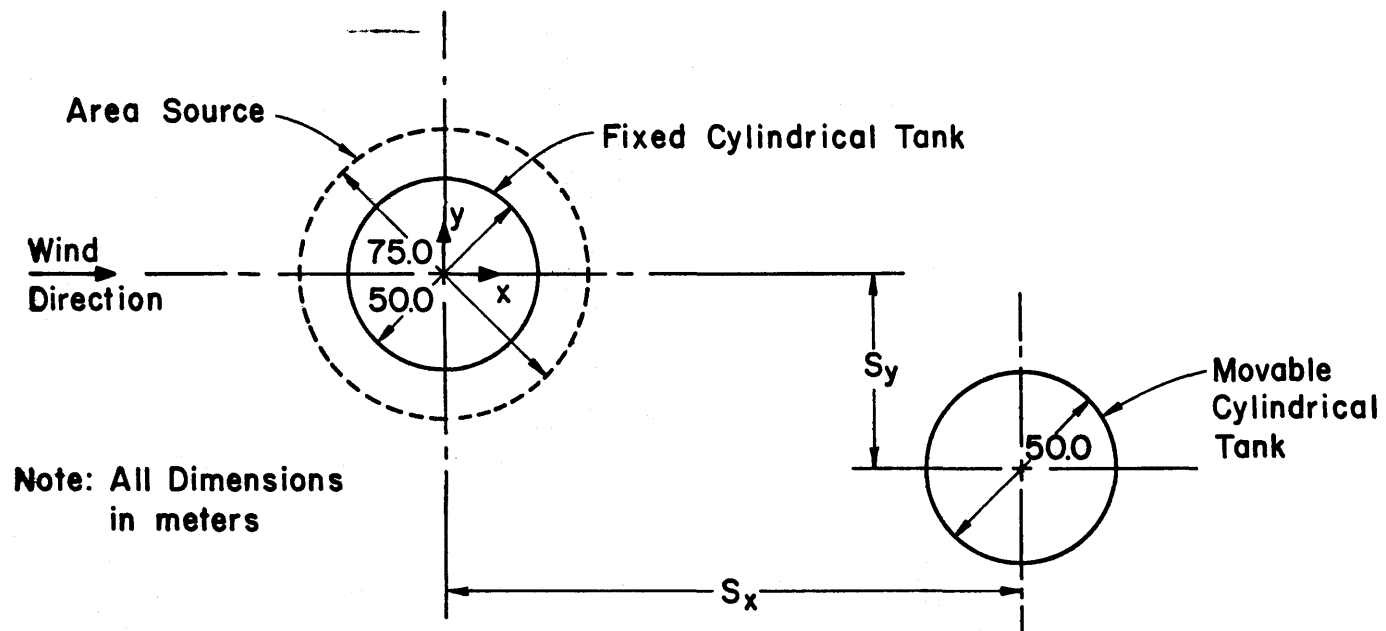
Configuration	Displacement in x Direction S_x, meters	Displacement in y Direction S_y, meters
10	150.0	0.0
11	150.0	-50.0
12	250.0	0.0

Figure 12. Configurations 10 to 12 Identification

Figure 13. Configurations 13 to 17 Identification

Movable Cylindrical Tank

Wind Direction

Four Cubical Buildings 18.75 × 18.75 × 18.75

Area Source

50.0

75.0

75.0

75.0

75.0

75.0

S_x

Note: All Dimensions in meters
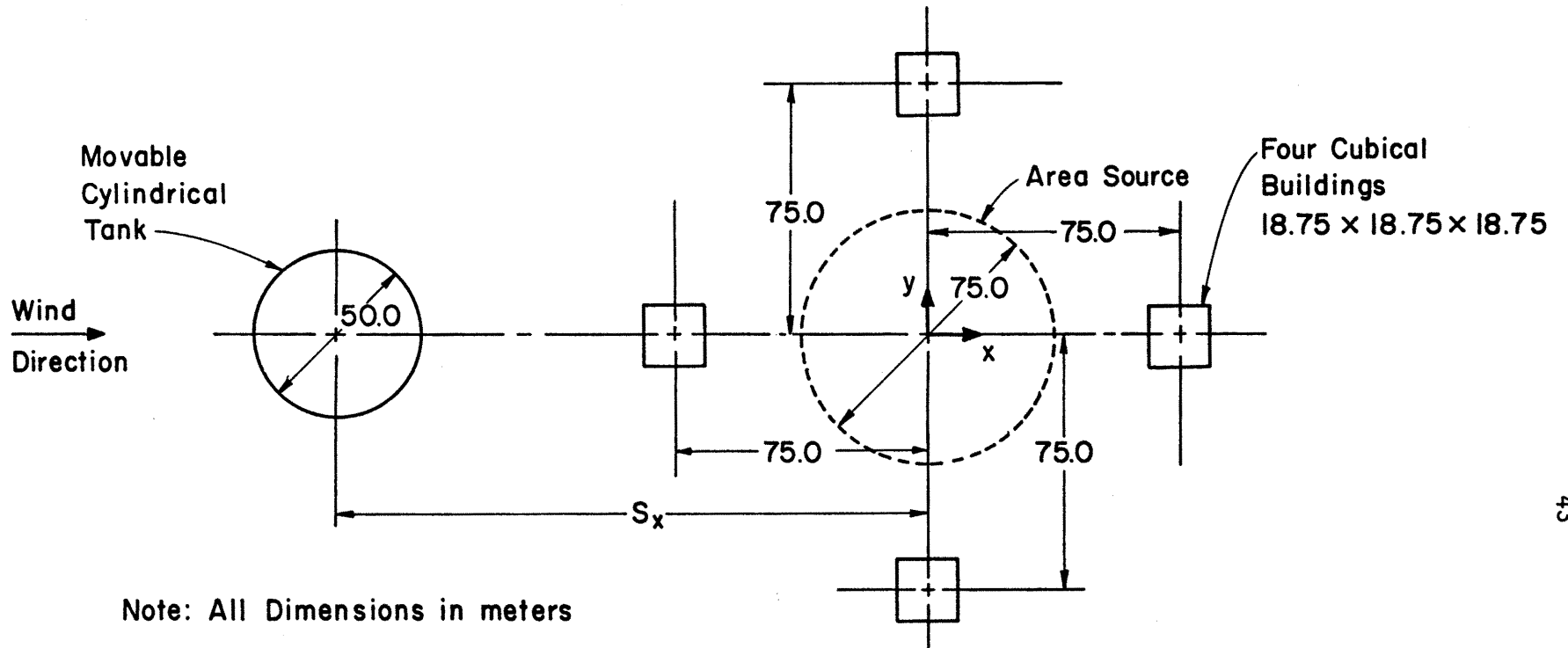
Configuration	Displacement in x Direction S_x, meters
13	-250.0
14	-150.0
15	0.0
16	150.0
17	250.0

Area Source

Moveable
Cylindrical
Tank

Wind
Direction

50.0

y 75.0

x

S_x

75.0

Tree Line
Approximate Height 7.5 meters
and Porosity ~30%

300.0

Note: All Dimensions
in meters

44
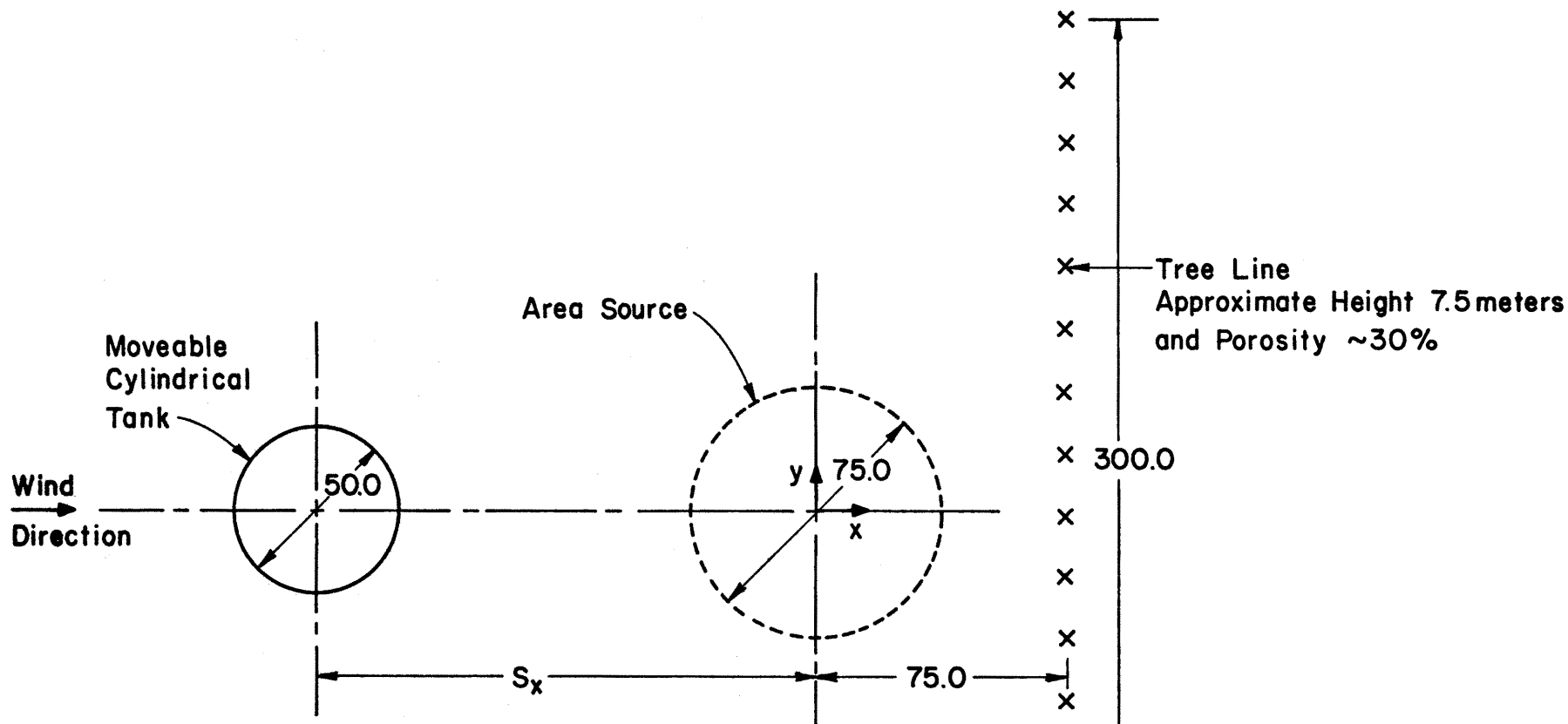
Configuration	Displacement in x Direction S_x, meters
18	-250.0
19	-150.0
20	0.0
21	150.0
22	250.0

Figure 14.   Configurations 18 to 22 Identification

Table 1. Summary of Tests

Configuration Number	Source Density-Neutral				Source at Specific Gravity of LNG at Boiloff Temperature			
	Prototype Wind Speed @ 10 m height	Run Number	Prototype Wind Speed @ 10 m height	Run Number	Prototype Wind Speed @ 10 m height	Run Number	Prototype Wind Speed @ 10 m height	Run Number
1		1		23		45		67
2		2		24		46		68
3		3		25		47		69
4		4		26		48		70
5		5		27		49		71
6		6		28		50		72
7		7		29		51		73
8		8		30		52		74
10		10		32		54		76
11		11		33		55		77
12	4.0 m/sec	12	7.0 m/sec	34	4.0 m/sec	56	7.0 m/sec	78
13		13		35		57		79
14		14		36		58		80
15		15		37		59		81
16		16		38		60		82
17		17		39		61		83
18		18		40		62		84
19		19		41		63		85
20		20		42		64		86
21		21		43		65		87
22		22		44		66		88

Note:

1. Boiloff rate from area source = 30 m^3/min.
2. Neutral density source runs were performed with the equivalent amount of vapor generation from 30 m^3/min LNG, but with neutral density.

45

$$L_m = \frac{1}{L.S.} \, L_p \; ,$$

with LNG plume,

$$U_m = \left(\frac{S.G._m - 1}{S.G._p - 1}\right)^{1/2} \left(\frac{L_m}{L_p}\right)^{1/2} U_p \; ,$$

$$Q_m = \left(\frac{S.G._m - 1}{S.G._p - 1}\right)^{1/2} \left(\frac{L_m}{L_p}\right)^{5/2} Q_p \; ,$$

and with Neutral Density plume,

$$U_m = \left(\frac{L_m}{L_p}\right)^{1/2} U_p \; ,$$

$$Q_m = \left(\frac{L_m}{L_p}\right)^{5/2} Q_p \; ,$$

where,

L is length,

U is reference wind speed at 10 m height,

Q is plume flow rate at the source,

L.S. is length scale factor (250),

S.G. is plume specific gravity at the source, and subscripts m and p indicate model and prototype (field) conditions, respectively.

4.1 RESULTS AND DISCUSSION

4.1.1 Approach Velocities

The approach flow velocity profiles were measured at the location of the area source center. The model approach velocities were slightly higher for neutral density plumes dispersion tests as compared with LNG plume dispersion tests because of the difference in modeling source gas. The characteristic mean velocity and turbulence profiles are displayed

in Figures 15 and 16 for neutral density and LNG dispersion tests, respectively. The average value of the velocity profile power-law exponent was 0.22. The average values of the frictional velocity, u_*, were 0.25 m/sec and 0.44 m/sec corresponding to prototype wind speeds of 4 m/sec and 7 m/sec at 10 m height. The average value of the surface roughness parameter, z_0 for prototype conditions was 4 cm.

4.1.2 Flow Visualization Results

The various configurations of the scaled model were installed in the wind tunnel and flow visualization was performed with 30 m^3/min LNG equivalent flow rate and two wind speeds. For each test, 4x5 black and white still photographs, 35 mm color slides, and 16 mm silent movie were obtained to determine the plume geometry.

4.1.3 Concentration Measurement Results

Concentration measurements from twenty-one different configurations are grouped into four categories to determine the effects of cylindrical tanks, two cylindrical tanks, buildings and a cylindrical tank, and a tree line and a cylindrical tank on the plume dispersion. The neutral density plume results are presented as mean concentration, whereas LNG plume data are given in the form of mean concentration and peak concentration. All concentration data are given in Appendix B.

Figures 17 through 20 show the plots of mean concentration against downwind distance for various configurations and both wind speeds for a neutral density plume. Figures 21 through 24 and Figures 25 to 28 present peak concentration and mean concentration, respectively, as a function of downwind distance for different configurations and both wind speeds for a LNG plume. For both types of plumes, the highest concentrations were observed without any suface obstacle. The surface
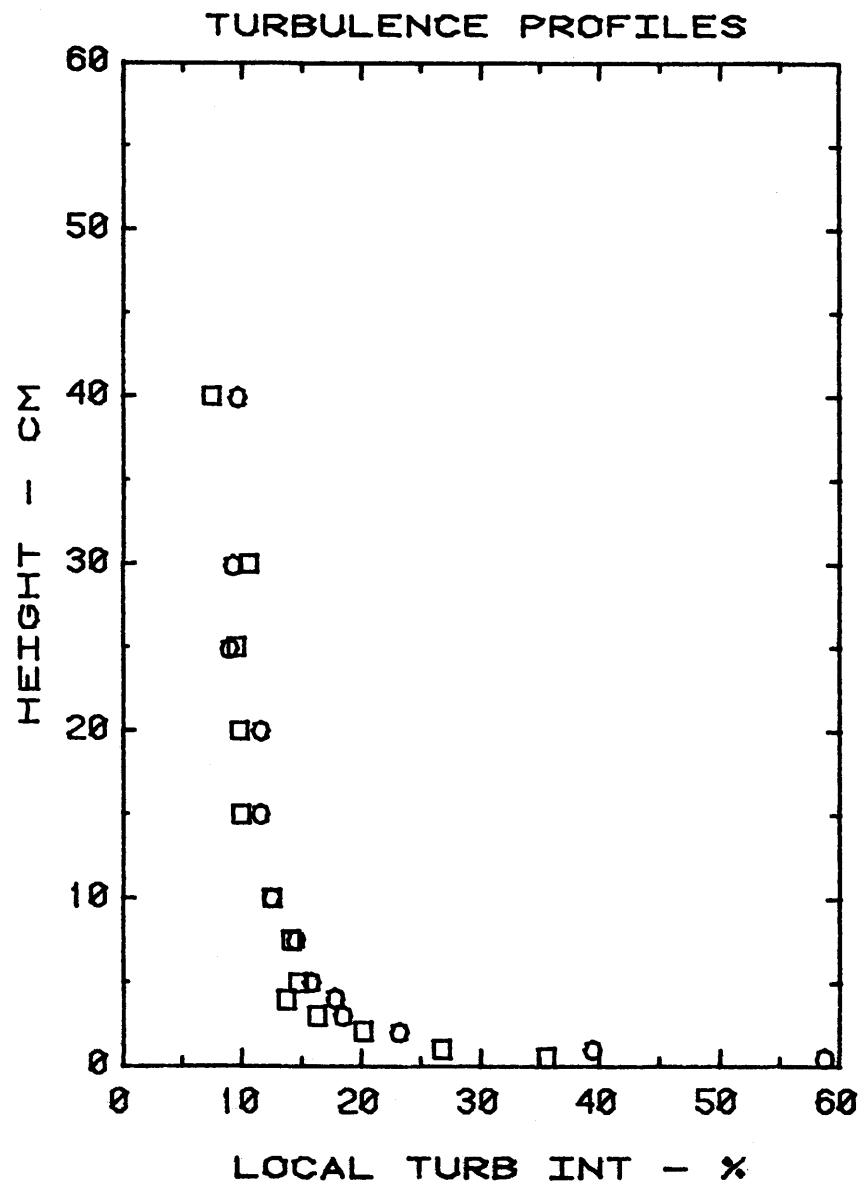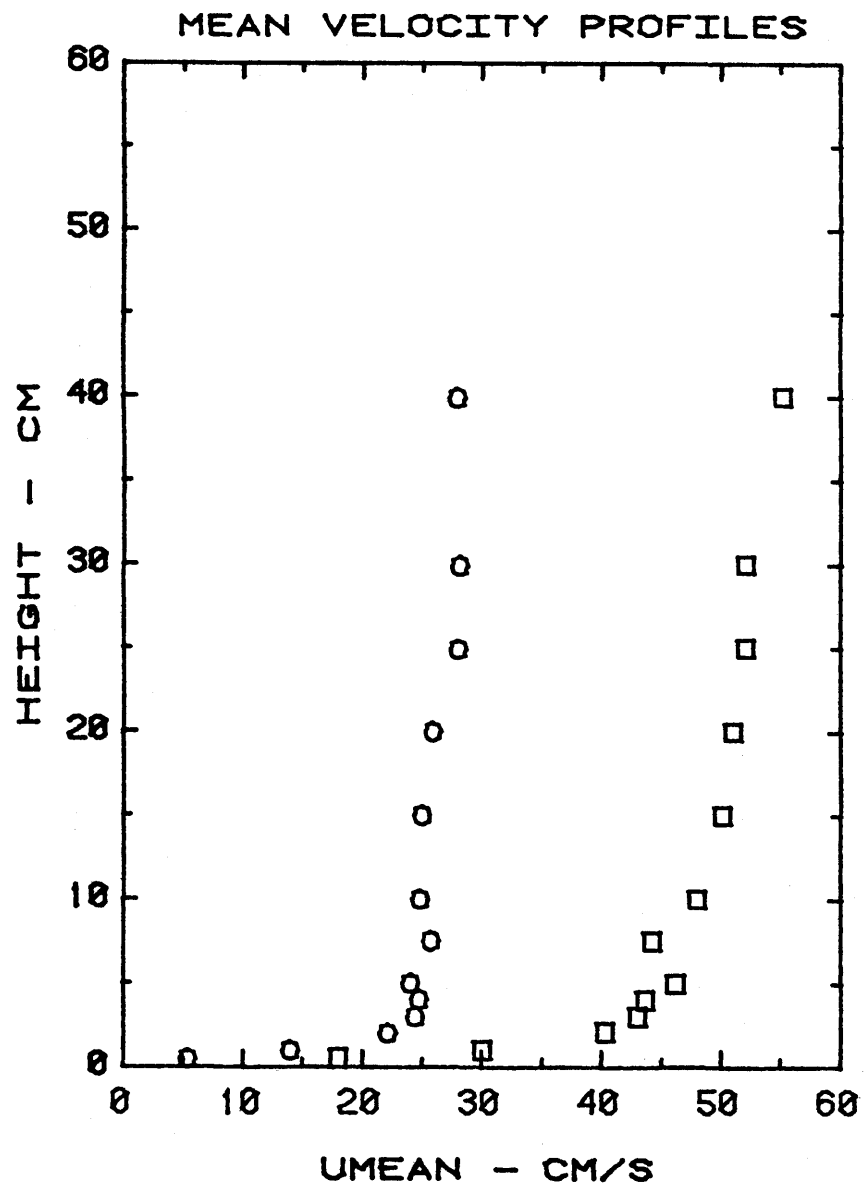
Figure 15. Velocity and Turbulence Profiles Utilized with Neutral Density Plume
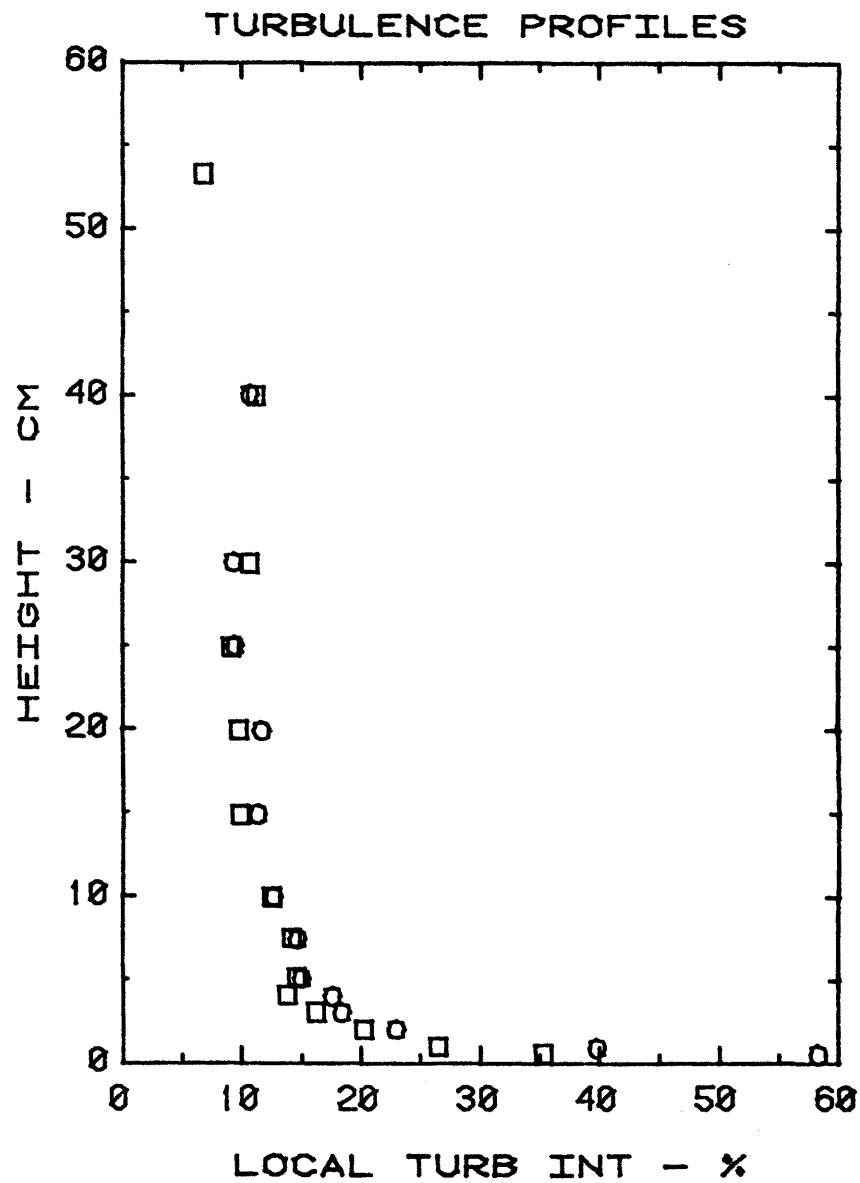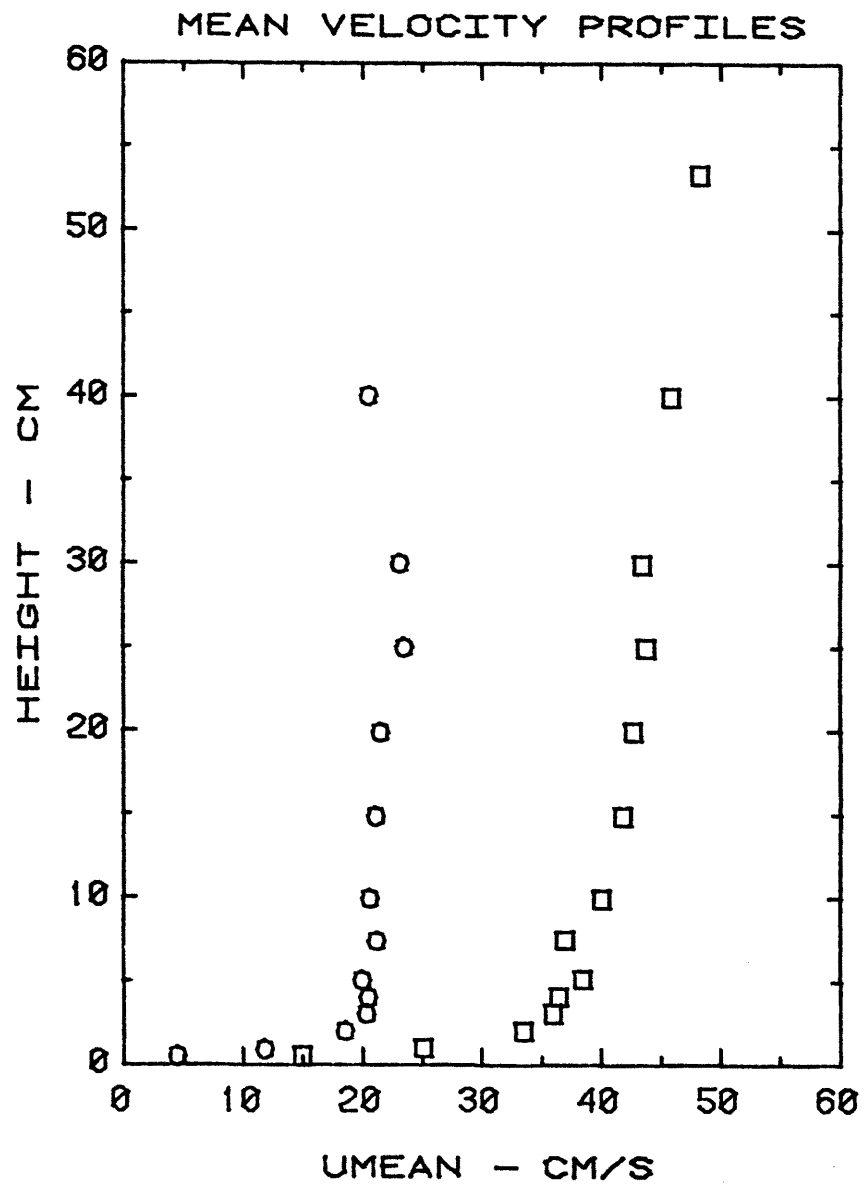
Figure 16. Velocity and Turbulence Profiles Utilized with Negatively Buoyant Plume (LNG)
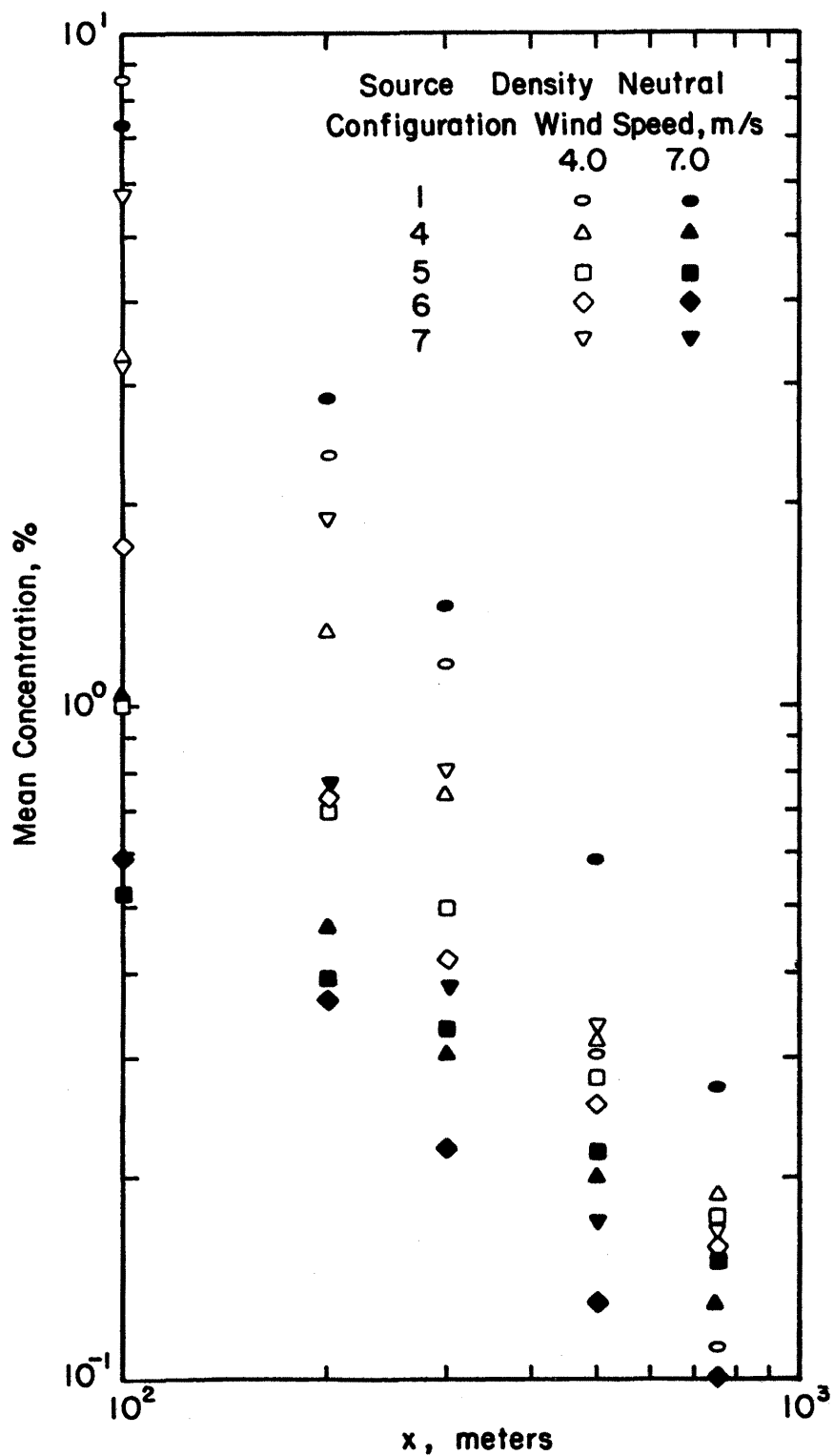
Figure 17.   Mean Concentration vs.   x   (Neutral Density Plume)
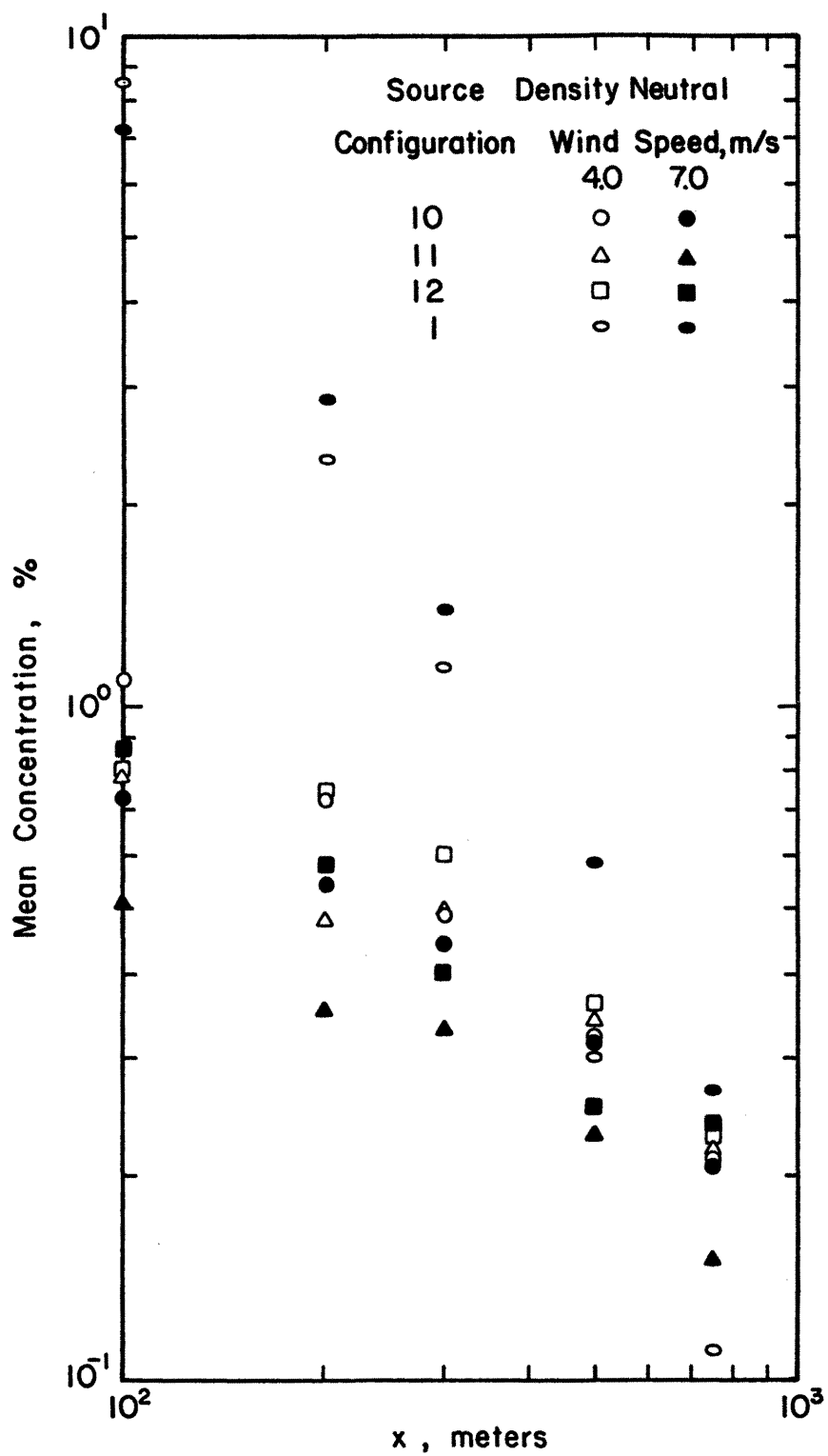
Figure 18. Mean Concentration vs. x (Neutral Density Plume)
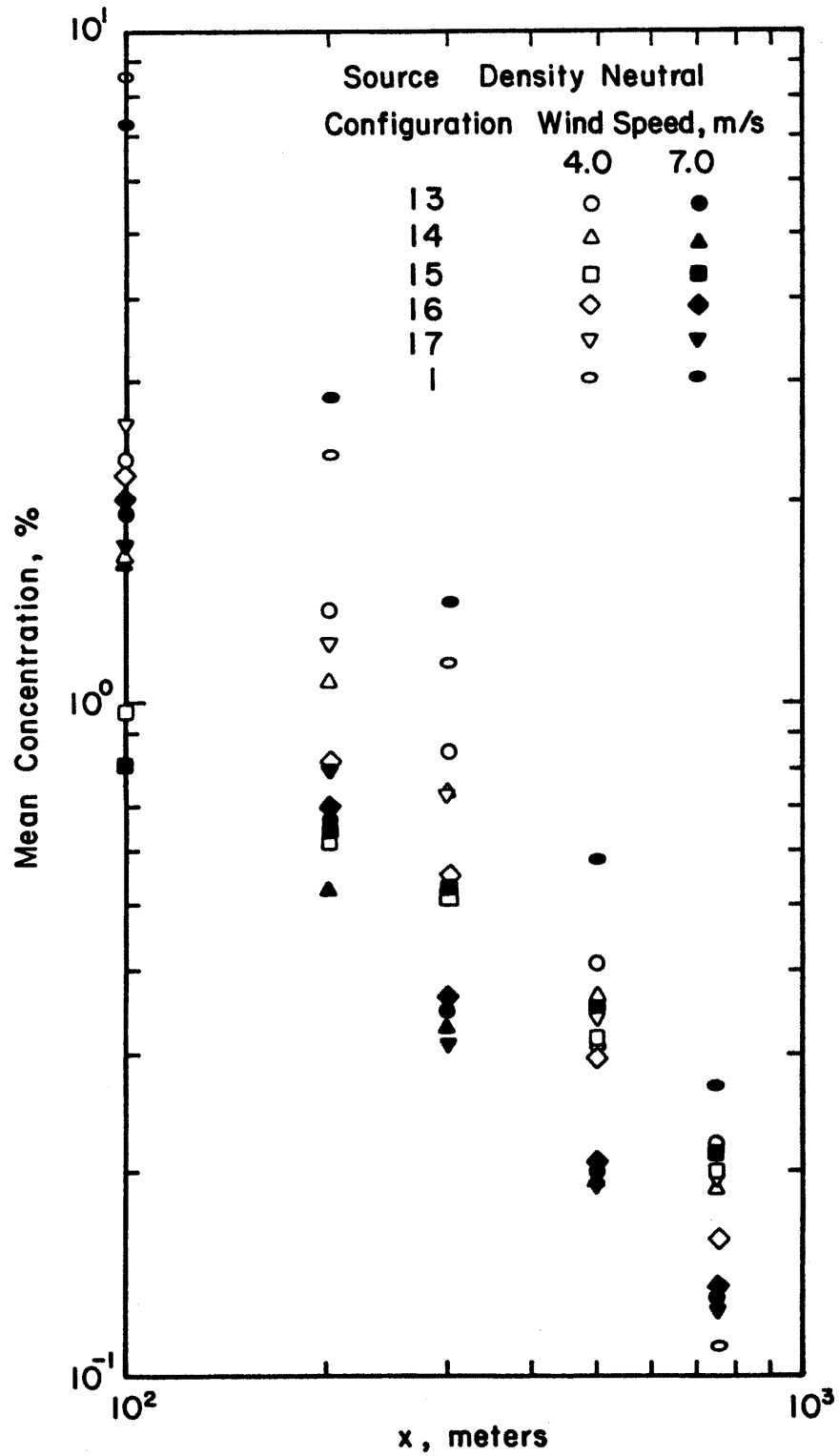
Figure 19. Mean Concentration vs. x (Neutral Density Plume)
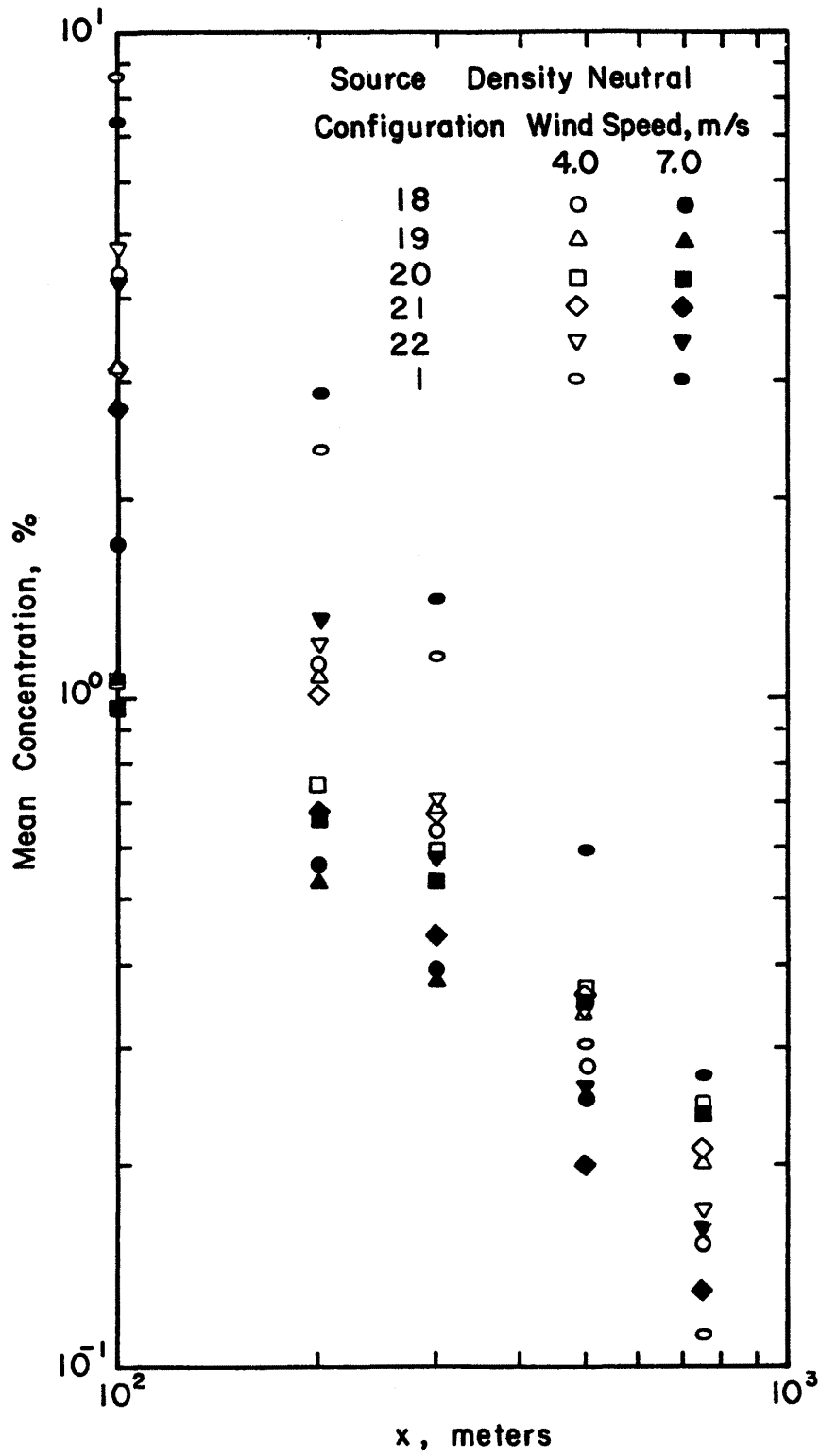
Figure 20.   Mean Concentration vs.   x   (Neutral Density Plume)
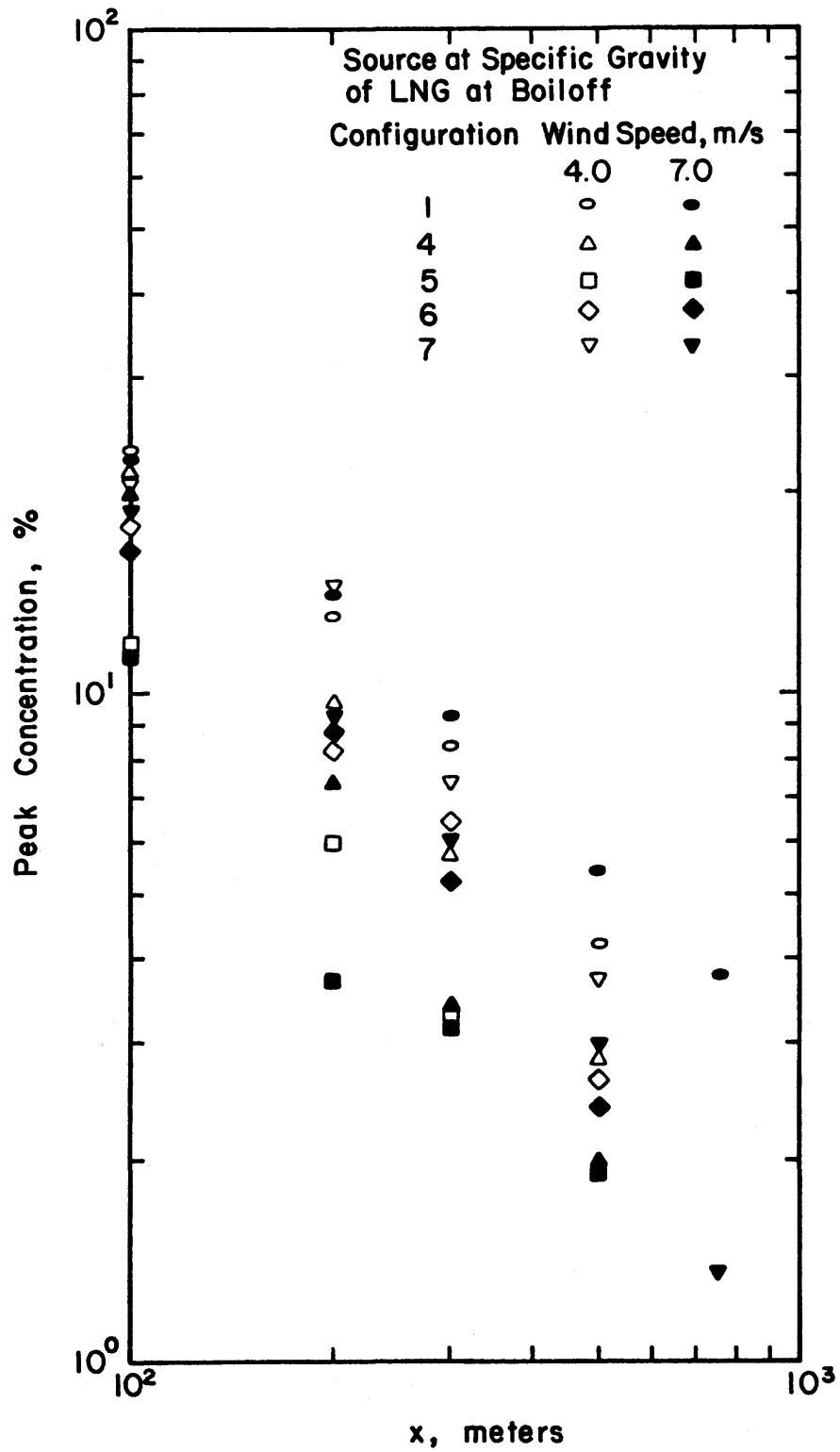
Figure 21. Peak Concentration vs. x (LNG Plume)
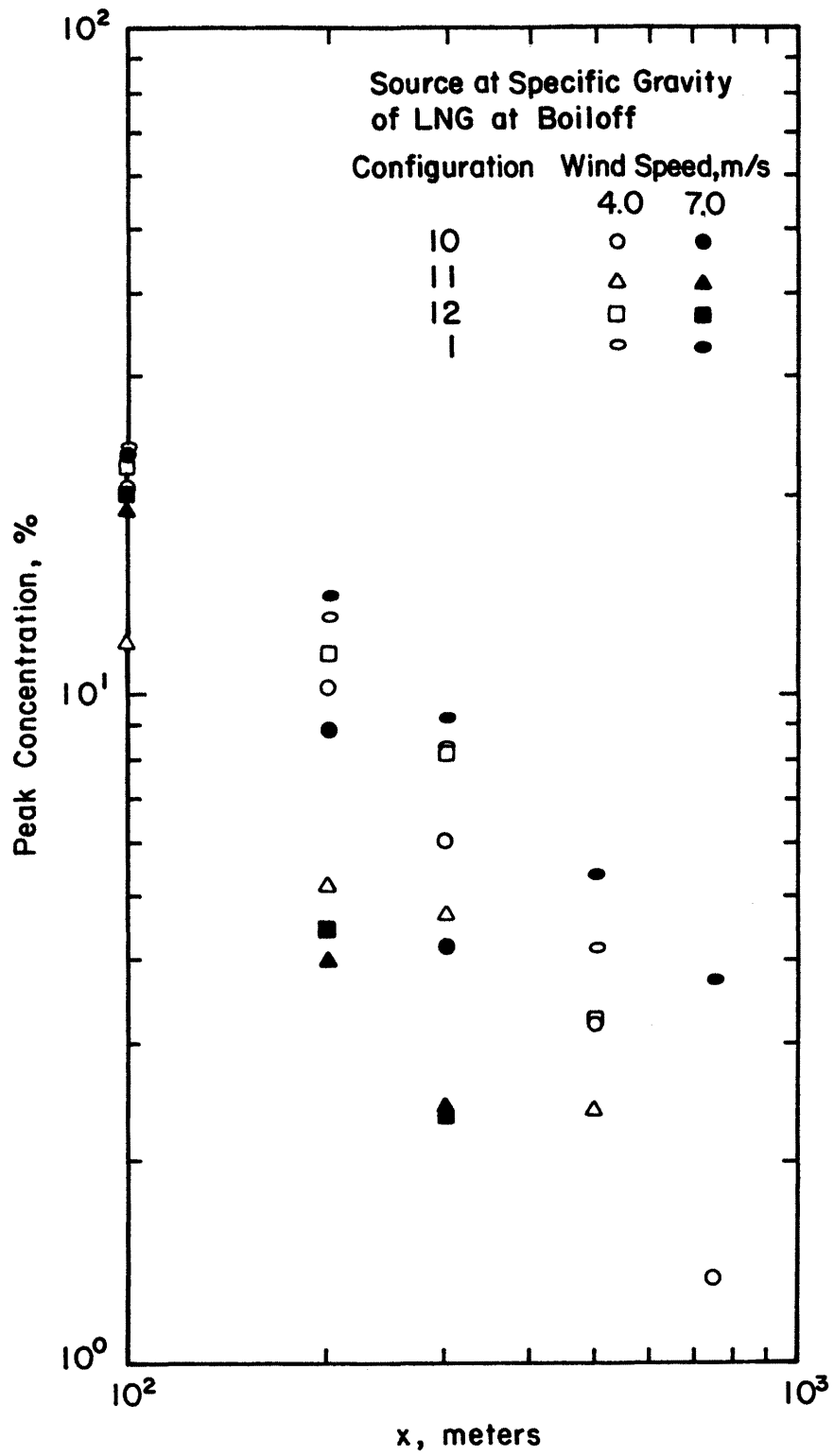
Figure 22.   Peak Concentration vs.   x   (LNG Plume)
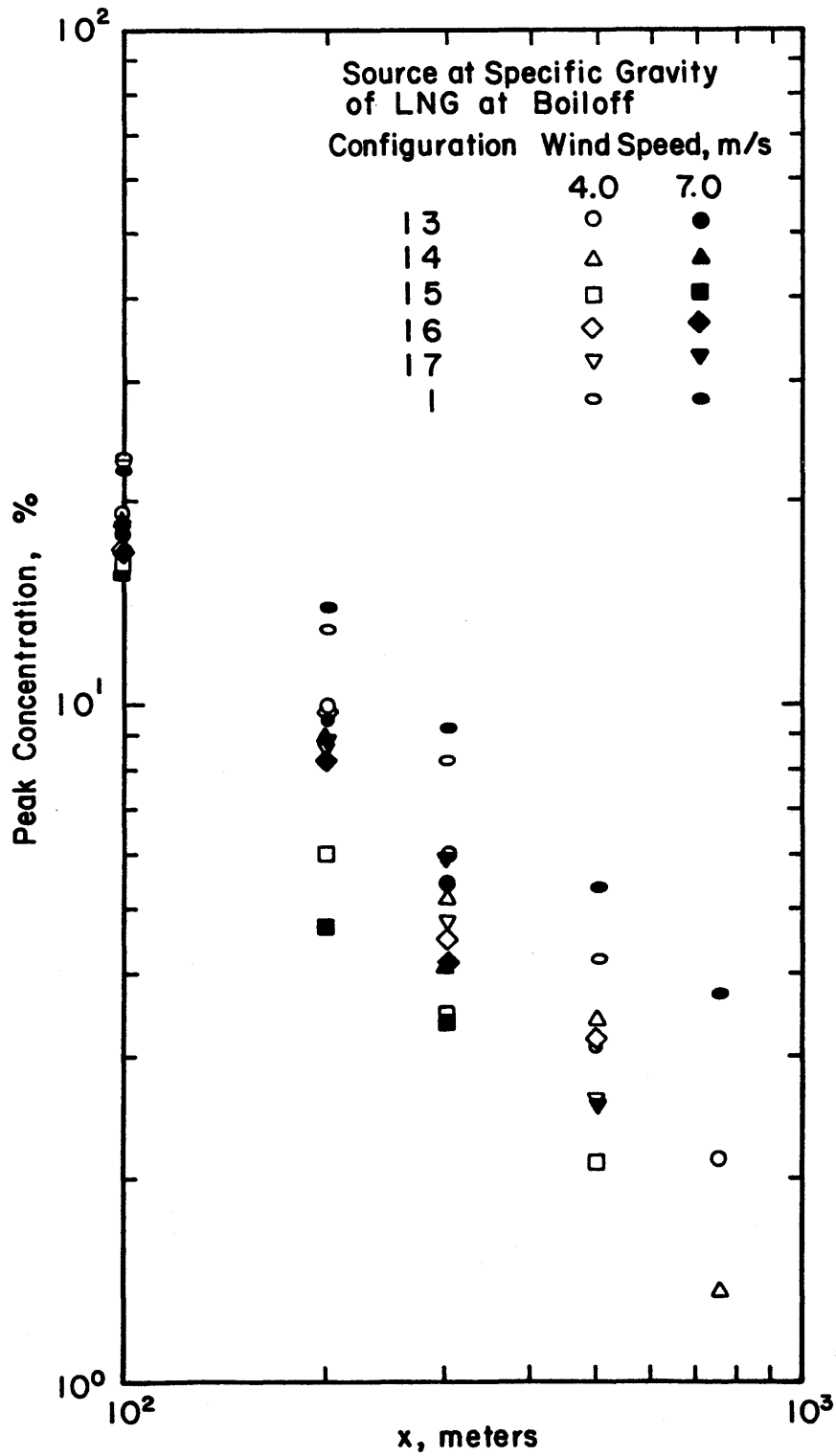
Figure 23.   Peak Concentration vs.   x   (LNG Plume)
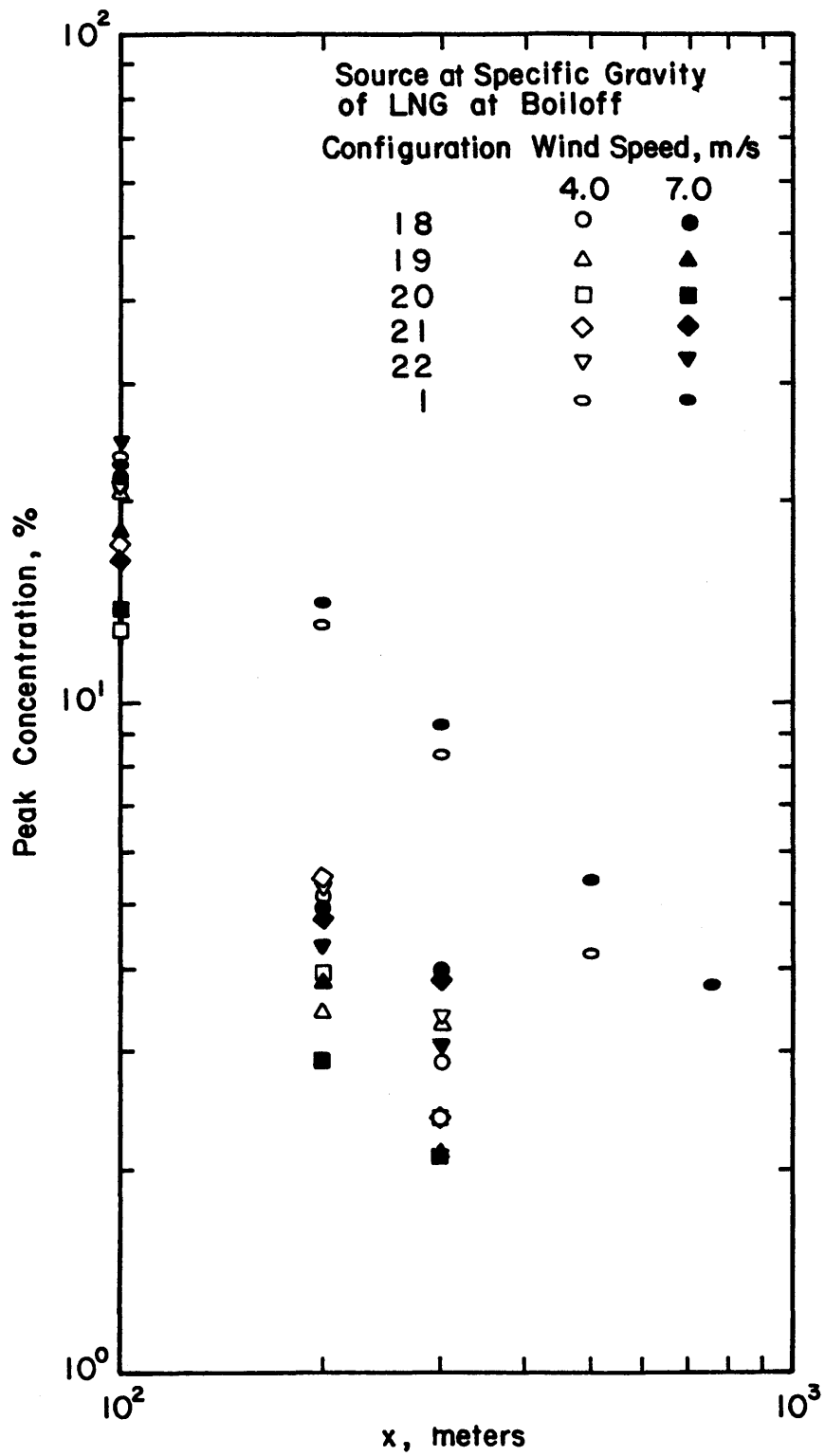
Figure 24.   Peak Concentration vs.   x   (LNG Plume)
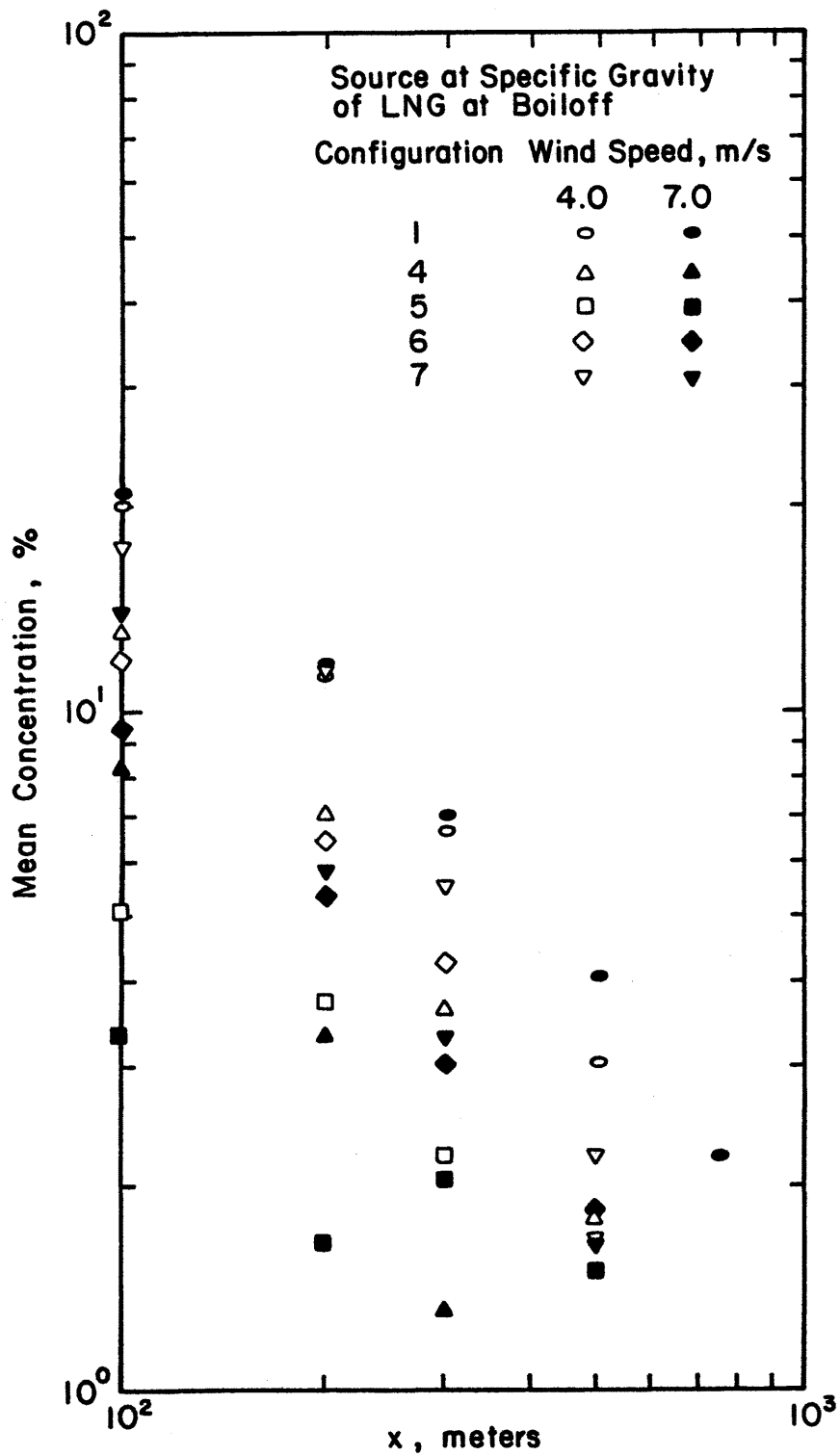
Figure 25. Mean Concentration vs. x (LNG Plume)
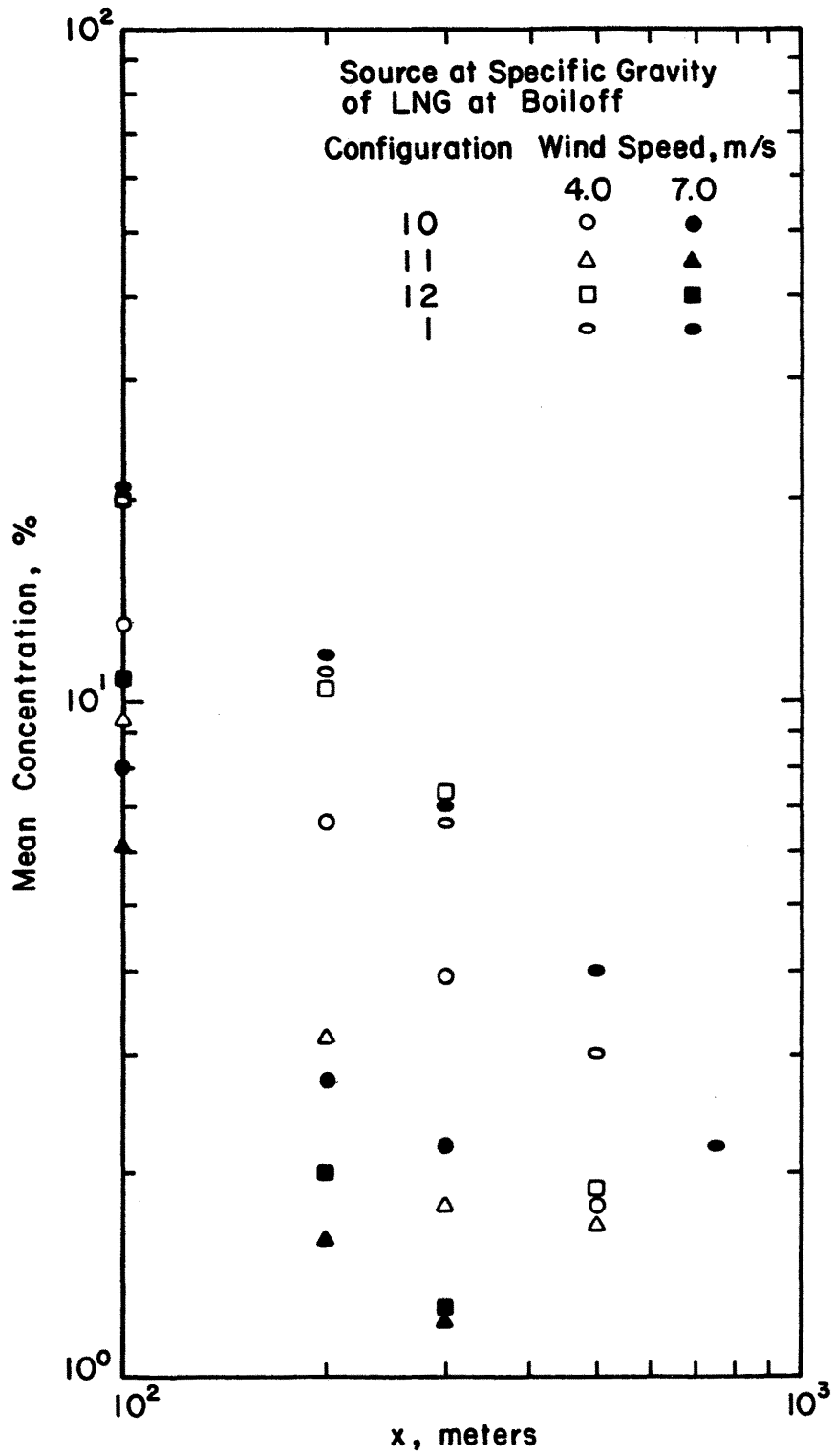
Figure 26. Mean Concentration vs. x (LNG Plume)
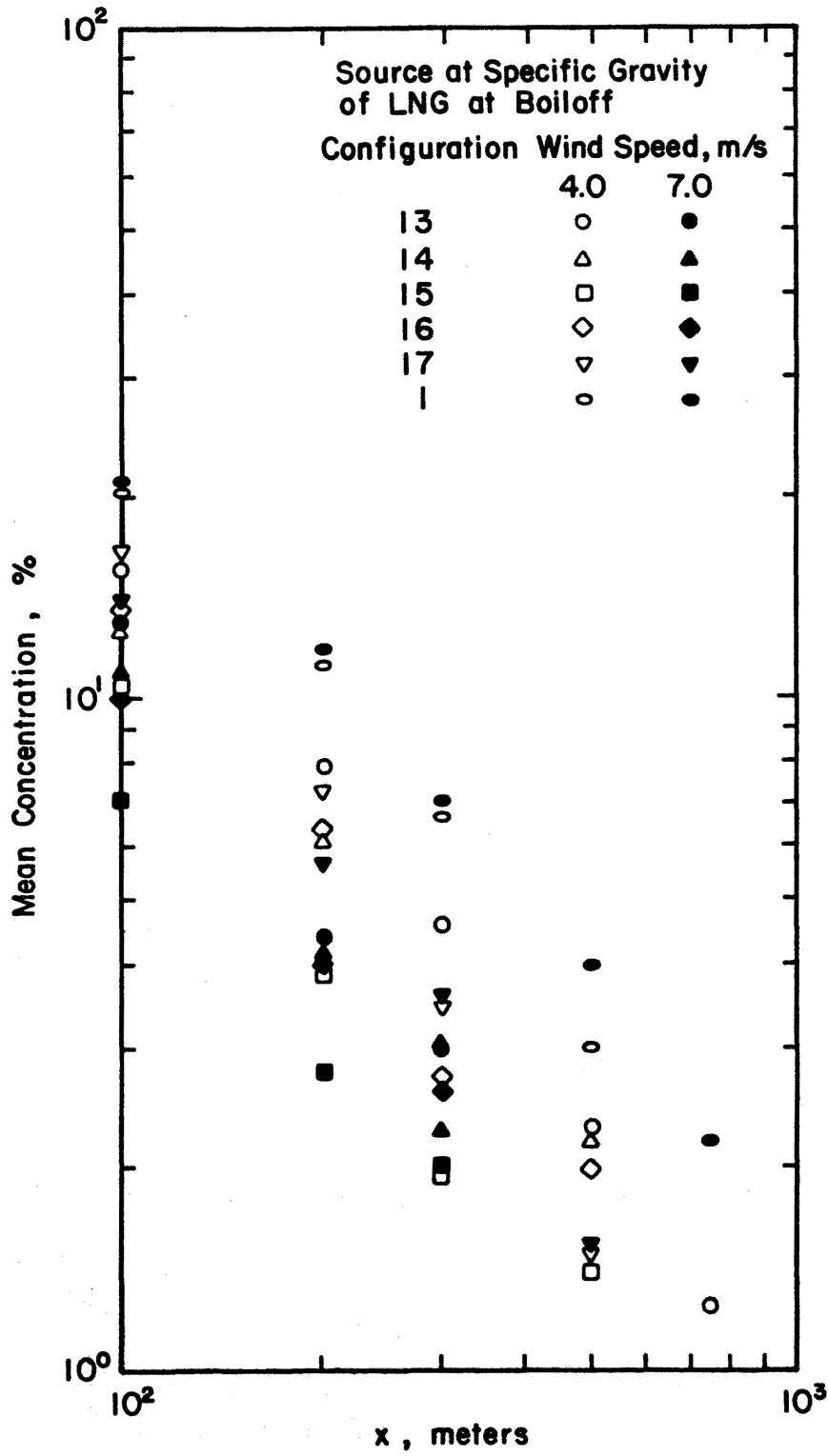
Figure 27. Mean Concentration vs. x (LNG Plume)
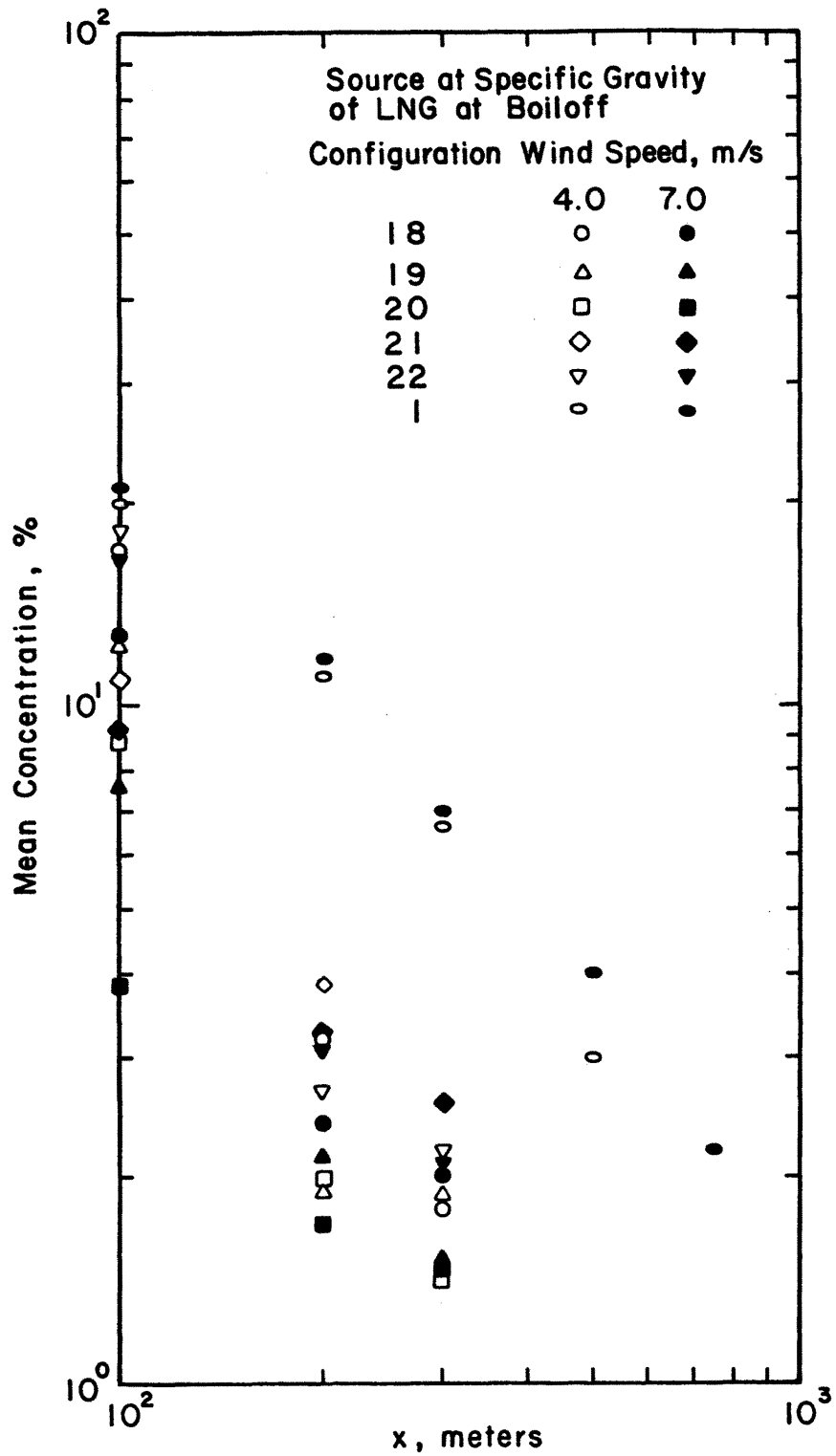
Figure 28. Mean Concentration vs. x (LNG Plume)

obstacle generates excess turbulence intensity in the wake (Kothari et al. [29], Woo et al. [30], Hansen et al. [31], Castro and Robins [32], Counihan [33]) and hence quicker plume dilution. Also in general, the lower wind speed resulted in higher ground-level concentration when the surface obstacle interacts with the plume. However, for the unobstructed case, the higher wind speed gave the maximum concentration. The mean concentration measured with the neutral density plume are about 3 to 5 times smaller in magnitude than those observed with LNG plume. With the cylindrical tank upstream of the spill area, the initial dilution (measured at 100 m downwind) was generally about 2 to 3 times smaller with the LNG plume as compared to the neutral plume data. This emphasizes that even with the excess turbulence generated by the presence of the cylindrical tank, the entrainment of air into the heavier LNG plume was smaller when compared with the neutral plume. Hence, even under the influence of the wake of cylindrical tank, it is important to account for the initial gravity spread of the LNG plume. As expected, with the cylinderical tank upstream and closest to the spill area, the highest plume dilution was observed. Concentration isopleths for selected configurations and both wind speeds are displayed in Figures 29 through 54.

It is evident that, at lower wind speed, plume spread is larger when compared with higher wind speed, and hence results in shorter flammability limit (LFL) distances for the plane area source (Figures 29 and 30). Configurations where the plume is affected by the surface obstacles gave longer LFL distances at the lower wind speed. The measured LNG plume concentration tends to have its maximum off the centerline, in particular, when the surface obstacle is on the
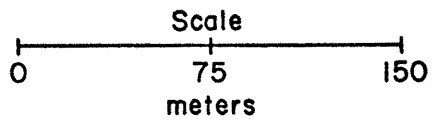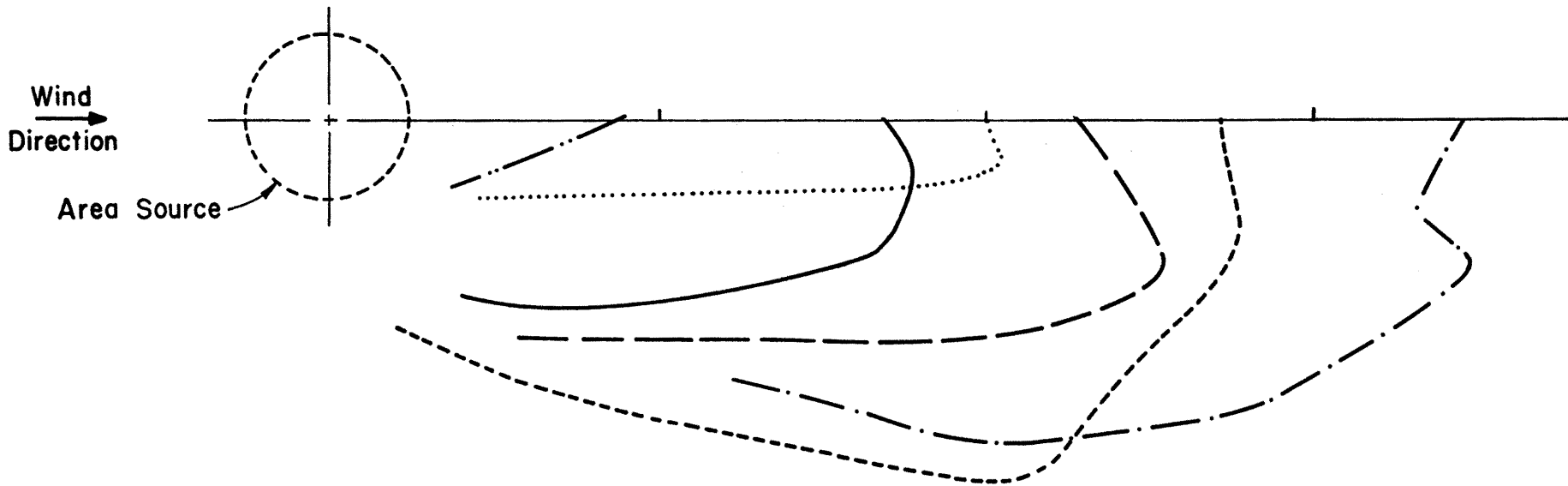
Wind
Direction

Area Source

Scale

0 ———— 75 ———— 150
meters

Configuration I
Wind Speed 4m/sec at 10m Height
Source Gas
Negatively Buoyant   Neutral
CONCENTRATION

————————— 10.0% Peak   — ·· — ·· 5.0% Mean
– – – – – – – 5.0% Peak   ················ 1.0% Mean
— — — — 5.0% Mean
— · — · — · 2.5% Mean

Figure 29. Concentration Isopleths for Configuration 1 and
Wind Speed 4 m/sec

63

Configuration I
Wind Speed 7m/sec at IOm Height
Source Gas
Negatively Buoyant   Neutral
CONCENTRATION
——————————10.0% Peak   ——··——··— 5.0% Mean
———————— 5.0% Peak   ················· 1.0% Mean
— — — — 5.0% Mean
—·——·——·— 2.5% Mean

Scale
0   75   150
meters
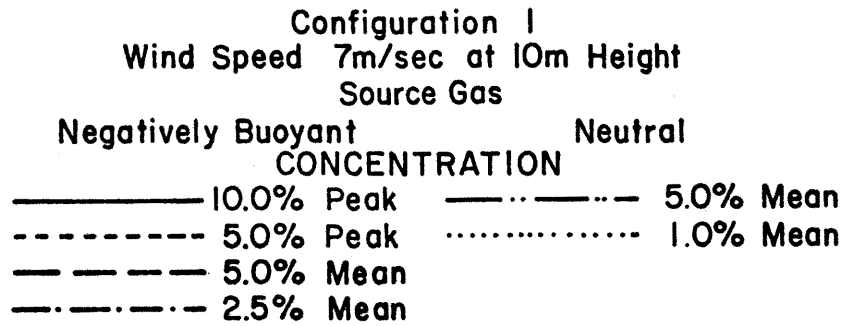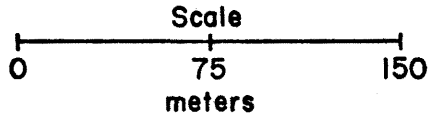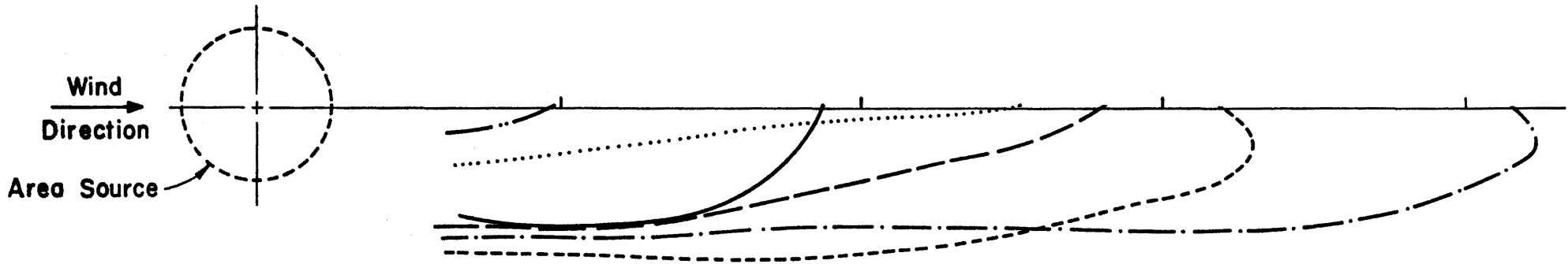
Figure 30. Concentration Isopleths for Configuration 1 and
Wind Speed 7 m/sec

Wind Direction →

Area Source

Cylindrical Tank

65

Configuration 4
Wind Speed 4m/sec at 10m Height
Source Gas

Negatively Buoyant   Neutral
CONCENTRATION

————————— 10.0% Peak   ——··——··—— 2.5% Mean
— — — — — — — 5.0% Peak   ·················· 1.0% Mean
— — — — — — 5.0% Mean
——·——·——·— 2.5% Mean

Scale

0   75   150

meters
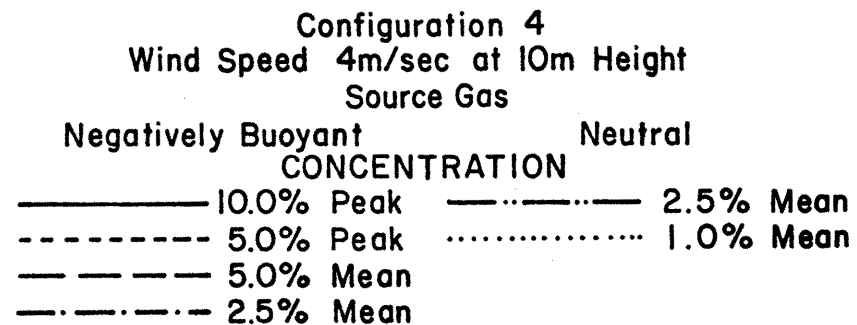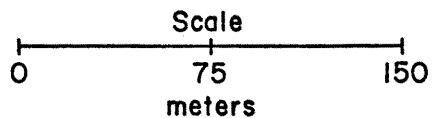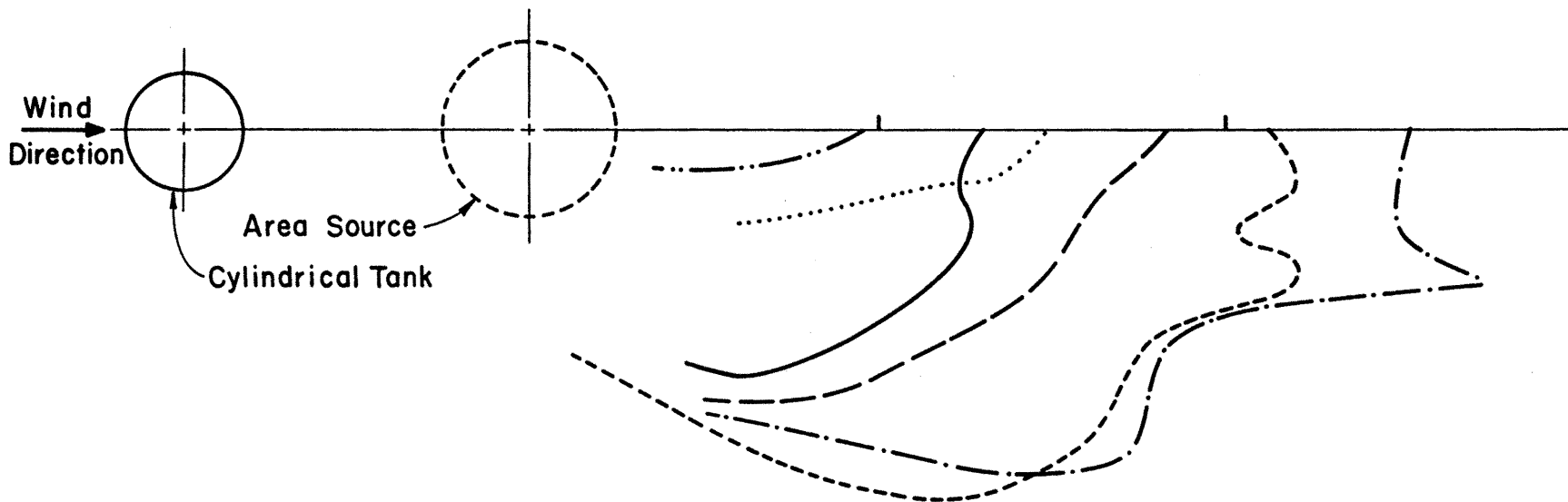
Figure 31.   Concentration Isopleths for Configuration 4 and
Wind Speed 4 m/sec

Wind
Direction

Area Source

Cylindrical Tank

Scale

0   75   150
      meters

Configuration 4
Wind Speed 7m/sec at 10m Height
Source Gas

Negatively Buoyant   Neutral
              CONCENTRATION
——————— 10.0% Peak   —··—··— 1.0% Mean
————————— 5.0% Peak   ·············· 0.5% Mean
— — — — 5.0% Mean
—·—·—·— 2.5% Mean
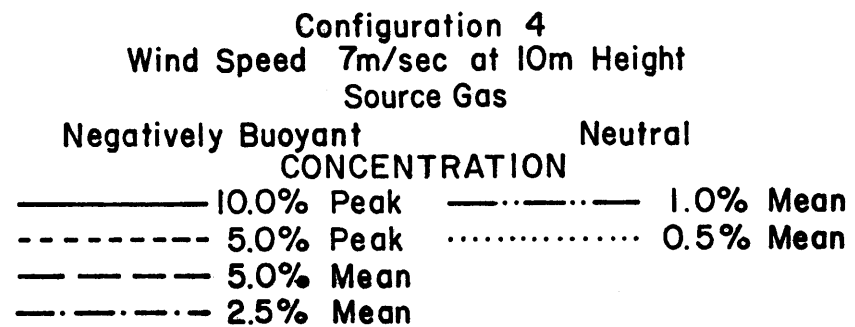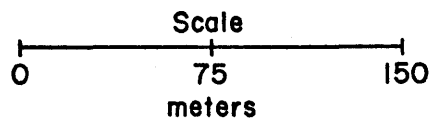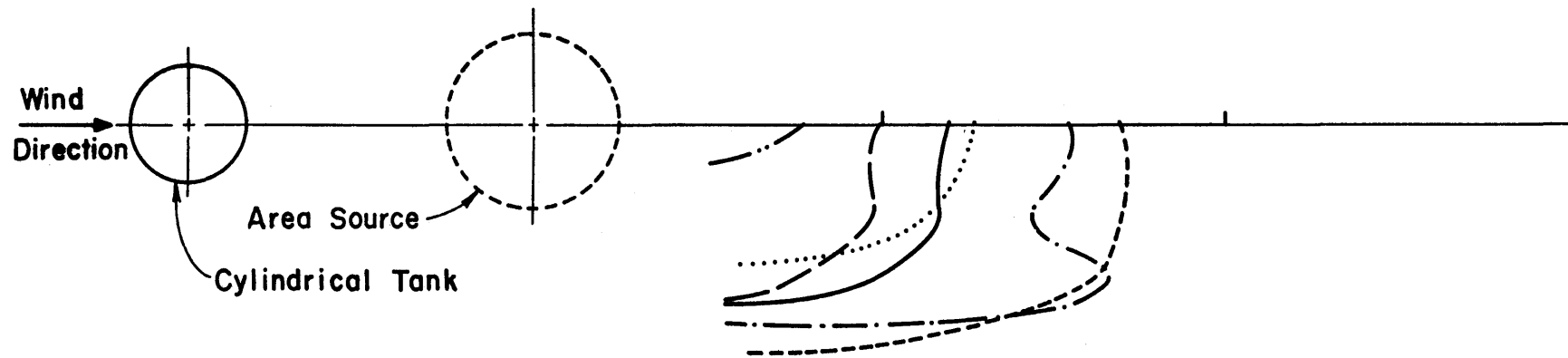
Figure 32. Concentration Isopleths for Configuration 4 and
Wind Speed 7 m/sec
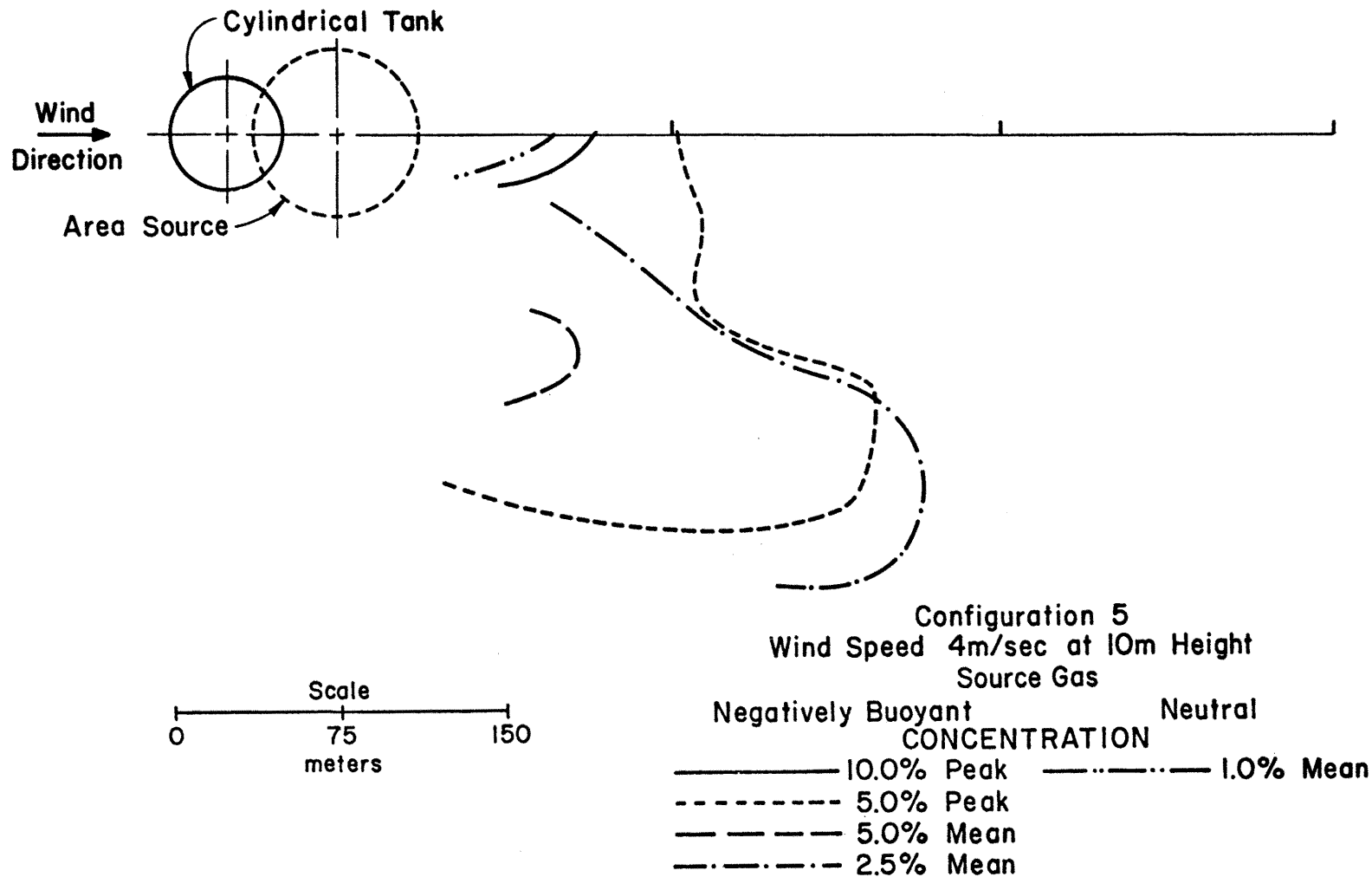
Figure 33. Concentration Isopleths for Configuration 5 and
Wind Speed 4 m/sec

Wind
Direction

Cylindrical Tank

Area Source

Scale

0   75   150

meters

Configuration 5
Wind Speed 7m/sec at 10m Height
Source Gas

Negatively Buoyant   Neutral
CONCENTRATION

————————10.0% Peak   ——··——··—— 0.5% Mean

- - - - - - - - 5.0% Peak

— — — — 2.5% Mean
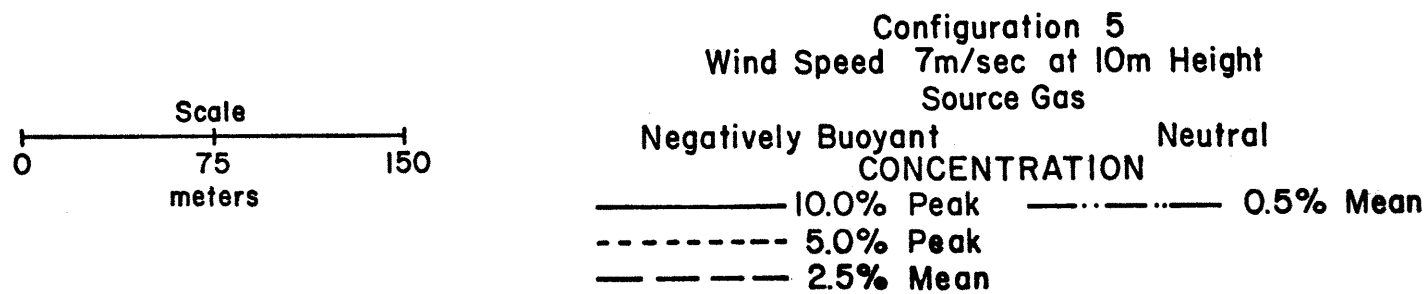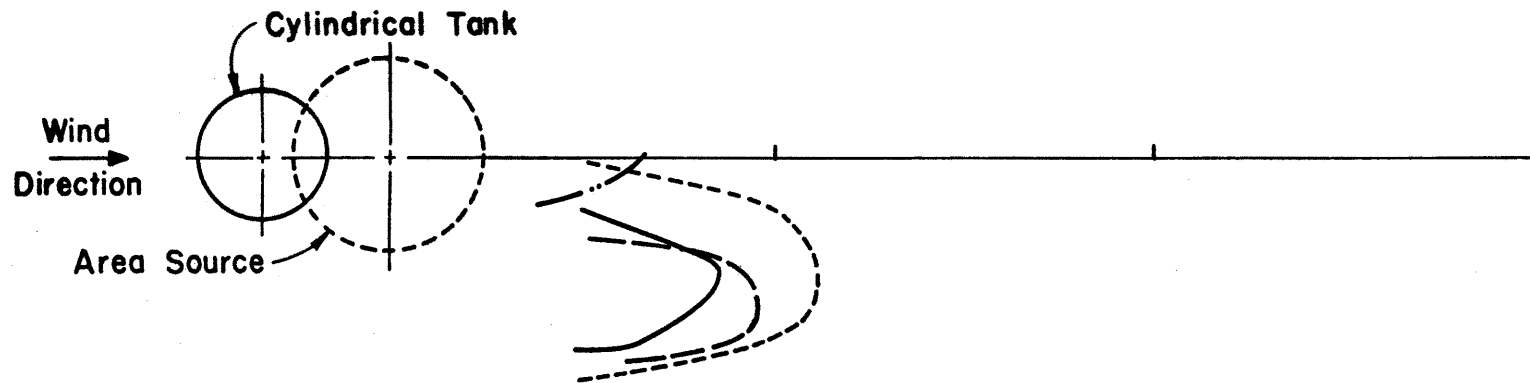
Figure 34. Concentration Isopleths for Configuration 5 and
Wind Speed 7 m/sec

Wind Direction →

Cylindrical Tank

Area Source

Scale

0   75   150
        meters

Configuration 6
Wind Speed 4m/sec at 10m Height
Source Gas
Negatively Buoyant   Neutral
                CONCENTRATION
————————— 10.0% Peak   —··——··— 0.5% Mean
- - - - - - - 5.0% Peak
— — — — 5.0% Mean
—·—·—·— 2.5% Mean
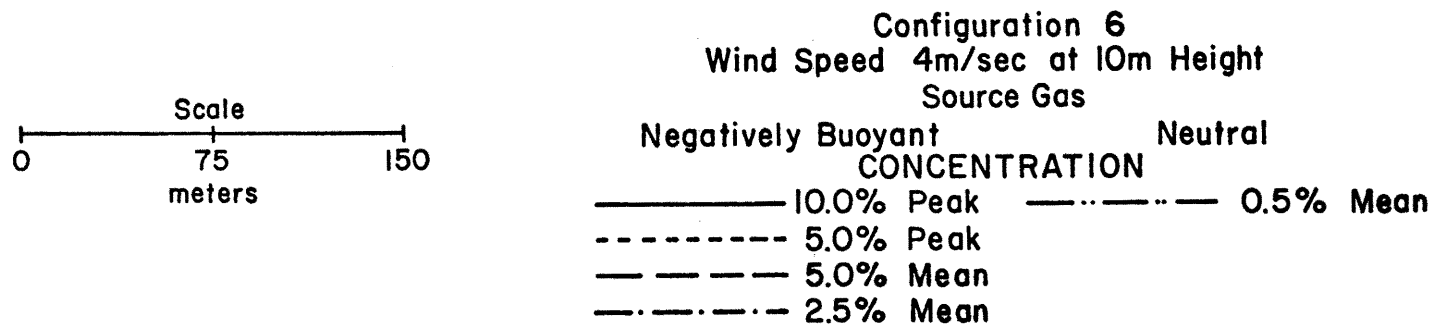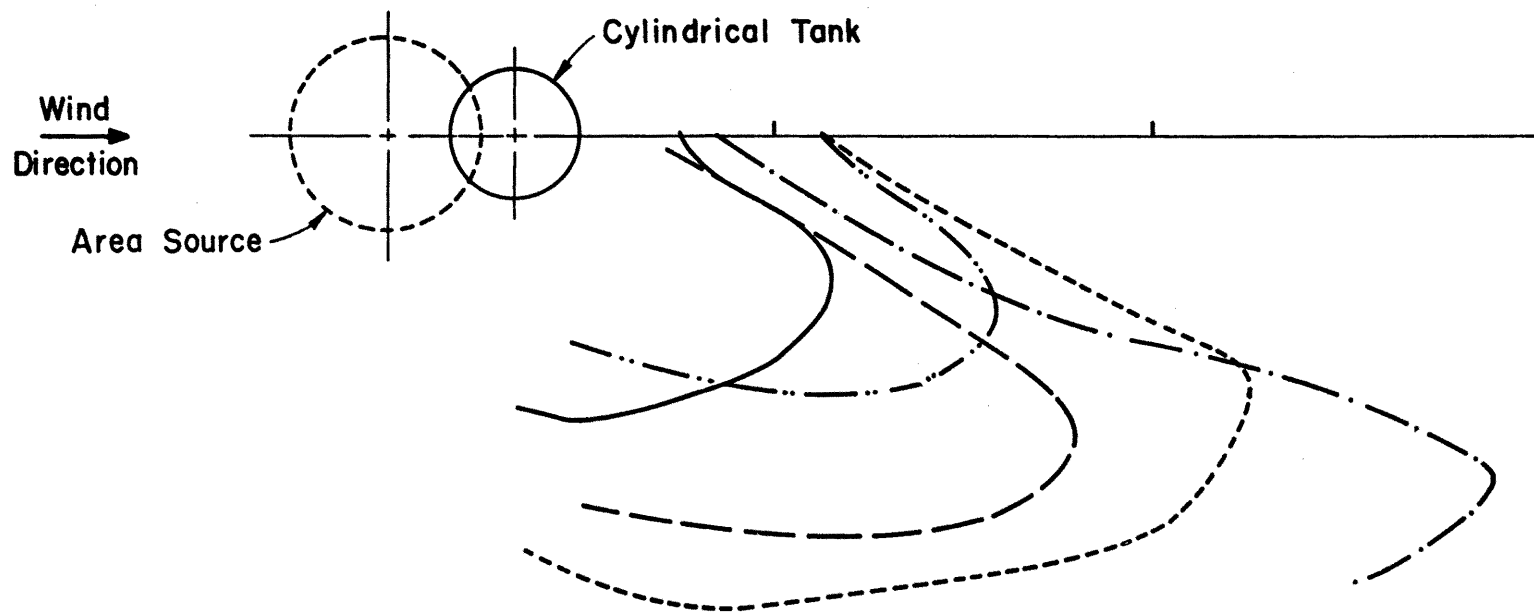
Figure 35.   Concentration Isopleths for Configuration 6 and
             Wind Speed 4/sec
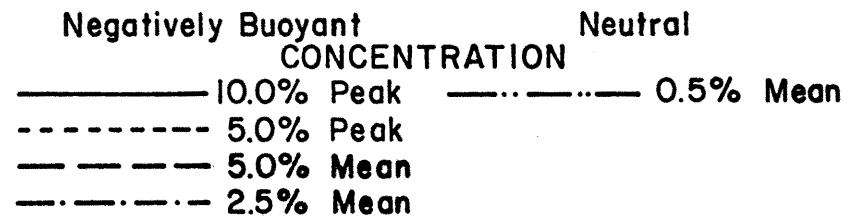
Figure 36. Concentration Isopleths for Configuration 6 and Wind Speed 7 m/sec

Wind Direction →

Cylindrical Tank

Area Source
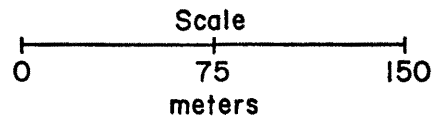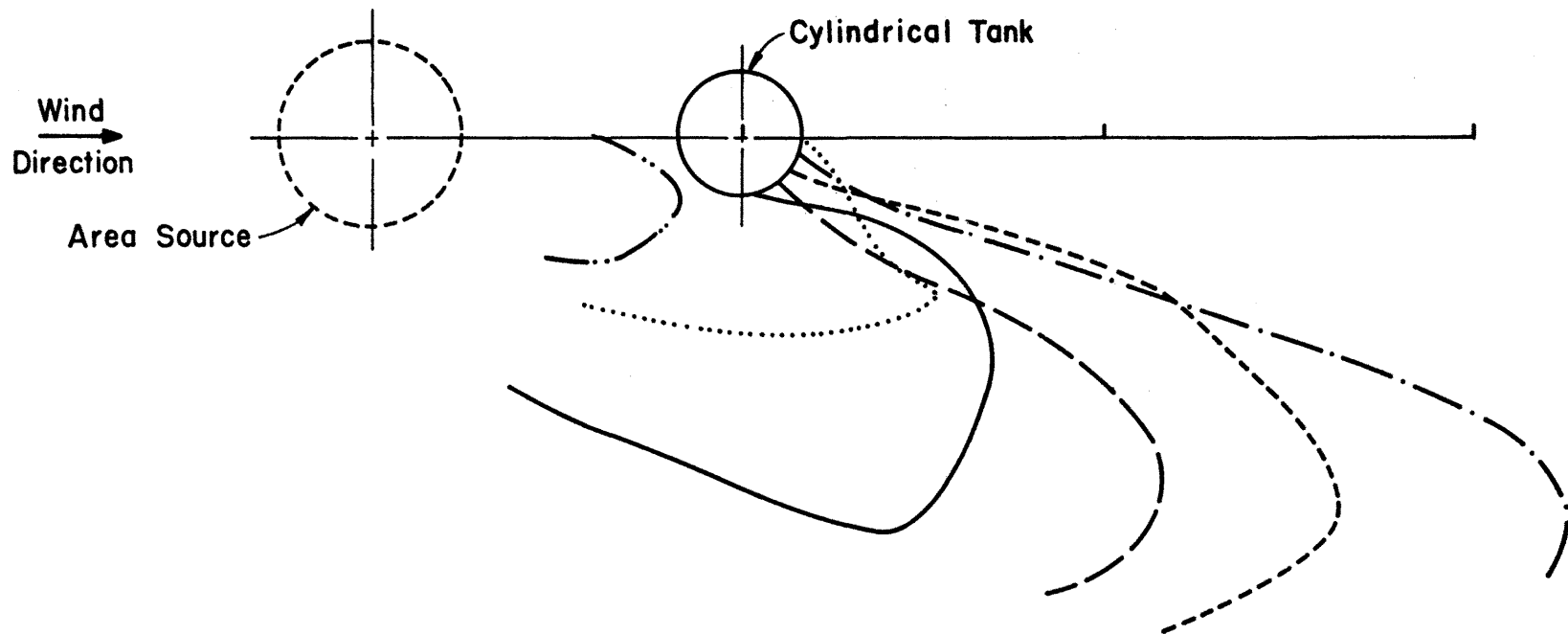
Configuration 7
Wind Speed 4m/sec at 10m Height
Source Gas

Negatively Buoyant   Neutral
CONCENTRATION

————————— 10.0% Peak   — ··— ··— 5.0% Mean

— — — — — — 5.0% Peak   ················ 1.0% Mean

— — — — 5.0% Mean

—·—·—··— 2.5% Mean

Scale

0   75   150
        meters

Figure 37.   Concentration Isopleths for Configuration 7 and
             Wind Speed 4 m/sec

71

Wind Direction

Area Source

Cylindrical Tank

Configuration 7
Wind Speed 7m/sec at 10m Height
Source Gas

Scale

0   75   150
meters

Negatively Buoyant   Neutral
CONCENTRATION

——————— 10.0% Peak   ——··—··— 1.0% Mean
- - - - - - - - - 5.0% Peak
— — — — 5.0% Mean
—·—·—·— 2.5% Mean
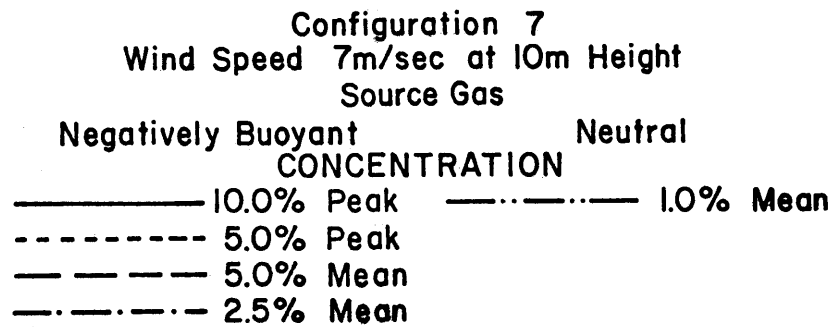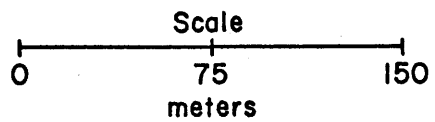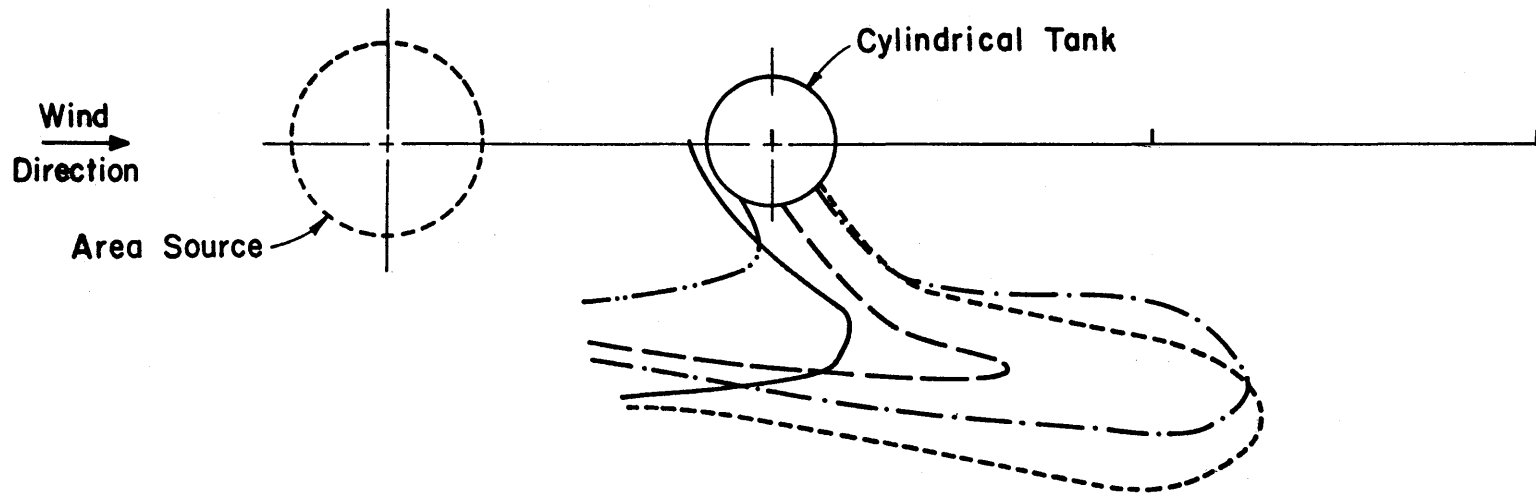
Figure 38.   Concentration Isopleths for Configuration 7 and
Wind Speed 7 m/sec

Figure 39. Concentration Isopleths for Configuration 10 and
Wind Speed 4 m/sec

Wind Direction →

Cylindrical Tank

Area Source

Scale

0   75   150

meters
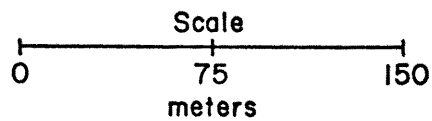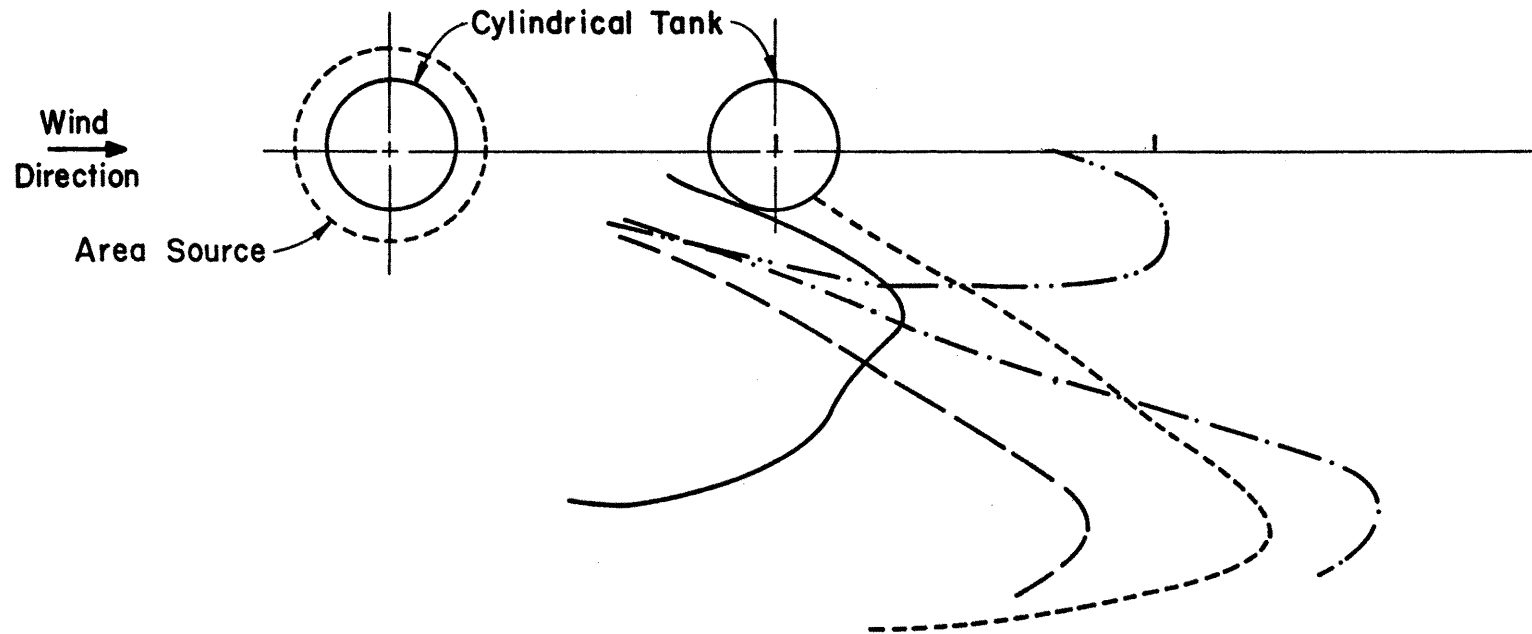
Configuration 10
Wind Speed 7m/sec at 10m Height
Source Gas

Negatively Buoyant   Neutral
CONCENTRATION

—————— 10.0% Peak   —··——··—— 0.5% Mean

– – – – – – – 5.0% Peak

— — — — 5.0% Mean

—·—·—·— 2.5% Mean
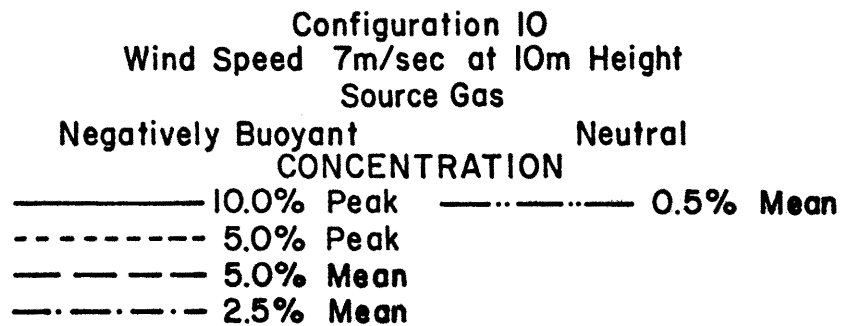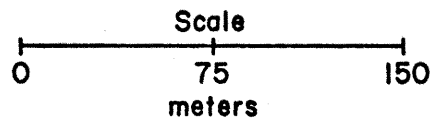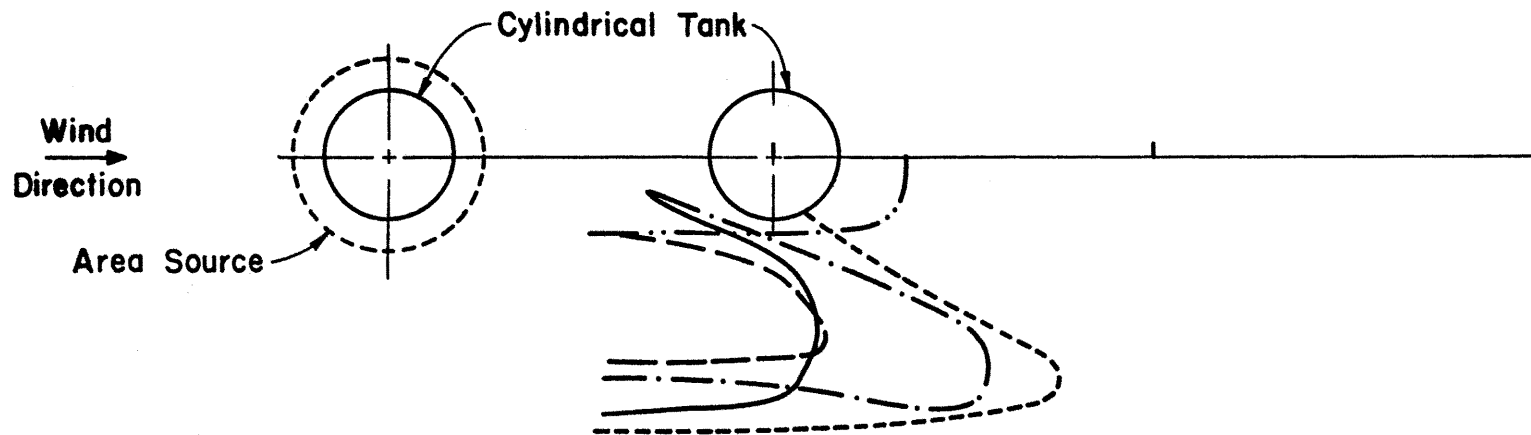
Figure 40. Concentration Isopleths for Configuration 10 and
Wind Speed 7 m/sec
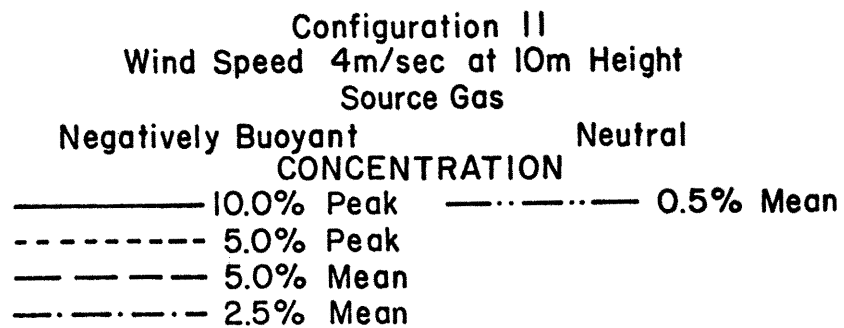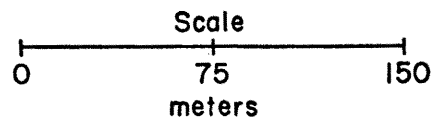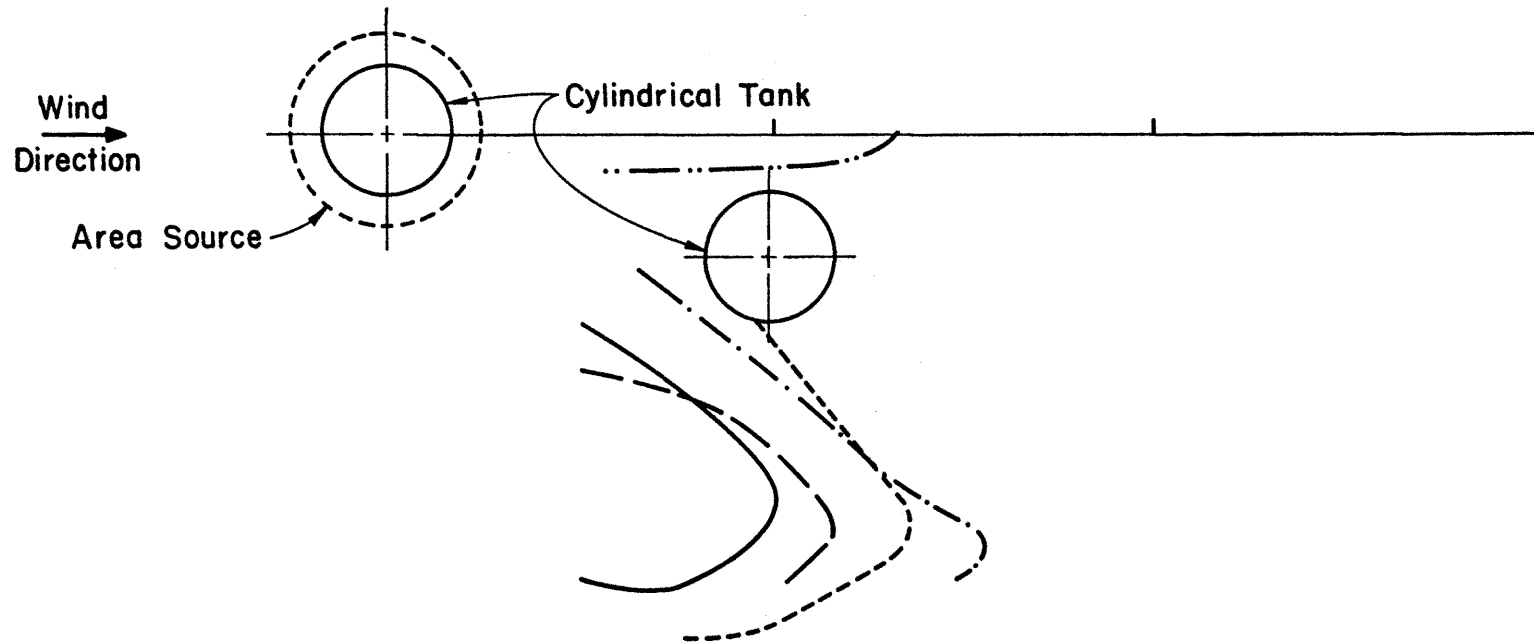
Figure 41. Concentration Isopleths for Configuration 11 and Wind Speed 4/sec

Wind
Direction →

Area Source

Cylindrical Tank

Scale

0   75   150

meters

Configuration II
Wind Speed 7m/sec at 10m Height
Source Gas

Negatively Buoyant   Neutral
CONCENTRATION

——————— 10.0% Peak   — ··— ··— 0.5% Mean

- - - - - - - - 5.0% Peak

— — — — 2.5% Mean
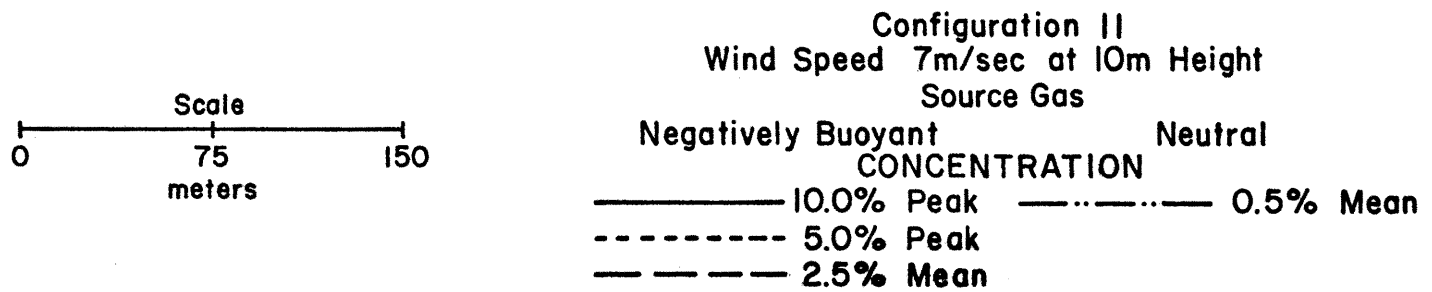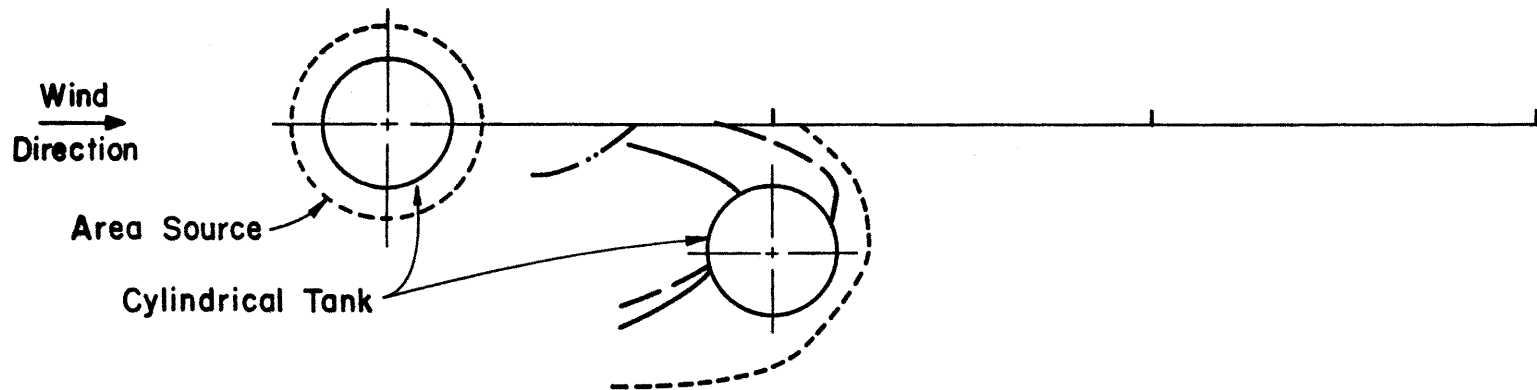
Figure 42.   Concentration Isopleths for Configuration 11 and
Wind Spped 7 m/sec

Configuration 14
Wind Speed 4m/sec at 10m Height
Source Gas

Negatively Buoyant   Neutral
                   CONCENTRATION
————————10.0% Peak   —— ·· —— ·· —— 0.5% Mean
---------- 5.0% Peak
—— —— —— 5.0% Mean
—— · —— · —— · 2.5% Mean

Scale

0   75   150
          meters
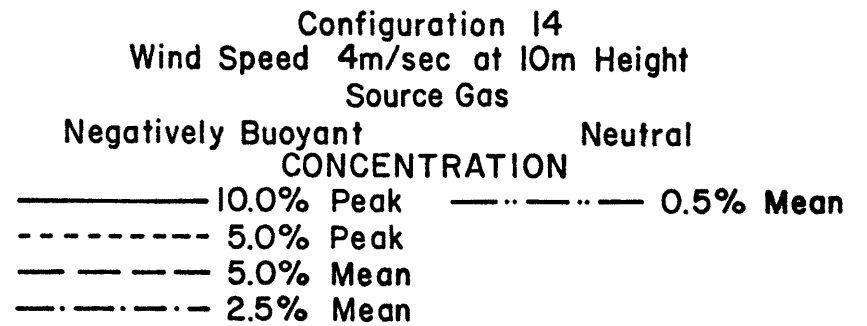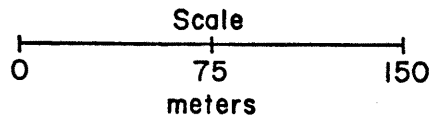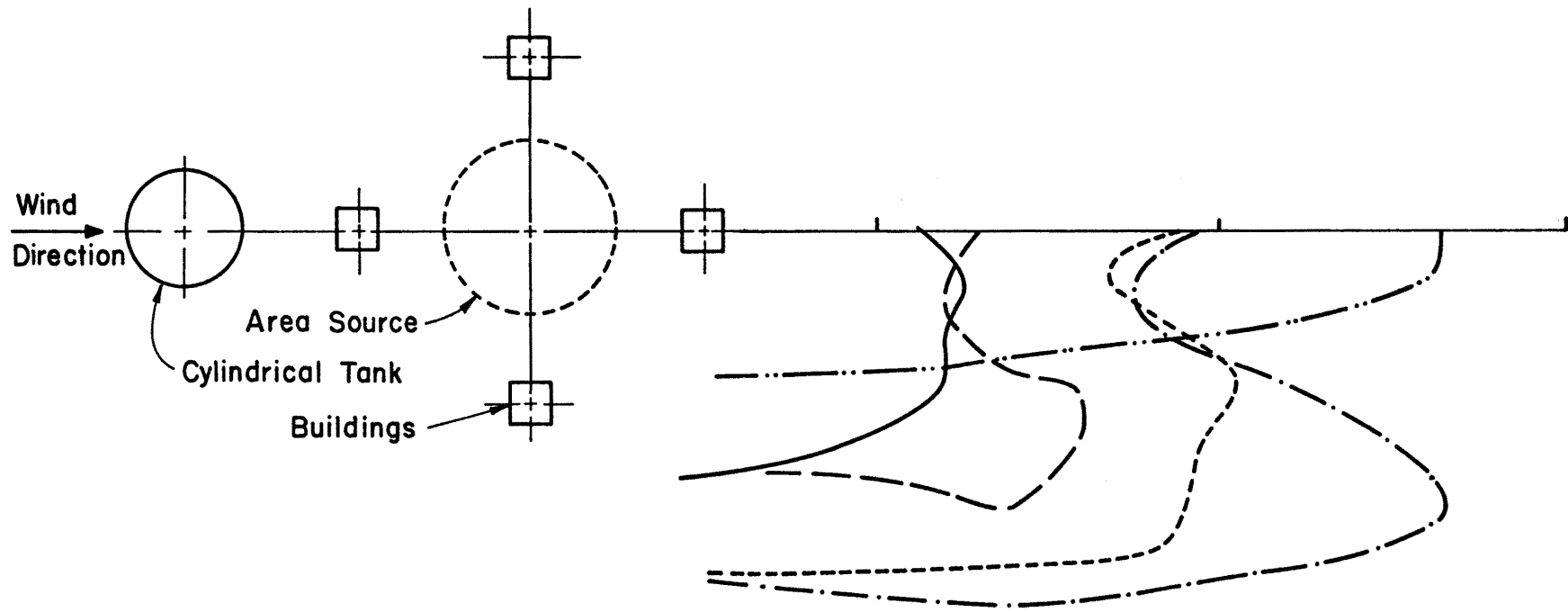
Figure 43.   Concentration Isopleths for Configuration 14 and
             Wind Speed 4 m/sec
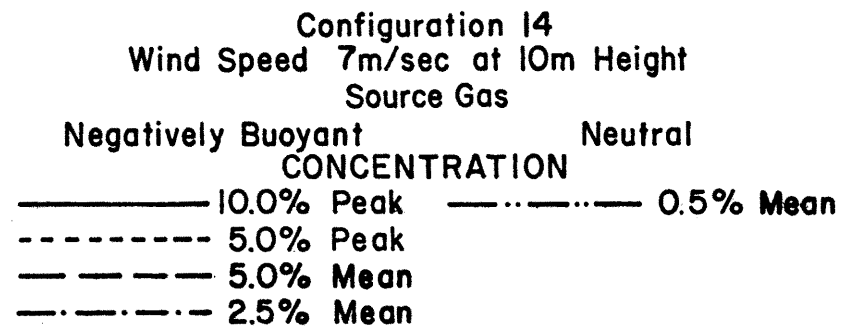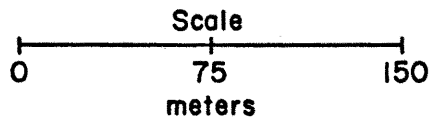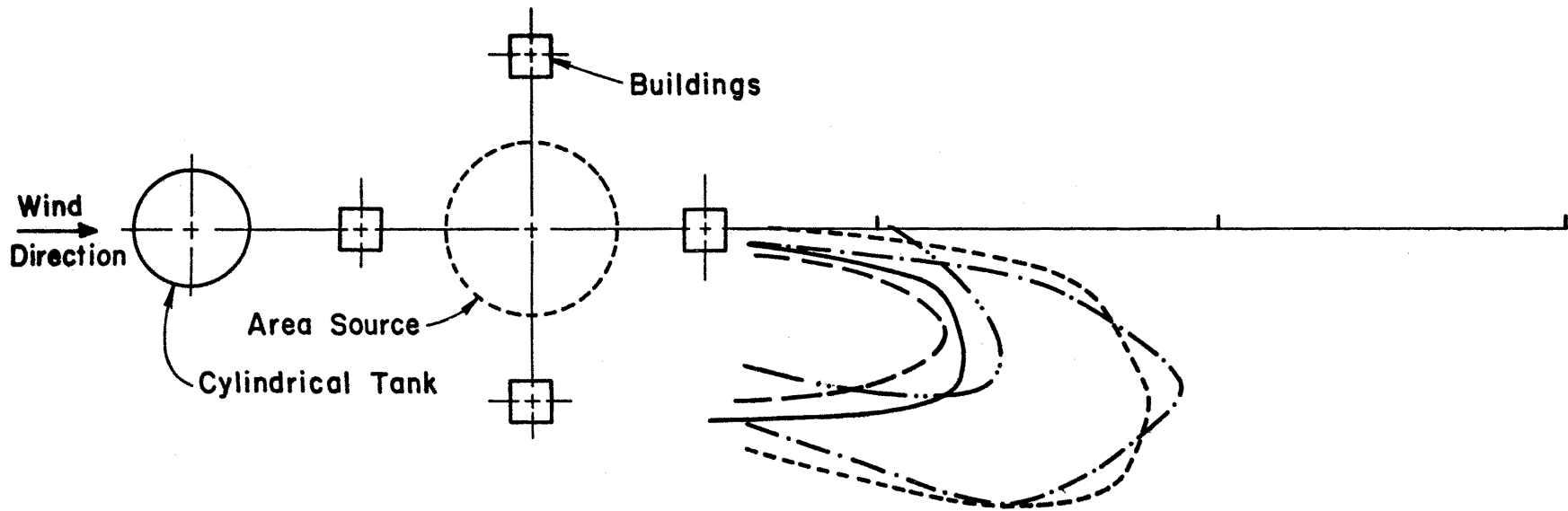
Figure 44. Concentration Isopleths for Configuration 14 and Wind Speed 7 m/sec

Wind Direction →

Cylindrical Tank

Area Source

Buildings

Scale

0   75   150

meters
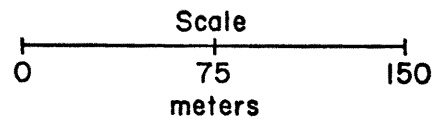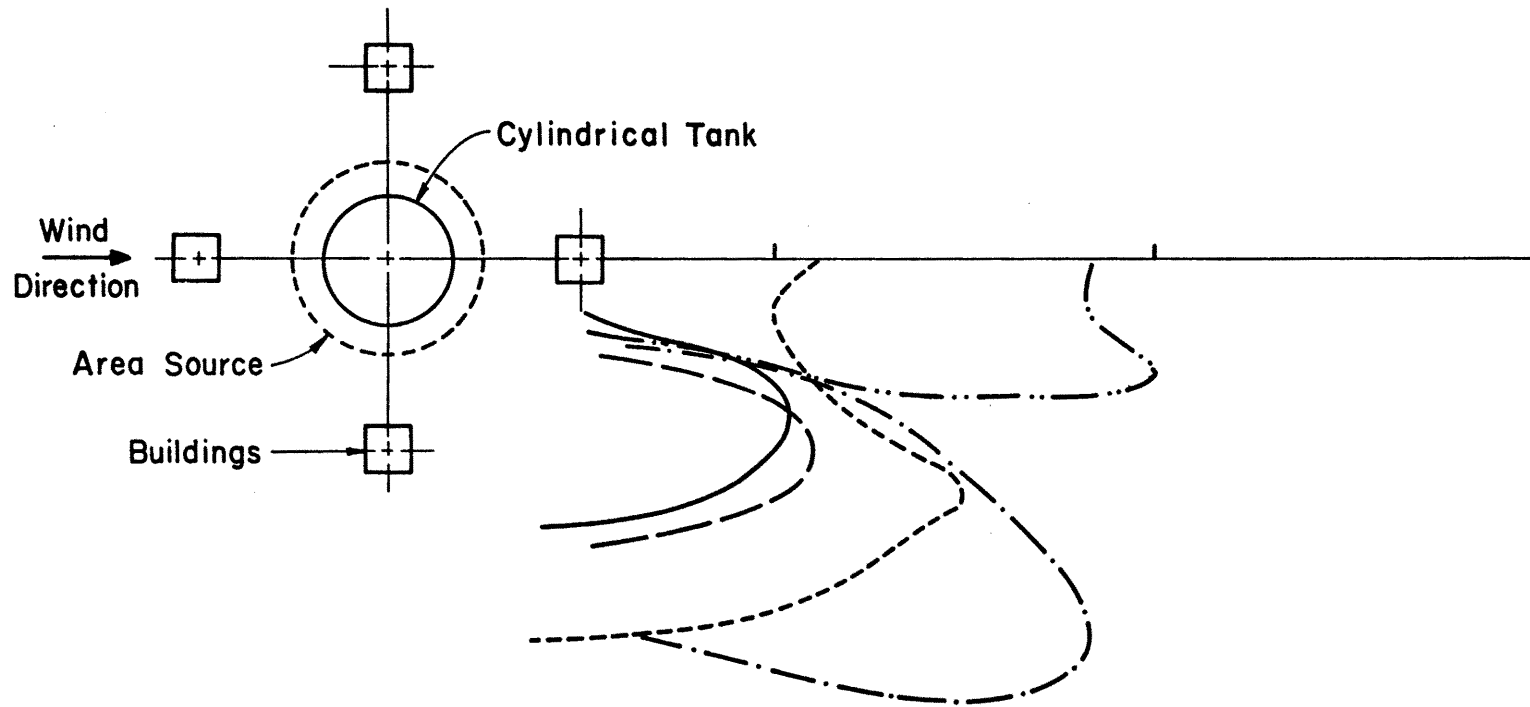
Configuration 15
Wind Speed 4m/sec at 10m Height
Source Gas

Negatively Buoyant   Neutral
CONCENTRATION

—————— 10.0% Peak   —··—··— 0.5% Mean

--------- 5.0% Peak

— — — — 5.0% Mean

—·—··—·— 2.5% Mean
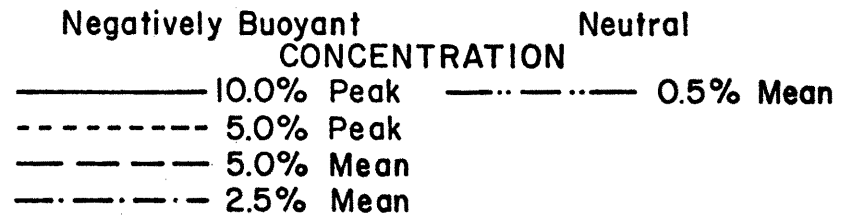
Figure 45.   Concentration Isopleths for Configuration 15 and
             Wind Speed 4 m/sec
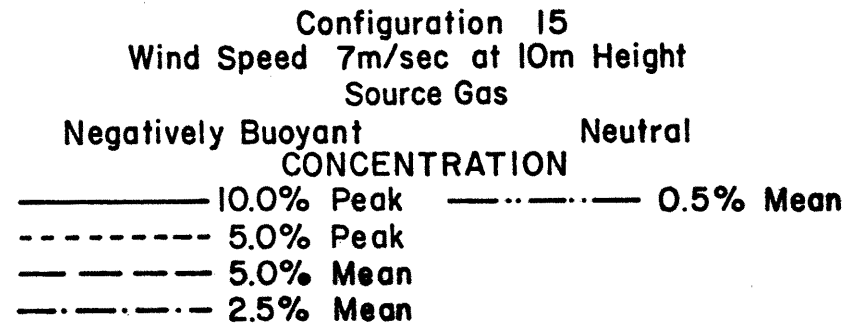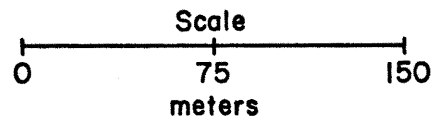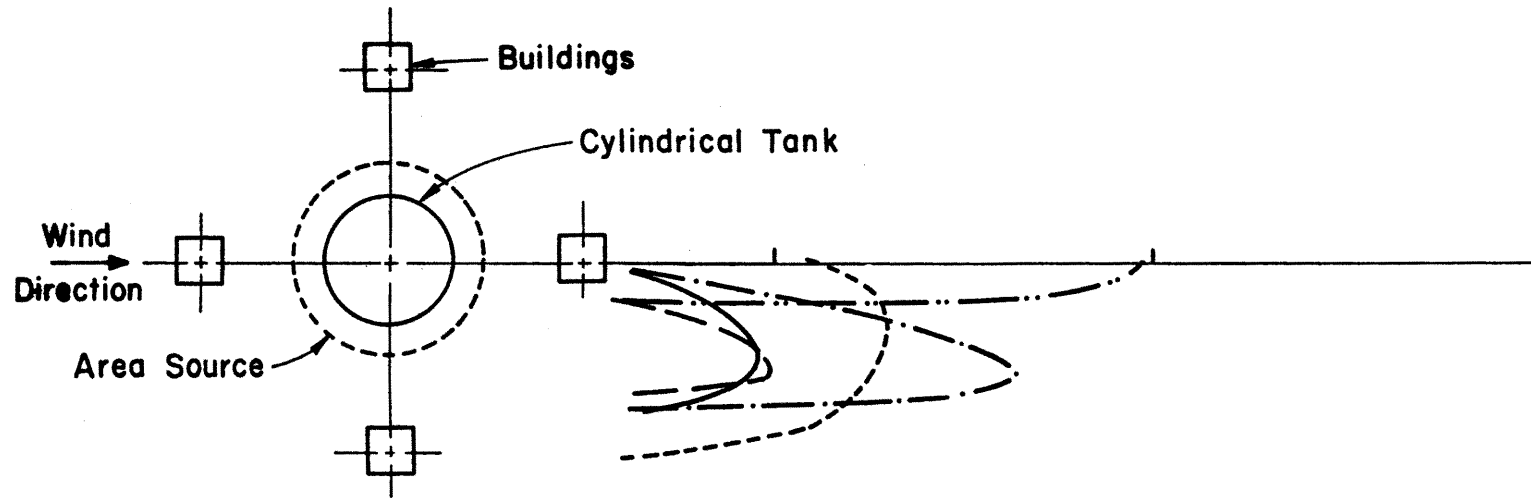
Figure 46. Concentration Isopleths for Configuration 15 and Wind Speed 7 m/sec
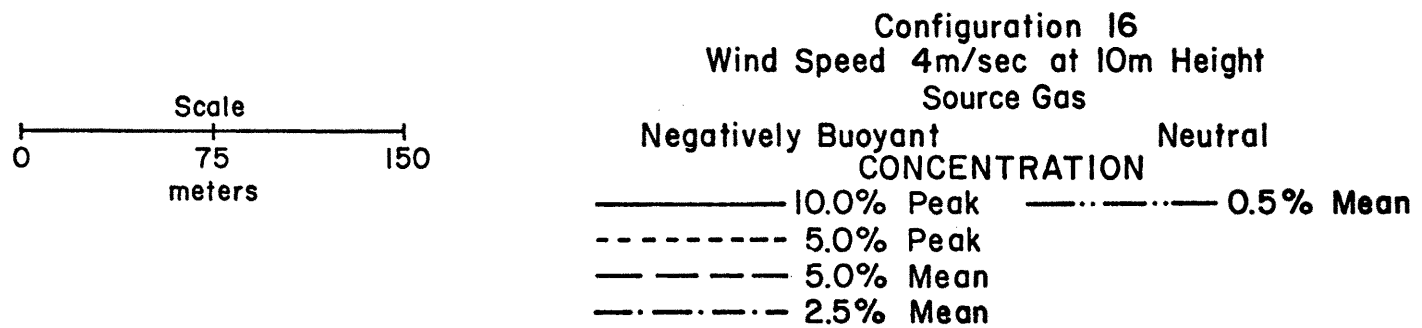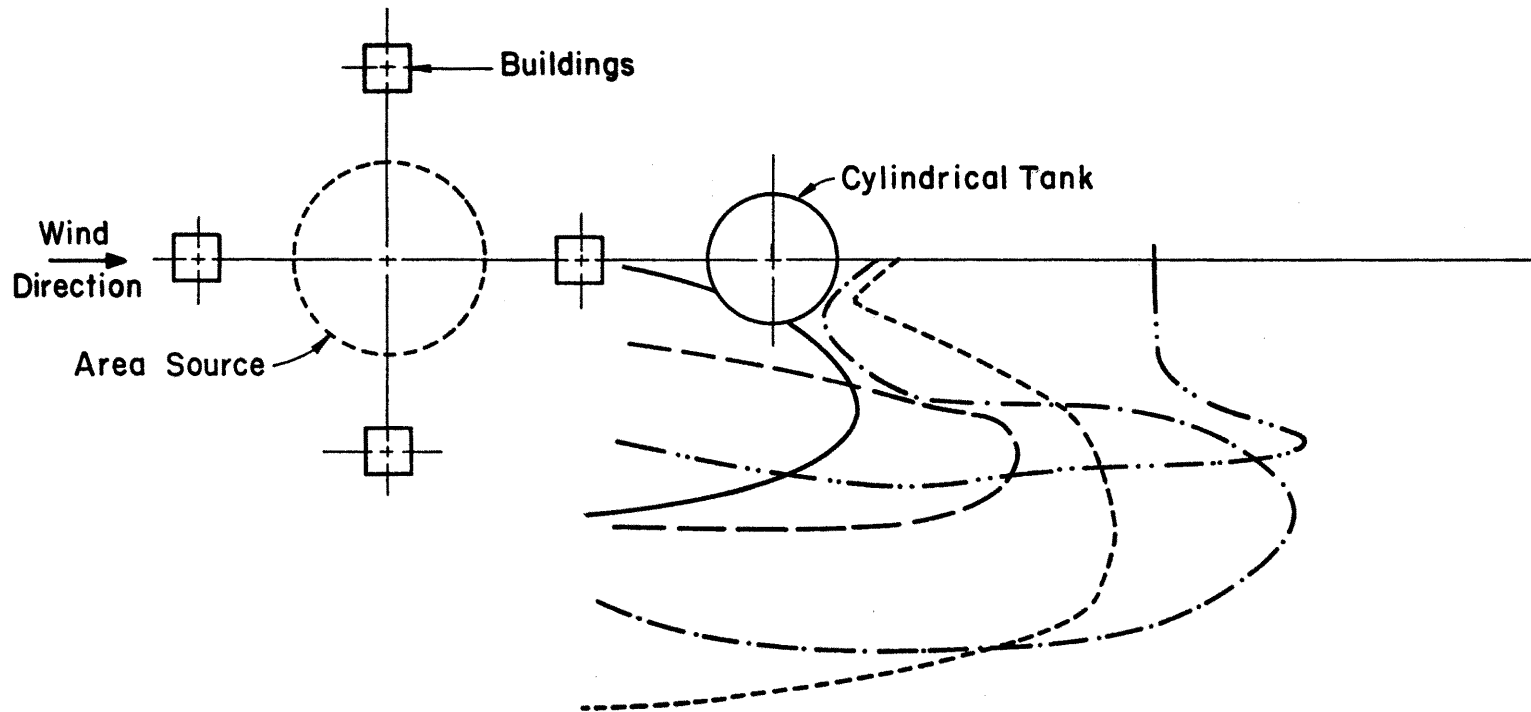
Figure 47. Concentration Isopleths for Configuration 16 and Wind Speed 4 m/sec

Wind
Direction →

Buildings

Cylindrical Tank

Area Source

Scale

0	75	150

meters

Configuration 16
Wind Speed 7m/sec at 10m Height
Source Gas

Negatively Buoyant   Neutral
CONCENTRATION

——————— 10.0% Peak   ——··—··— 0.5% Mean
---------- 5.0% Peak
—— —— —— 5.0% Mean
—·—·—·— 2.5% Mean
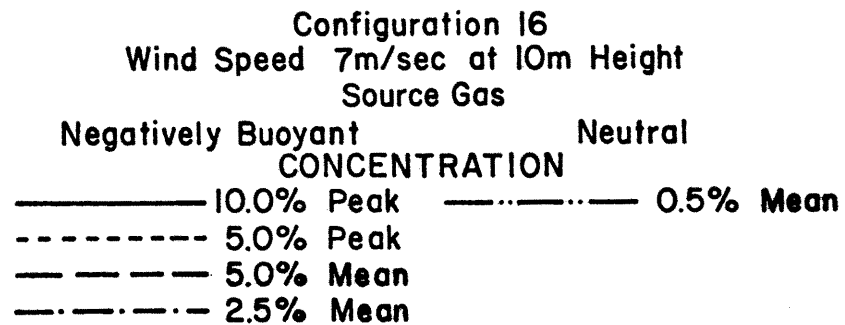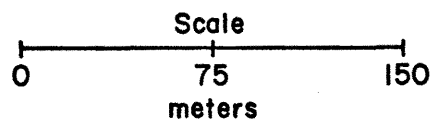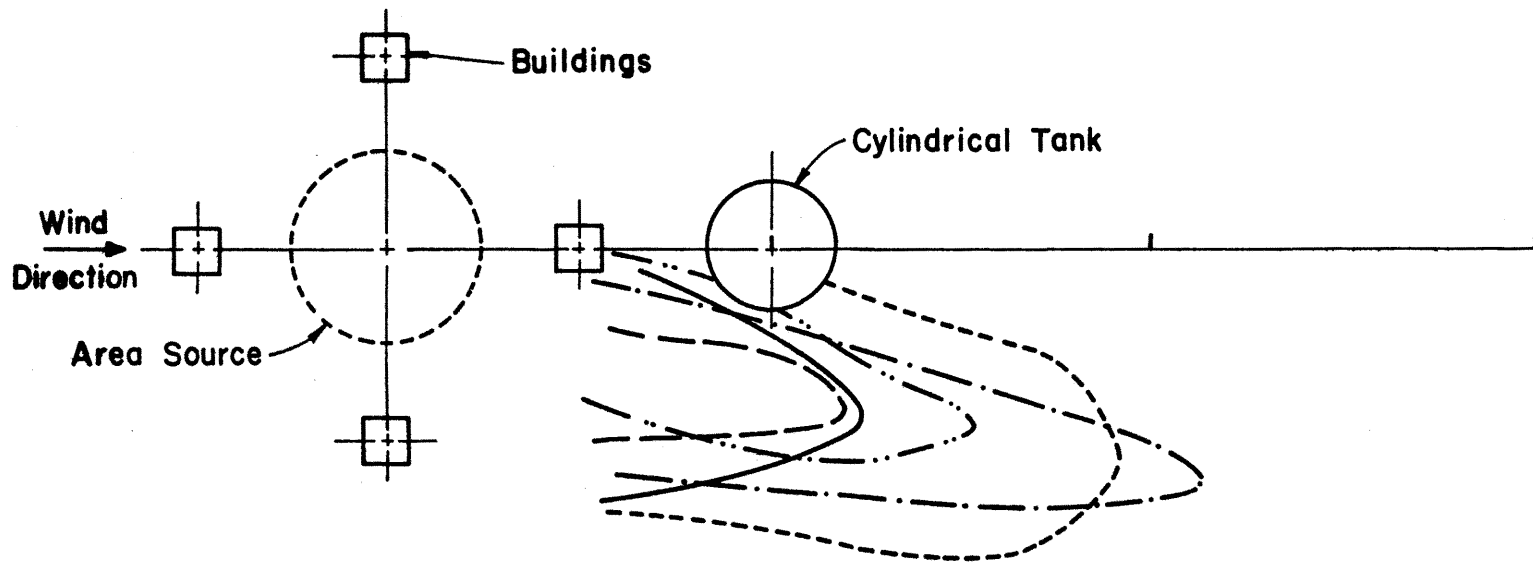
Figure 48. Concentration Isopleths for Configuration 16 and
Wind Speed 7 m/sec
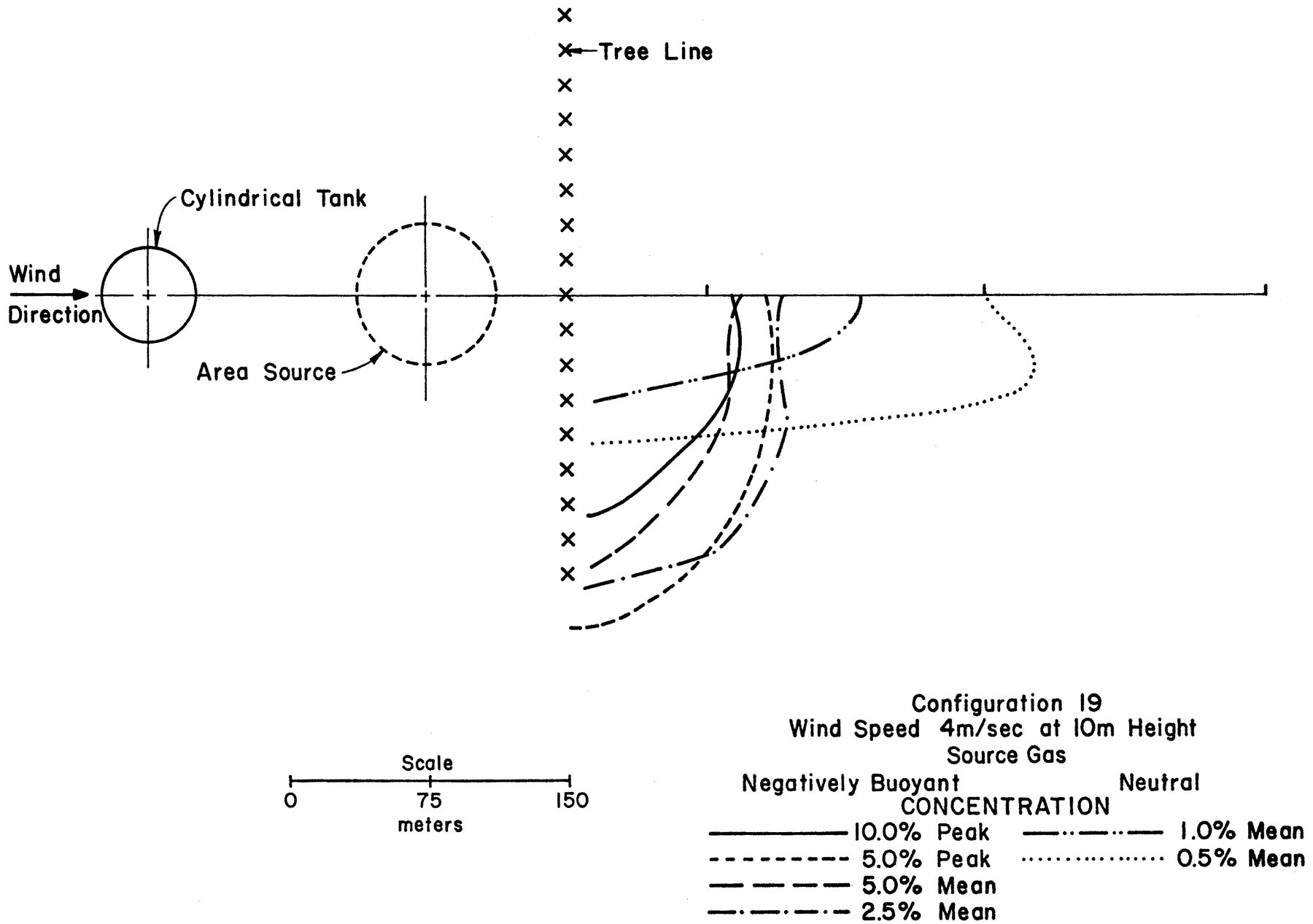
Figure 49.   Concentration Isopleths for Configuration 19 and
Wind Speed 4 m/sec
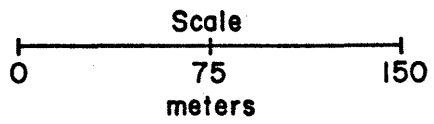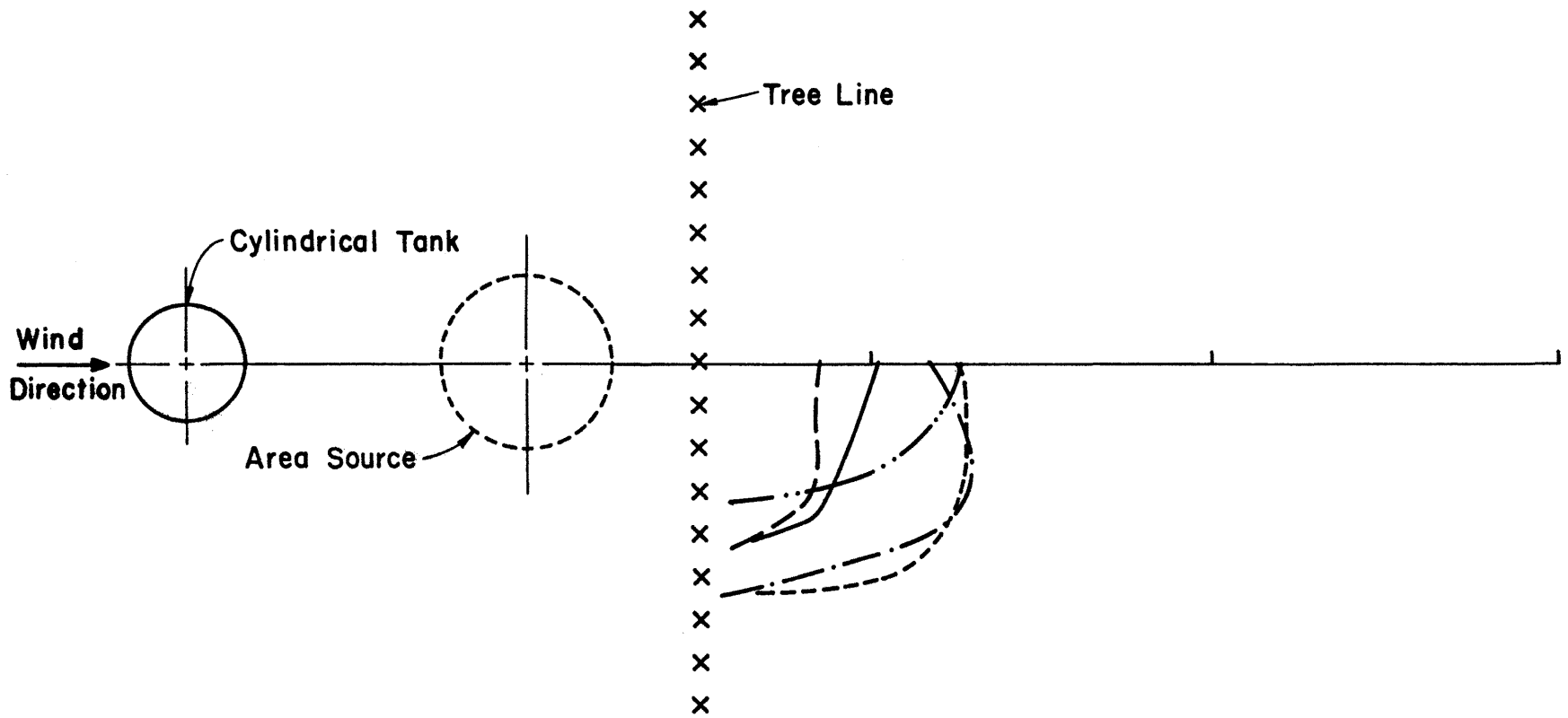
Figure 50. Concentration Isopleths for Configuration 19 and Wind Speed 7 m/sec

×

×

× ←——Tree Line

×

×

Cylindrical Tank

Wind Direction →

Area Source

Scale

0   75   150

meters
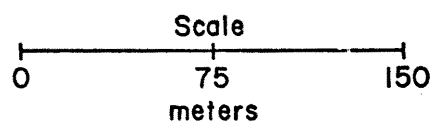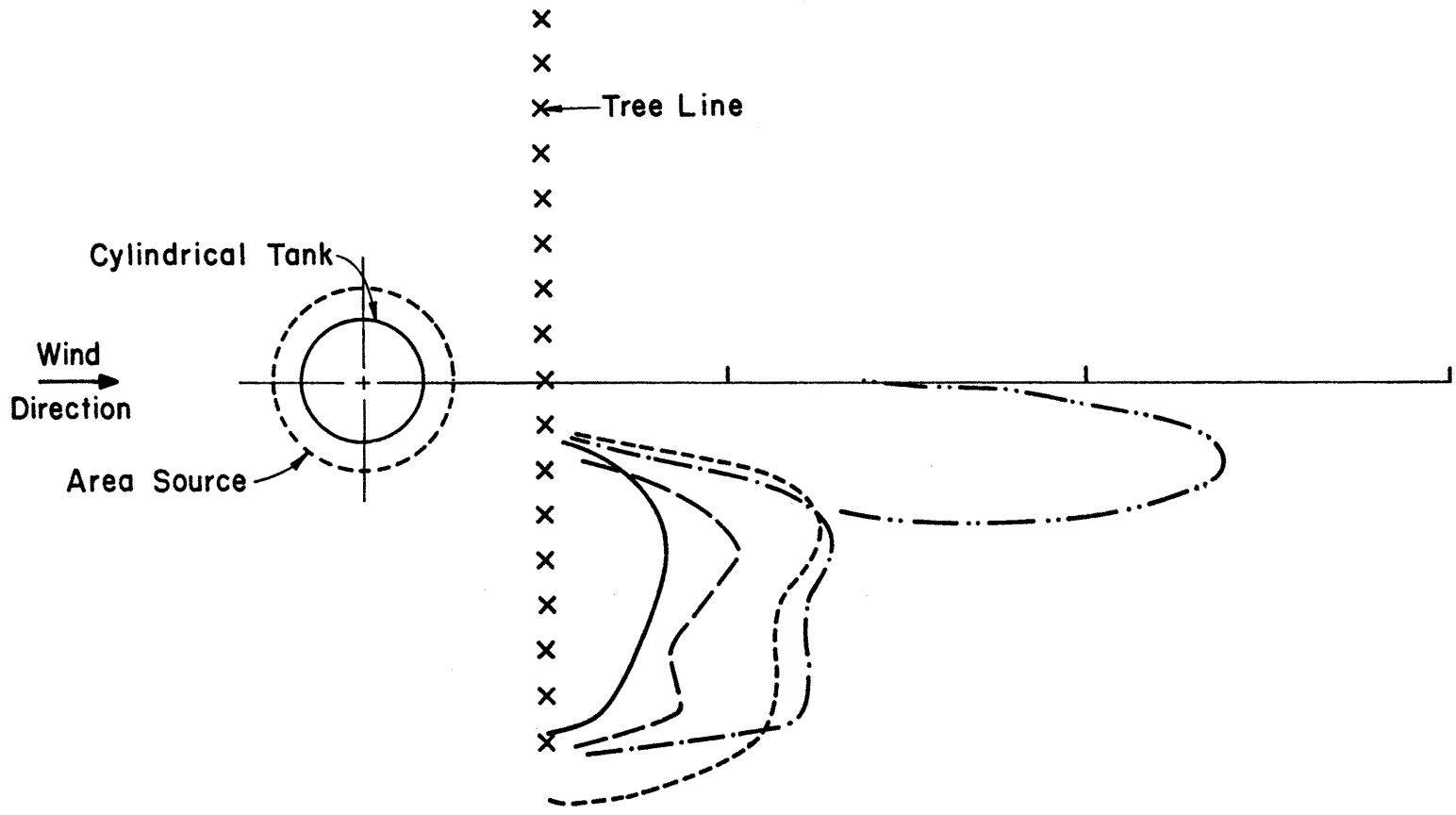
Configuration 20
Wind Speed 4m/sec at 10m Height
Source Gas

Negatively Buoyant   Neutral
CONCENTRATION

———————10.0% Peak   —··——··—— 0.5% Mean

- - - - - - 5.0% Peak

— — — — 5.0% Mean

—·——·——·— 2.5% Mean

Figure 51.   Concentration Isopleths for Configuration 20 and
Wind Speed 4 m/sec

Figure 52.   Concentration Isopleths for Configuration 20 and
Wind Speed 7 m/sec

× ×—Tree Line

Cylindrical Tank

Wind Direction

Area Source

87

Configuration 21
Wind Speed 4m/sec at 10m Height
Source Gas

Negatively Buoyant   Neutral
CONCENTRATION

Scale

|————|————|————|————|
0   75   150
meters

———————————10.0% Peak   —··—··— 1.0% Mean
— — — — — — 5.0% Peak   ·············· 0.5% Mean
— — — — 5.0% Mean
—·—·—··— 2.5% Mean

Figure 53. Concentration Isopleths for Configuration 21 and
Wind Speed 4 m/sec

Figure 54. Concentration Isopleths for Configuration 21 and
Wind Speed 7 m/sec

downstream side of the spill area (Figures 33 to 42). This could be attributed to the following:

1. Higher turbulence intensity in the wake of the tank results in higher entrainment and correspondingly lower concentration in the wake region,

2. The experimental measurements of cylindrical obstacle wake of Kothari et al. [34] indicate the presence of horseshoe surface vortices with their axis in the longitudinal direction on either sides of a cylindrical obstacle. These horseshoe vortices deflect the lower concentration air downward from the top of the turbulent boundary layer along the centerline of the obstacle and results in lower surface concentrations, or

3. The plume is laterally displaced by the presence of the surface obstacle.

The concentration patterns with and without the additional small auxiallary building obstacles appear similar (Figures 37 and 47 or Figures 38 and 48). However, with these additional buildings there is a slight reduction in the LFL distances. Similar results were obtained by Dirkmaat [35]. The simulated tree line resulted in concentration contours approximately parallel to the tree line. However, this concentration was smaller than those measured with the similar configuration but no tree line (Figures 37 and 57 and Figures 38 and 54).

5.0 CONCLUSIONS

The wind-tunnel test program was conducted on a 1:250 scale model to determine the effects of surface obstacles on the dispersion of LNG and neutral density plumes. The tests were conducted with the continuous LNG boiloff rate of 30 m^3/min, two wind speeds; 4 m/sec and 7 m/sec, and 21 different surface obstacle configurations. The tests were repeated with the neutral density source gas plume and a flow rate equivalent to 30 m^3/min continuous LNG plume boiloff rate, two winds (4 and 7 m/sec) and 21 different surface obstacle configurations. The experimental measurements led to the following conlusions:

- At the same downwind locations, the highest concentrations were observed without any surface obstacles, i.e., surface obstacles enhance LNG vapor dispersion, resulting in a reduction of LFL distances.

- In general, a lower wind speed resulted in higher ground-level concentration when the surface obstacle interacted with the plume. However, for the unobstructed case, the higher wind speed gave higher concentration for the wind speeds tested.

- The mean concentrations measured with neutral density plumes were about 1/3 to 1/5 of the magnitude of those observed with the LNG plume. This indicates the importance of the buoyancy effect.

- The measured LNG plume concentration tended to have its maximum off the centerline, in particular, when the surface obstacle was on the downstream side of the spill area. This could be attributed to the following:

1. Higher turbulence intensity in the tank wake, which leads to higher entrainment and correspondingly lower concentration in the wake region,

2. The horseshoe vortices on the either side of cylindrical tank deflect lower concentration air from the top of the turbulent boundary layer along the obstacle centerline and results in lower surface concentration, or

3. The plume is laterally displaced by the presence of the surface obstacle.

-   The addition of smaller buildings gave only slight reduction in the LFL distances.

-   The simulated treeline resulted in concentration contours parallel to the treeline. But, this concentration was smaller in magnitude when compared with similar configurations but without tree line.

REFERENCES

1. Fay, J. A. (1973) "Unusual Fire Hazard of LNG Tanker Spills," _Combustion Science and Technology_, Vol. 7, pp. 47-49.

2. Burgess, D. S., Biardi, J., and Murphy, J. N. (1972) "Hazards of Spillage of LNG into Water," Bureau of Mines, MIPR No. Z-70099-9-12395.

3. American Gas Association (1974) "LNG Safety Program, Interim Report on Phase II Work," Report on American Gas Association Project IS-3-1, Battelle Columbus Laboratories.

4. Neff, D. E., Meroney, R. N., and Cermak, J. E. (1976) "Wind Tunnel Study of Negatively Buoyant Plume Due to an LNG Spill," Report prepared for R & D Associates, California, Fluid Dynamics and Diffusion Laboratory Report CER76-77DEN-RNM-JEC22, Colorado State University, Fort Collins, Colorado, 241 p.

5. Hinze, J. O. (1975) _Turbulence_, McGraw-Hill, 790 p.

6. Pasquill, F. (1974) _Atmospheric Diffusion_, D. von Nostrand Co., 429 p.

7. Cermak, J. E. (1971) "Laboratory Simulation of the Atmospheric Boundary Layer," _AIAA Jl._, Vol. 9, No. 9, pp. 1746-1754, September.

8. Kline, S. J. (1965) _Similitude and Approximation Theory_, McGraw-Hill, 229 p.

9. Cermak, J. E. (1975) "Applications of Fluid Mechanics to Wind Engineering, A Freeman Scholar Lecture," _J. of Fluid Engineering_, Vol. 97, Ser. 1, No. 1, pp. 9-38.

10. Schlichting, H. (1968) _Boundary Layer Theory_, McGraw-Hill, New York.

11. Zoric, D. and Sandborn, V. A. (1972) "Similarity of Large Reynolds Number Boundary Layers," _Boundary-Layer Meteorology_, Vol. 2, No. 3, March, pp. 326-333.

12. Halitsky, J. (1969) "Validation of Scaling Procedures for Wind Tunnel Model Testing of Diffusion Near Buildings," Geophysical Sciences Laboratory, Report No. TR-69-8, New York University, New York.

13. Plate, E. J. and Cermak, J. E. (1963) "Micro-Meteorological Wind-Tunnel Facility: Description and Characteristics," Fluid Dynamics and Diffusion Laboratory Report CER63-ELP-JEC9, Colorado State University, Fort Collins, Colorado.

14. Counihan, J. (1975) "Adiabatic Atmospheric Boundary Layers: A Review and Analysis of Data from the Period 1880-1972," _Atmospheric Environment_, Vol. 9, pp. 871-905.

15. Hoot, T. G., et al. (1974) "Wind Tunnel Tests of Negatively Buoyant Plumes," Fluid Dynamics and Diffusion Laboratory Report CER73-74TGH-RNM-JAP-13, Colorado State University, Fort Collins, Colorado, October.

16. Skinner, G. T. and Ludwig, G. R. (1978) "Physical Modeling of Dispersion in the Atmospheric Boundary Layer," Calspan Advanced Technology Center, Calspan Report No. 201, May.

17. Snyder, W. H. (1972) "Similarity Criteria for the Application of Fluid Models to the Study of Air Pollution Meteorology," Boundary Layer Meteorology, Vol. 3, No. 1, September.

18. Boyle, G. J. and Kneebone, A. (1973) "Laboratory Investigation into the Characteristics of LNG Spills on Water, Evaporation, Spreading and Vapor Dispersion," Shell Research, Ltd., Report to API, March.

19. Meroney, R. N., Neff, D. E., Cermak, J. E., and Megahed, M. (1977) "Dispersion of Vapor from LNG Spills - Simulation in a Meteorological Wind Tunnel," Report prepared for R & D Associates, California, Fluid Dynamics and Diffusion Laboratory Report CER76-77RNM-JEC-DEN-MM57, Colorado State University, Fort Collins, Colorado, 151 p.

20. Meroney, R. N., et al. (1974) "Wind Tunnel Study of Stack Gas Dispersal at the Avon Lake Power Plant," Fluid Dynamics and Diffusion Laboratory Report CER73-74RNM-JEC-BTY-SKN35, Colorado State University, Fort Collins, Colorado, April.

21. Kothari, K. M. and Meroney, R. N. (1979) "Building Effects on National Transonic Facility Exhaust Plume," A Technical Report Prepared for NASA, Hampton, Virginia, also, Colorado State University Report CER79-80KMK-RNM35.

22. Bodurtha, F. T., Jr. (1961) "The Behavior of Dense Stack Gases," J. of APCA, Vol. 11, No. 9, pp. 431-437.

23. van Ulden, A. P. (1974) "On the Spreading of a Heavy Gas Released Near the Ground," Loss Prevention and Safety Promotion Seminar, Delft, Netherlands, 6 p.

24. Fay, J. A. (1980) "Gravitational Spread and Dilution of Heavy Vapor Clouds," Second International Symposium on Stratified Flows, the Norwegian Institute of Technology, Trondheim, Norway, 24-27 June.

25. Sandborn, V. A. (1972) Resistance Temperature Transducers, Metrology Press, 545 p.

26. Blackshear, P. L., Jr., and Fingerson, L. (1962) "Rapid Response Heat Flux Probe for High Temperature Gases," ARS Journal, November 1962, pp. 1709-1715.

27. Brown, G. L. and Rebollo, M. R. (1972) "A Small, Fast Response Probe to Measure Composition of a Binery Gas Mixture," AIAA Journal, Vol. 10, No. 5, pp. 649-752.

28. Kuretsky, W. H. (1967) "On the Use of an Aspirating Hot-Film Anemometer for the Instantaneous Measurement of Temperature," Thesis, Master of Mechanical Engineering, University of Minnesota, Minneapolis, Minnesota.

29. Kothari, K. M., Peterka, J. A., and Meroney, R. N. (1979) "Stably Stratified Building Wakes," U.S. Nuclear Regulatory Commission Report NUREG/CR-1247.

30. Woo, H. G. C., Peterka, J. A., and Cermak, J. E. (1976) "Wind Tunnel Meaurements in the Wakes of Structures," Colorado State University Report CER75-76-HGCW-JAP-JEC40, Colorado State University, Fort Collins, Colorado.

31. Hansen, A. C. and Cermak, J. E. (1975) "Vortex-Containing Wakes of Surface Obstacles," Colorado State University Report CER75-76ACH-JEC16, Colorado State University, Fort Collins, Colorado.

32. Castro, J. P., and Robins, A. G. (1975) "The Effect of a Thick Incident Boundary Layer on the Flow Around a Small Surface Mounted Cube," Central Electricity Generating Board Report R/M/N795, England.

33. Counihan, J. (1971) "An Experimental Investigation of the Cube behind a Two-Dimensional Block and behind a Cube in a Simulated Boundary Layer Flow," Centered Electricity Generating Board Report RD/L/N115/71.

34. Kothari, K. M., Meroney, R. N., and Peterka, J. A. (1981) "The Flow and Diffusion Structure in the Wakes of Cylindrical Obstacles," A paper presented at 4th U.S. National Conference on Wind Engineering Research, Seattle, Washington, 26-29 July.

35. Dirkmaat, J. J. (1981) "Experimental Studies on the Dispersion of Heavy Gases in the Vicinity of Structures and Buildings," TNO Report 81-05564.

36. Neff, D. E. and Meroney, R. N. (1981) "The Behavior of LNG Vapor Clouds: Wind-Tunnel Simulation of 40 m^3 LNG Spill Tests at China Lake Naval Weapons Center, California," Colorado State University Report CER81-82DEN-RNM1 for Gas Research Institute, Contract No. 5014-52-0203, pp.

APPENDIX A

THE CALCULATION OF MODEL SCALE FACTORS

APPENDIX A - THE CALCULATION OF MODEL SCALE FACTORS

As discussed previously in Section 2.3 the dominant scaling criteria for the simulation of LNG vapor cloud physics are the Froude number and the volume flux ratio. By setting these parameters equal for model and prototype one obtains the following relationships.

$$(U_a)_m = \left(\frac{S.G._m - 1}{S.G._p - 1}\right)^{1/2} \left(\frac{1}{L.S.}\right)^{1/2} (U_a)_p$$

$$Q_m = \left(\frac{S.G._m - 1}{S.G._p - 1}\right)^{1/2} \left(\frac{1}{L.S.}\right)^{5/2} Q_p$$

$$L_m = \left(\frac{1}{L.S.}\right) L_p$$

In addition to these scaling parameters which govern the flow physics, one must also scale the mole fractions (concentrations) measured in the model to those that would occur in the prototype. This scaling is required since the number of moles being released in a thermal plume are different from the number of moles being released in a isothermal plume. To be more precise the relationship between the molar flow rate of source gas in the model and the prototype is

$$n_p = (T_m/T_p)_{@\ b.o.} \quad n_m = (2.70)\ n_m$$

By definition the concentration of LNG vapor is expressed as:

$$X_p = n_{NG}/(n_{NG} + n_a)$$

Substituting model equivalents into the above expression yields

$$X_p = \frac{(T_m/T_p)_{@b.o.} n_{Ar}}{(T_m/T_p)_{@b.o.} n_{Ar} + n_a} = \frac{n_{Ar}}{n_{Ar} + n_a(T_p/T_m)_{@b.o.}}$$

or

$$X_p = \frac{X_m}{X_m + (1 - X_m)(0.37)}$$

This equation was used to correct the modeled measurements to those that would be observed in the field.

APPENDIX B

DATA TABLE

CONFIGURATION NUMBER 1

RUN NUMBER 1   RUN NUMBER 45

SOURCE DENSITY – NEUTRAL   SOURCE AT SPECIFIC GRAVITY OF
                                                LNG AT BOILOFF

SAMPLE POINT	NONDIMENSIONAL CONCENTRATION COEFFICIENT,K	MEAN CONCENTRATION PERCENT	PEAK PERCENT	CONCENTRATION MEAN PERCENT	RMS PERCENT
1	17.73	8.68	23.09	20.00	1.50
2	8.83	4.32	21.70	18.30	1.81
3	1.02	.50	19.65	16.51	2.46
4	.02	.01	15.38	11.76	2.35
5	0.00	0.00	9.88	6.15	2.04
6	0.00	0.00	5.98	1.04	1.95
7	0.00	0.00	0.00	0.00	0.00
8	.00	.00	0.00	0.00	0.00
9	4.92	2.41	12.91	11.25	.87
10	4.08	2.00	13.14	11.32	.74
11	1.16	.57	11.99	10.56	.81
12	.22	.11	11.30	9.31	1.25
13	.01	.01	8.20	6.45	1.61
14	0.00	0.00	6.98	4.04	1.96
15	0.00	0.00	6.73	1.53	1.99
16	.00	.00	3.70	0.00	.97
17	1.91	.94	7.47	5.66	.92
18	2.33	1.14	7.47	5.96	.86
19	1.06	.52	7.71	6.55	.70
20	.26	.13	8.20	6.64	.60
21	.03	.02	6.98	5.60	.70
22	.00	.00	5.98	4.50	1.04
23	0.00	0.00	5.73	3.64	1.29
24	0.00	0.00	5.48	2.59	1.49
25	.53	.26	4.21	2.85	.60
26	.62	.30	3.95	2.57	.81
27	.55	.27	3.95	2.34	.94
28	.25	.12	4.21	2.99	.86
29	.34	.17	3.95	2.42	.87
30	.02	.01	3.44	1.54	.92
31	.00	.00	3.18	1.54	.86
32	0.00	0.00	2.66	.71	1.11
33	.18	.09	--	--	--
34	.22	.11	--	--	--
35	.21	.10	--	--	--
36	.16	.08	--	--	--
37	.08	.04	--	--	--
38	.04	.02	--	--	--
39	.01	.00	--	--	--
40	0.00	0.00	--	--	--

CONFIGURATION NUMBER   2

RUN NUMBER   2   RUN NUMBER 46

SOURCE DENSITY - NEUTRAL   SOURCE AT SPECIFIC GRAVITY OF
                                                 LNG AT BOILOFF

SAMPLE POINT	NONDIMENSIONAL CONCENTRATION COEFFICIENT,K	MEAN CONCENTRATION PERCENT	PEAK PERCENT	CONCENTRATION MEAN PERCENT	RMS PERCENT
1	2.25	1.14	15.16	1.72	2.77
2	1.24	.62	13.59	2.50	2.60
3	.33	.17	20.48	9.24	4.69
4	.01	.01	19.03	14.16	3.16
5	.00	.00	16.04	13.44	1.80
6	.00	.00	14.94	10.69	2.97
7	0.00	0.00	10.83	3.83	3.99
8	.00	.00	.54	.10	.16
9	1.37	.69	1.87	.14	.28
10	1.26	.64	3.18	.04	.67
11	.82	.42	5.23	.83	1.07
12	1.26	.64	8.20	3.80	1.75
13	.08	.04	5.98	3.48	1.43
14	.01	.00	8.93	5.93	1.54
15	.00	.00	8.44	6.05	1.47
16	.00	.00	7.96	4.97	1.93
17	.98	.49	.54	.11	.19
18	1.03	.52	.54	0.00	.35
19	.83	.42	1.34	.22	.44
20	.63	.32	2.66	1.12	.61
21	.27	.13	4.47	2.03	.87
22	.06	.03	4.47	2.73	1.05
23	.01	.01	4.97	3.07	.73
24	.00	.00	4.47	2.81	.70
25	.54	.27	--	--	--
26	.59	.30	--	--	--
27	.41	.21	--	--	--
28	.60	.30	--	--	--
29	.60	.30	--	--	--
30	.23	.12	--	--	--
31	.11	.06	--	--	--
32	.04	.02	--	--	--
33	.30	.15	--	--	--
34	.33	.17	--	--	--
35	.35	.18	--	--	--
36	.38	.19	--	--	--
37	.37	.19	--	--	--
38	.29	.15	--	--	--
39	.21	.11	--	--	--
40	0.00	0.00	--	--	--

CONFIGURATION NUMBER   3

	RUN NUMBER 3		RUN NUMBER 47		
	SOURCE DENSITY - NEUTRAL		SOURCE AT SPECIFIC GRAVITY OF LNG AT BOILOFF		

SAMPLE POINT	NONDIMENSIONAL CONCENTRATION COEFFICIENT,K	MEAN CONCENTRATION PERCENT	PEAK PERCENT	CONCENTRATION MEAN PERCENT	RMS PERCENT
1	12.16	6.32	25.04	21.65	2.14
2	7.72	4.01	23.29	18.48	3.20
3	2.67	1.39	20.48	15.98	2.42
4	.46	.24	17.12	11.21	2.94
5	.03	.02	12.45	7.79	2.46
6	0.00	0.00	9.88	4.28	3.01
7	0.00	0.00	2.13	.53	.35
8	0.00	0.00	0.00	0.00	0.00
9	3.60	1.87	11.53	8.73	1.53
10	3.43	1.78	11.99	8.55	1.76
11	2.27	1.18	11.06	7.85	1.55
12	1.16	.60	10.59	7.53	1.58
13	.52	.27	8.69	5.31	1.66
14	.14	.07	7.71	4.42	1.53
15	.02	.01	7.47	3.59	2.05
16	.00	.00	5.48	.79	1.73
17	1.60	.83	7.22	5.49	.83
18	1.78	.92	7.71	5.23	1.07
19	1.58	.82	7.22	5.13	.91
20	1.13	.59	7.47	5.54	.86
21	.65	.34	6.98	4.25	1.13
22	.33	.17	6.98	4.57	.95
23	.09	.05	7.22	4.27	1.29
24	.02	.01	5.98	3.27	1.44
25	.52	.27	3.95	2.39	.57
26	.64	.33	4.21	2.51	.74
27	.66	.34	3.70	2.19	.86
28	.64	.33	3.70	2.27	.77
29	.65	.34	3.18	1.92	.70
30	.38	.20	2.92	1.58	.68
31	.24	.12	3.18	1.83	.63
32	.07	.04	3.18	1.68	.58
33	.22	.11	--	--	--
34	.28	.14	--	--	--
35	.31	.16	--	--	--
36	.32	.17	--	--	--
37	.30	.15	--	--	--
38	.29	.15	--	--	--
39	.25	.13	--	--	--
40	0.00	0.00	--	--	--

CONFIGURATION NUMBER 4

RUN NUMBER 4   RUN NUMBER 48

SOURCE DENSITY - NEUTRAL   SOURCE AT SPECIFIC GRAVITY OF
                                                LNG AT BOILOFF

SAMPLE POINT	NONDIMENSIONAL CONCENTRATION COEFFICIENT,K	MEAN CONCENTRATION PERCENT	PEAK PERCENT	CONCENTRATION MEAN PERCENT	RMS PERCENT
1	6.38	3.36	22.50	13.06	5.03
2	3.54	1.86	21.09	12.69	3.86
3	1.45	.76	22.90	12.16	3.35
4	.43	.23	18.19	10.35	2.56
5	.06	.03	14.04	8.00	2.01
6	.00	.00	10.36	5.44	2.54
7	0.00	0.00	7.47	.83	2.05
8	0.00	0.00	.81	.26	.17
9	2.43	1.28	9.65	7.22	1.50
10	1.92	1.01	8.69	6.43	1.53
11	1.23	.65	8.93	5.81	1.59
12	.80	.42	8.44	5.55	1.27
13	.44	.23	6.23	4.37	1.20
14	.12	.06	6.23	4.02	1.20
15	.03	.01	5.48	3.35	1.38
16	0.00	0.00	4.97	1.40	1.78
17	1.42	.75	5.23	3.73	.85
18	1.21	.63	5.73	2.91	.95
19	1.01	.53	4.97	2.65	1.08
20	.72	.38	5.48	3.51	1.09
21	.49	.26	3.95	1.88	.79
22	.31	.17	3.44	1.66	1.01
23	.10	.05	4.21	2.21	1.00
24	.03	.01	3.70	1.82	1.18
25	.61	.32	1.87	.91	.51
26	.61	.32	2.13	.68	.66
27	.58	.31	2.13	1.12	.69
28	.50	.27	2.92	1.82	.77
29	.52	.28	2.40	1.00	.54
30	.34	.18	2.40	1.04	.53
31	.24	.13	2.13	1.14	.46
32	.03	.02	2.13	.97	.55
33	.33	.17	--	--	--
34	.35	.19	--	--	--
35	.36	.19	--	--	--
36	.34	.18	--	--	--
37	.30	.16	--	--	--
38	.27	.14	--	--	--
39	.21	.11	--	--	--
40	0.00	0.00	--	--	--

CONFIGURATION NUMBER 5

RUN NUMBER 5   PUN NUMBER 49

SOURCE DENSITY - NEUTRAL   SOURCE AT SPECIFIC GRAVITY OF
                                                                    LNG AT BOILOFF

SAMPLE POINT	NONDIMENSIONAL CONCENTRATION COEFFICIENT,K	MEAN CONCENTRATION PERCENT	PEAK PERCENT	CONCENTRATION MEAN PERCENT	RMS PERCENT
1	2.08	1.03	11.99	.54	1.22
2	1.75	.87	8.69	1.22	1.34
3	1.00	.50	9.41	3.00	1.95
4	.33	.17	10.12	4.68	1.90
5	.02	.01	8.69	5.07	1.79
6	0.00	0.00	8.69	4.94	1.72
7	0.00	0.00	8.44	4.79	1.75
8	0.00	0.00	5.48	.12	1.85
9	1.26	.63	1.61	.51	.29
10	1.38	.69	.81	.03	.27
11	1.04	.52	2.92	.60	.48
12	.72	.36	3.44	1.70	.67
13	.28	.14	4.21	1.93	.86
14	.05	.03	5.98	3.20	1.09
15	.01	.00	5.48	3.65	.81
16	0.00	0.00	5.48	2.75	.70
17	.79	.39	.54	0.00	.27
18	1.02	.51	.54	0.00	.27
19	.97	.48	0.00	0.00	0.00
20	.73	.36	1.34	.19	.33
21	.39	.19	1.34	.32	.40
22	.16	.08	2.13	1.21	.37
23	.04	.02	3.18	1.79	.56
24	.00	.00	3.44	2.42	.57
25	.39	.19	--	--	--
26	.51	.25	--	--	--
27	.57	.28	--	--	--
28	.53	.27	--	--	--
29	.56	.28	--	--	--
30	.28	.14	--	--	--
31	.13	.07	--	--	--
32	.03	.02	--	--	--
33	.20	.10	--	--	--
34	.25	.13	--	--	--
35	.33	.16	--	--	--
36	.35	.18	--	--	--
37	.32	.16	--	--	--
38	.25	.12	--	--	--
39	.20	.10	--	--	--
40	0.00	0.00	--	--	--

CONFIGURATION NUMBER 6

RUN NUMBER 6   RUN NUMBER 50

SOURCE DENSITY - NEUTRAL   SOURCE AT SPECIFIC GRAVITY OF
                                        LNG AT BOILOFF

SAMPLE POINT	NONDIMENSIONAL CONCENTRATION COEFFICIENT,K	MEAN CONCENTRATION PERCENT	PEAK PERCENT	CONCENTRATION MEAN PERCENT	RMS PERCENT
1	1.15	.58	10.83	2.63	1.85
2	1.23	.62	12.22	6.07	2.58
3	2.08	1.05	18.19	10.15	3.36
4	3.45	1.74	17.12	12.09	2.07
5	.97	.49	12.22	9.66	1.19
6	.02	.01	9.88	7.82	.98
7	0.00	0.00	9.65	6.57	2.28
8	0.00	0.00	8.69	1.61	3.11
9	1.06	.54	3.18	.75	.71
10	.91	.46	4.21	.96	.83
11	1.15	.58	6.23	2.39	1.44
12	1.43	.72	7.22	5.00	1.25
13	1.19	.60	7.71	6.05	.76
14	.49	.25	8.20	6.53	.76
15	.09	.05	7.71	5.94	.88
16	0.00	0.00	7.71	5.02	1.68
17	.89	.45	1.87	.53	.37
18	.73	.37	2.66	.70	.61
19	.70	.35	3.18	1.02	.64
20	.84	.42	4.72	1.52	1.03
21	.83	.42	6.48	3.09	1.08
22	.55	.28	5.98	3.85	.77
23	.23	.12	5.48	4.27	.64
24	.06	.03	4.97	3.72	.97
25	.50	.26	1.87	.19	.40
26	.48	.24	1.61	.07	.28
27	.47	.24	0.00	0.00	0.00
28	.43	.21	1.07	.30	.23
29	.44	.22	1.34	.46	.29
30	.38	.19	1.07	.22	.36
31	.28	.14	2.66	1.72	.49
32	.08	.04	2.66	1.62	.61
33	.29	.14	--	--	--
34	.30	.15	--	--	--
35	.29	.15	--	--	--
36	.29	.15	--	--	--
37	.26	.13	--	--	--
38	.25	.12	--	--	--
39	.19	.10	--	--	--
40	0.00	0.00	--	--	--

CONFIGURATION NUMBER 7

RUN NUMBER 7   RUN NUMBER 51

SOURCE DENSITY - NEUTRAL   SOURCE AT SPECIFIC GRAVITY OF
                                            LNG AT BOILOFF

SAMPLE POINT	NONDIMENSIONAL CONCENTRATION COEFFICIENT,K	MEAN CONCENTRATION PERCENT	PEAK PERCENT	CONCENTRATION MEAN PERCENT	RMS PERCENT
1	9.14	4.75	16.25	13.24	2.28
2	11.08	5.76	16.47	12.47	2.77
3	9.40	4.89	20.07	17.45	1.67
4	2.09	1.09	20.27	17.09	1.69
5	.05	.02	15.60	11.80	2.39
6	0.00	0.00	10.83	7.56	2.21
7	0.00	0.00	9.65	3.82	4.01
8	0.00	0.00	0.00	0.00	0.00
9	1.01	.53	1.87	.87	.23
10	1.37	.71	4.47	1.22	.72
11	2.19	1.14	10.83	4.43	2.29
12	3.65	1.89	12.22	9.60	1.31
13	1.53	.80	13.37	11.45	.96
14	.20	.10	11.76	10.01	1.16
15	.00	.00	11.06	8.47	1.58
16	0.00	0.00	10.59	6.73	2.29
17	.88	.46	2.40	.90	.51
18	.90	.47	3.18	.51	.68
19	1.24	.65	3.70	1.17	.94
20	1.54	.80	5.48	3.79	1.14
21	1.36	.71	5.98	3.91	.85
22	.58	.30	6.98	5.34	.95
23	.11	.06	7.47	5.52	1.00
24	.01	.00	7.47	5.23	1.05
25	.52	.27	1.61	.94	.32
26	.52	.27	2.13	.99	.40
27	.51	.26	2.13	.89	.48
28	.57	.29	2.66	.56	.84
29	.51	.26	1.87	.41	.76
30	.61	.32	2.40	1.02	.69
31	.38	.20	3.44	2.12	.75
32	.12	.06	3.70	2.24	.72
33	.31	.16	--	--	--
34	.32	.17	--	--	--
35	.32	.17	--	--	--
36	.32	.17	--	--	--
37	.32	.17	--	--	--
38	.32	.17	--	--	--
39	.30	.15	--	--	--
40	0.00	0.00	--	--	--

CONFIGURATION NUMBER 8

RUN NUMBER 8   RUN NUMBER 52

SOURCE DENSITY - NEUTRAL   SOURCE AT SPECIFIC GRAVITY OF
                                              LNG AT BOILOFF

SAMPLE POINT	NONDIMENSIONAL CONCENTRATION COEFFICIENT,K	MEAN CONCENTRATION PERCENT	PEAK PERCENT	CONCENTRATION MEAN PERCENT	RMS PERCENT
1	17.23	8.44	24.46	21.38	1.30
2	10.74	5.26	24.46	21.02	1.67
3	3.64	1.78	21.50	18.59	1.53
4	.30	.15	17.97	14.19	2.15
5	.00	.00	13.82	9.80	2.43
6	0.00	0.00	10.83	4.22	3.78
7	0.00	0.00	6.73	.72	1.46
8	0.00	0.00	.54	.32	.11
9	2.17	1.06	11.30	7.53	1.41
10	3.41	1.67	8.69	6.10	.89
11	4.56	2.24	11.99	9.20	1.07
12	2.18	1.07	11.76	10.14	1.01
13	.70	.34	9.88	7.56	1.56
14	.06	.03	8.69	5.59	1.73
15	0.00	0.00	6.48	2.36	2.36
16	0.00	0.00	3.18	0.00	.57
17	.69	.34	1.87	1.03	.22
18	1.00	.49	1.87	.50	.33
19	1.31	.64	4.21	1.86	.91
20	1.70	.83	6.98	5.23	1.06
21	.95	.47	8.44	7.49	.46
22	.35	.17	8.93	7.53	.80
23	.05	.03	8.44	6.50	1.08
24	0.00	0.00	7.96	5.02	2.00
25	.36	.18	2.66	1.08	.39
26	.47	.23	2.92	1.26	.54
27	.53	.26	3.95	1.91	.63
28	.59	.29	3.95	1.91	.81
29	.53	.26	3.44	1.75	.61
30	.37	.18	3.95	2.76	.56
31	.22	.11	4.47	3.08	.76
32	.04	.02	4.21	2.87	1.04
33	.20	.10	1.07	.40	.21
34	.28	.14	1.61	.86	.31
35	.32	.15	1.87	.85	.31
36	.34	.17	1.87	.78	.33
37	.32	.16	2.13	.96	.39
38	.28	.14	1.87	.72	.47
39	.19	.09	1.61	.76	.49
40	0.00	0.00	1.61	.50	.63

CONFIGURATION NUMBER 10

RUN NUMBER 10   RUN NUMBER 54

SOURCE DENSITY - NEUTRAL   SOURCE AT SPECIFIC GRAVITY OF
                                              LNG AT BOILOFF

SAMPLE POINT	NONDIMENSIONAL CONCENTRATION COEFFICIENT,K	MEAN CONCENTRATION PERCENT	PEAK PERCENT	CONCENTRATION MEAN PERCENT	RMS PERCENT
1	2.19	1.09	3.95	0.00	.63
2	2.02	1.00	11.53	.11	3.07
3	.74	.37	18.19	6.06	4.46
4	.11	.05	20.48	12.84	4.34
5	.00	.00	16.04	13.07	1.69
6	0.00	0.00	11.99	9.66	1.59
7	0.00	0.00	10.12	4.85	3.49
8	0.00	0.00	1.07	0.00	.29
9	1.24	.61	1.87	.77	.24
10	1.47	.73	1.34	.69	.24
11	1.25	.62	4.72	.88	.76
12	.70	.35	10.12	2.33	2.05
13	.25	.12	7.47	3.74	1.95
14	.06	.03	9.17	5.54	1.41
15	.00	.00	8.93	6.59	1.31
16	0.00	0.00	8.93	6.55	1.97
17	.81	.40	.81	0.00	.19
18	.98	.49	.54	0.00	.16
19	.94	.46	.54	.19	.15
20	.76	.38	3.18	.80	.67
21	.45	.22	3.70	1.72	.81
22	.19	.09	4.97	2.97	.79
23	.06	.03	5.48	3.85	.69
24	.00	.00	5.98	3.91	.73
25	.44	.22	1.61	1.01	.22
26	.59	.29	1.87	1.13	.21
27	.64	.32	.54	.40	.13
28	.59	.29	1.07	.31	.19
29	.60	.30	1.61	.71	.33
30	.37	.18	1.87	1.18	.32
31	.20	.10	2.92	1.45	.48
32	.05	.03	3.18	1.84	.44
33	.26	.13	1.34	.53	.30
34	.34	.17	.54	0.00	.28
35	.40	.20	0.00	0.00	0.00
36	.42	.21	.27	0.00	.10
37	.39	.19	0.00	0.00	0.00
38	.33	.16	0.00	0.00	0.00
39	.28	.14	0.00	0.00	0.00
40	0.00	0.00	0.00	0.00	0.00

CONFIGURATION NUMBER 11

RUN NUMBER 11   RUN NUMBER 55

SOURCE DENSITY - NEUTRAL   SOURCE AT SPECIFIC GRAVITY OF
                                              LNG AT BOILOFF

SAMPLE POINT	NONDIMENSIONAL CONCENTRATION COEFFICIENT,K	MEAN CONCENTRATION PERCENT	PEAK PERCENT	CONCENTRATION MEAN PERCENT	RMS PERCENT
1	1.53	.79	6.73	3.07	1.48
2	.63	.33	7.22	3.17	1.75
3	.11	.06	5.98	2.19	1.53
4	.03	.01	6.73	2.91	1.66
5	.00	.00	9.17	3.38	2.25
6	0.00	0.00	10.83	6.45	2.25
7	0.00	0.00	11.30	8.93	1.23
8	0.00	0.00	11.99	9.48	1.94
9	.94	.48	1.87	1.56	.15
10	.78	.40	3.44	2.65	.24
11	.64	.33	3.18	2.55	.29
12	.35	.18	1.61	.91	.15
13	.04	.02	2.66	1.77	.29
14	.01	.01	2.66	1.59	.46
15	.00	.00	3.18	1.70	.59
16	0.00	0.00	5.23	3.15	.89
17	.88	.45	4.72	1.75	.79
18	.97	.50	2.66	1.20	.38
19	.91	.47	1.61	.76	.25
20	.73	.37	1.07	.44	.20
21	.42	.22	1.87	.81	.30
22	.12	.06	2.40	.92	.40
23	.03	.02	2.40	1.04	.47
24	.00	.00	3.18	1.80	.60
25	.56	.29	2.40	1.05	.53
26	.66	.34	1.87	.69	.46
27	.62	.32	2.40	1.25	.28
28	.56	.29	1.07	.74	.12
29	.57	.29	1.87	1.69	.13
30	.39	.20	1.87	1.52	.15
31	.24	.12	1.34	.87	.21
32	.06	.03	1.07	.48	.25
33	.33	.17	--	--	--
34	.42	.22	--	--	--
35	.43	.22	--	--	--
36	.41	.21	--	--	--
37	.37	.19	--	--	--
38	.32	.16	--	--	--
39	.26	.13	--	--	--
40	.00	.00	--	--	--

CONFIGURATION NUMBER 12

RUN NUMBER 12   RUN NUMBER 56

SOURCE DENSITY - NEUTRAL   SOURCE AT SPECIFIC GRAVITY OF
                                          LNG AT BOILOFF

SAMPLE POINT	NONDIMENSIONAL CONCENTRATION COEFFICIENT,K	MEAN CONCENTRATION PERCENT	PEAK PERCENT	CONCENTRATION MEAN PERCENT	RMS PERCENT
1	0.00	0.00	22.90	19.97	1.29
2	1.63	.81	20.89	18.01	1.40
3	.53	.26	19.03	15.98	1.63
4	.06	.03	17.12	12.74	2.03
5	.00	.00	10.83	7.02	1.69
6	0.00	0.00	7.47	1.96	2.58
7	0.00	0.00	0.00	0.00	0.00
8	0.00	0.00	0.00	0.00	0.00
9	1.27	.63	10.36	9.06	.77
10	1.51	.75	10.12	7.96	.93
11	1.29	.64	10.83	10.06	.37
12	.74	.37	11.53	10.46	.48
13	.29	.15	11.06	9.37	.70
14	.07	.03	9.41	7.55	.90
15	.01	.00	8.44	6.29	1.10
16	0.00	0.00	7.22	3.03	2.37
17	.97	.48	2.66	1.70	.32
18	1.20	.60	3.44	1.17	.67
19	1.20	.59	4.72	2.57	1.11
20	.89	.44	7.47	6.17	.95
21	.58	.29	8.20	7.30	.53
22	.27	.13	7.71	6.50	1.01
23	.07	.04	7.71	5.97	1.17
24	.01	.01	6.98	4.14	1.67
25	.55	.28	1.07	.09	.25
26	.71	.36	.54	.07	.15
27	.73	.36	.81	.12	.16
28	.70	.35	1.07	.39	.22
29	.69	.34	6.73	6.00	.39
30	.46	.23	2.66	.58	.48
31	.32	.16	2.40	1.40	.40
32	.12	.06	3.18	1.87	.37
33	.33	.16	.27	0.00	.14
34	.40	.20	0.00	0.00	0.00
35	.47	.23	0.00	0.00	0.00
36	.46	.23	.54	.25	.07
37	.43	.22	.54	.47	.11
38	.41	.20	.54	.22	.12
39	.36	.18	.81	.13	.20
40	0.00	0.00	.54	0.00	.27

CONFIGURATION NUMBER 14

RUN NUMBER 14   RUN NUMBER 58

SOURCE DENSITY - NEUTRAL   SOURCE AT SPECIFIC GRAVITY OF
                                          LNG AT BOILOFF

SAMPLE POINT	NONDIMENSIONAL CONCENTRATION COEFFICIENT,K	MEAN CONCENTRATION PERCENT	PEAK PERCENT	CONCENTRATION MEAN PERCENT	RMS PERCENT
1	3.38	1.65	13.82	9.34	1.98
2	3.08	1.51	16.47	10.47	3.36
3	2.69	1.32	17.33	13.31	2.66
4	.95	.47	16.69	11.44	2.93
5	.17	.09	12.45	6.48	3.00
6	.03	.02	7.47	2.91	1.94
7	.00	.03	5.98	2.70	1.32
8	.00	.00	4.72	1.56	1.77
9	2.20	1.08	7.71	4.75	1.69
10	1.40	.69	5.73	3.15	1.30
11	1.10	.54	7.47	4.20	1.40
12	.99	.48	8.44	6.12	1.29
13	.68	.33	7.71	5.85	1.28
14	.32	.16	7.71	5.34	1.59
15	.10	.05	6.73	4.20	1.61
16	.01	.01	5.98	3.44	1.26
17	1.51	.74	3.95	2.68	.75
18	1.14	.56	3.70	2.13	.64
19	.92	.45	4.21	2.19	.89
20	.72	.35	5.23	2.93	.72
21	.61	.30	4.21	2.98	.59
22	.46	.23	4.47	3.04	.76
23	.28	.14	4.47	2.91	.74
24	.10	.05	3.44	2.29	.69
25	.75	.37	2.66	1.84	.38
26	.73	.36	3.18	2.20	.65
27	.61	.30	3.44	1.98	.61
28	.55	.27	2.66	1.49	.46
29	.57	.28	2.92	1.80	.58
30	.40	.20	3.18	2.07	.56
31	.36	.17	2.92	1.94	.42
32	.20	.10	2.40	1.63	.57
33	.38	.19	.81	.19	.22
34	.39	.19	0.00	0.00	0.00
35	.40	.19	.27	0.00	.14
36	.38	.19	.81	0.00	.30
37	.35	.17	.81	.27	.14
38	.34	.17	1.07	.39	.19
39	.30	.14	1.34	.71	.20
40	.00	.00	1.07	.52	.23

CONFIGURATION NUMBER 15

RUN NUMBER 15   RUN NUMBER 59

SOURCE DENSITY - NEUTRAL   SOURCE AT SPECIFIC GRAVITY OF
                                        LNG AT BOILOFF

SAMPLE POINT	NONDIMENSIONAL CONCENTRATION COEFFICIENT,K	MEAN CONCENTRATION PERCENT	PEAK PERCENT	CONCENTRATION MEAN PERCENT	RMS PERCENT
1	1.88	.97	8.69	3.26	2.29
2	1.39	.72	8.44	1.52	2.22
3	.60	.31	14.49	5.98	3.30
4	.15	.08	16.25	10.51	2.56
5	.01	.00	11.99	7.18	2.05
6	0.00	0.00	9.41	3.95	2.26
7	0.00	0.00	7.22	2.79	1.58
8	0.00	0.00	1.34	0.00	.30
9	1.08	.56	4.21	.90	1.11
10	1.42	.73	1.07	.03	.35
11	1.12	.58	2.92	.96	.74
12	.62	.32	4.72	2.53	.88
13	.22	.11	5.98	3.27	1.15
14	.03	.02	5.48	3.75	.87
15	.00	.00	5.73	4.13	.84
16	0.00	0.00	5.23	3.19	1.05
17	.60	.31	1.87	.58	.53
18	.54	.28	1.07	0.00	.25
19	1.01	.52	.81	0.00	.26
20	.75	.39	1.87	1.04	.44
21	.45	.23	1.87	1.24	.25
22	.16	.08	2.13	1.20	.42
23	.04	.02	3.44	1.88	.58
24	.01	.00	3.18	1.95	.66
25	.29	.15	1.34	.66	.29
26	.50	.26	1.61	.65	.28
27	.60	.31	1.07	.55	.19
28	.61	.32	1.07	.45	.19
29	.61	.32	1.34	.77	.21
30	.36	.19	2.13	1.40	.22
31	.23	.12	1.87	1.24	.26
32	.07	.04	1.87	1.08	.35
33	.18	.10	--	--	--
34	.29	.15	--	--	--
35	.34	.18	--	--	--
36	.37	.19	--	--	--
37	.38	.20	--	--	--
38	.33	.17	--	--	--
39	.28	.15	--	--	--
40	0.00	0.00	--	--	--

CONFIGURATION NUMBER 16

RUN NUMBER 16   RUN NUMBER 60

SOURCE DENSITY - NEUTRAL   SOURCE AT SPECIFIC GRAVITY OF
LNG AT BOILOFF

SAMPLE POINT	NONDIMENSIONAL CONCENTRATION COEFFICIENT,K	MEAN CONCENTRATION PERCENT	PEAK PERCENT	CONCENTRATION MEAN PERCENT	RMS PERCENT
1	4.28	2.20	7.71	.56	2.20
2	3.84	1.98	11.53	3.54	3.62
3	4.38	2.26	17.12	12.27	2.49
4	1.78	.92	16.90	13.91	1.23
5	.21	.11	11.76	8.14	2.88
6	.01	.00	7.71	2.59	2.59
7	0.00	0.00	6.23	2.62	1.44
8	0.00	0.00	5.48	3.19	1.16
9	1.44	.74	4.97	2.81	.65
10	1.48	.76	3.44	2.00	.39
11	1.59	.82	6.48	1.61	2.04
12	1.52	.78	9.88	6.31	1.59
13	.96	.49	9.17	5.80	1.40
14	.28	.14	7.22	4.27	1.51
15	.05	.03	6.48	3.14	1.55
16	.00	.00	4.97	2.01	8.87
17	1.00	.51	2.92	1.62	.72
18	.96	.49	3.95	1.35	.87
19	1.04	.54	3.70	1.53	1.07
20	1.08	.55	4.21	2.73	.79
21	.81	.42	3.95	2.73	.57
22	.38	.20	4.47	2.65	.77
23	.16	.08	4.21	2.62	.95
24	.03	.02	3.70	2.15	.97
25	.47	.24	1.61	1.09	.29
26	.51	.26	2.40	1.50	.26
27	.55	.29	2.66	1.54	.39
28	.57	.29	2.40	1.30	.45
29	.56	.29	3.18	1.96	.50
30	.37	.19	2.66	1.96	.47
31	.25	.13	2.66	1.90	.37
32	.08	.04	2.40	1.60	.33
33	.24	.12	--	--	--
34	.28	.14	--	--	--
35	.29	.15	--	--	--
36	.32	.16	--	--	--
37	.32	.16	--	--	--
38	.27	.14	--	--	--
39	.19	.10	--	--	--
40	0.00	0.00	--	--	--

CONFIGURATION NUMBER 17

	RUN NUMBER 17			RUN NUMBER 61	
	SOURCE DENSITY - NEUTRAL			SOURCE AT SPECIFIC GRAVITY OF LNG AT BOILOFF	
SAMPLE POINT	NONDIMENSIONAL CONCENTRATION COEFFICIENT,K	MEAN CONCENTRATION PERCENT	PEAK PERCENT	CONCENTRATION MEAN PERCENT	RMS PERCENT
1	4.65	2.31	10.36	6.79	2.89
2	5.36	2.67	17.33	9.86	3.95
3	4.06	2.02	20.27	16.56	2.15
4	1.01	.50	17.76	14.21	2.29
5	.04	.02	14.04	7.10	3.34
6	.00	.00	7.47	2.83	1.40
7	0.00	0.00	6.73	3.29	1.20
8	0.00	0.00	4.97	1.75	1.46
9	2.30	1.14	4.97	3.30	.89
10	2.46	1.22	4.72	2.75	1.02
11	2.14	1.06	7.22	3.97	1.31
12	1.60	.80	8.69	7.21	.81
13	.82	.41	8.44	6.72	.74
14	.14	.07	7.47	5.10	1.18
15	.02	.01	7.22	3.81	1.61
16	0.00	0.00	4.72	2.88	.98
17	1.11	.55	1.61	1.04	.24
18	1.38	.69	2.13	1.12	.32
19	1.46	.73	1.34	.19	.36
20	1.29	.64	4.72	3.15	.98
21	.89	.44	3.70	2.84	.49
22	.41	.20	4.72	3.45	.43
23	.10	.05	4.72	3.49	.66
24	.02	.01	3.95	2.26	.79
25	.60	.30	1.61	1.10	.25
26	.62	.31	1.87	1.18	.33
27	.65	.32	1.87	1.15	.32
28	.71	.35	2.66	1.02	.53
29	.67	.33	2.13	.80	.58
30	.49	.25	1.34	.19	.56
31	.25	.12	2.40	1.45	.41
32	.06	.03	2.13	1.14	.40
33	.30	.15	--	--	--
34	.35	.18	--	--	--
35	.36	.18	--	--	--
36	.37	.19	--	--	--
37	.38	.19	--	--	--
38	.34	.17	--	--	--
39	.25	.13	--	--	--
40	0.00	0.00	--	--	--

CONFIGURATION NUMBER 18

RUN NUMBER 18   RUN NUMBER 62

SOURCE DENSITY - NEUTRAL   SOURCE AT SPECIFIC GRAVITY OF
                                            LNG AT BOILOFF

SAMPLE POINT	NONDIMENSIONAL CONCENTRATION COEFFICIENT,K	MEAN CONCENTRATION PERCENT	PEAK PERCENT	CONCENTRATION MEAN PERCENT	RMS PERCENT
1	8.70	4.36	21.30	17.09	2.55
2	4.66	2.33	18.40	14.69	1.90
3	2.48	1.24	19.45	15.65	1.63
4	.81	.40	16.69	11.49	2.02
5	.17	.09	11.99	8.24	1.70
6	.01	.01	12.45	8.03	1.79
7	0.00	0.00	8.69	5.47	1.46
8	0.00	0.00	4.21	0.00	.59
9	1.99	1.00	4.97	3.15	.87
10	2.25	1.13	5.23	3.08	.81
11	1.58	.79	3.95	2.52	.63
12	.89	.45	4.72	2.59	.60
13	.37	.19	2.40	.01	.73
14	.13	.07	3.95	1.65	.85
15	.03	.02	3.44	1.49	.76
16	.00	.00	1.87	.54	.50
17	.84	.42	2.92	1.78	.48
18	1.25	.63	2.66	1.11	.58
19	1.20	.60	2.13	1.15	.51
20	.79	.40	2.66	1.61	.50
21	.51	.26	1.87	.87	.66
22	.24	.12	1.34	.21	.53
23	.10	.05	.81	0.00	.33
24	.02	.01	.27	0.00	.19
25	.29	.14	--	--	--
26	.44	.22	--	--	--
27	.56	.28	--	--	--
28	.55	.28	--	--	--
29	.55	.28	--	--	--
30	.31	.16	--	--	--
31	.20	.10	--	--	--
32	.08	.04	--	--	--
33	.12	.06	--	--	--
34	.20	.10	--	--	--
35	.27	.14	--	--	--
36	.32	.16	--	--	--
37	.32	.16	--	--	--
38	.28	.14	--	--	--
39	.21	.10	--	--	--
40	0.00	0.00	--	--	--

CONFIGURATION NUMBER 19

RUN NUMBER 19   RUN NUMBER 63

SOURCE DENSITY - NEUTRAL   SOURCE AT SPECIFIC GRAVITY OF
                                             LNG AT BOILOFF

SAMPLE POINT	NONDIMENSIONAL CONCENTRATION COEFFICIENT,K	MEAN CONCENTRATION PERCENT	PEAK PERCENT	CONCENTRATION MEAN PERCENT	RMS PERCENT
1	6.37	3.19	20.89	12.16	3.68
2	3.55	1.78	17.12	10.41	3.07
3	2.37	1.19	16.04	11.15	2.39
4	1.36	.68	12.45	8.77	1.66
5	.62	.31	11.53	7.10	1.35
6	.11	.06	10.12	7.21	1.40
7	.01	.00	8.20	5.69	1.62
8	0.00	0.00	5.98	.33	1.42
9	2.15	1.08	2.13	.79	.49
10	2.15	1.08	2.13	.98	.51
11	1.56	.78	2.92	1.15	.59
12	1.04	.52	3.44	1.87	.54
13	.63	.31	2.66	1.29	.56
14	.29	.14	1.34	0.00	.62
15	.05	.03	2.13	.38	.70
16	.00	.00	1.34	0.00	.60
17	1.06	.53	1.34	.47	.41
18	1.35	.68	1.07	0.00	.57
19	1.29	.65	1.61	.61	.36
20	1.02	.51	2.66	1.24	.43
21	.67	.34	3.44	1.87	.37
22	.44	.22	1.07	.01	.38
23	.15	.07	1.34	.15	.46
24	.02	.01	.81	0.00	.38
25	.44	.22	--	--	--
26	.58	.29	--	--	--
27	.65	.33	--	--	--
28	.68	.34	--	--	--
29	.65	.32	--	--	--
30	.48	.24	--	--	--
31	.30	.15	--	--	--
32	.08	.04	--	--	--
33	.19	.10	--	--	--
34	.27	.14	--	--	--
35	.35	.17	--	--	--
36	.39	.20	--	--	--
37	.39	.20	--	--	--
38	.37	.19	--	--	--
39	.31	.15	--	--	--
40	.00	.00	--	--	--

CONFIGURATION NUMBER 20

RUN NUMBER 20			RUN NUMBER 64	
SOURCE DENSITY - NEUTRAL			SOURCE AT SPECIFIC GRAVITY OF LNG AT BOILOFF	

SAMPLE POINT	NONDIMENSIONAL CONCENTRATION COEFFICIENT,K	MEAN CONCENTRATION PERCENT	PEAK PERCENT	CONCENTRATION MEAN PERCENT	RMS PERCENT
1	2.06	1.06	0.00	0.00	0.00
2	1.94	1.00	5.98	0.00	1.60
3	.97	.50	11.76	5.63	3.14
4	.57	.30	12.91	8.76	1.87
5	.39	.20	11.76	7.82	1.56
6	.04	.02	11.06	7.95	1.33
7	.00	.00	10.12	7.30	1.51
8	0.00	0.00	6.98	1.61	2.06
9	1.26	.65	.54	0.00	.12
10	1.44	.74	1.34	.20	.33
11	1.11	.57	2.92	1.04	.57
12	.61	.31	3.95	1.96	.72
13	.24	.13	3.18	1.24	.73
14	.09	.05	2.66	1.11	.76
15	.02	.01	2.92	1.21	.85
16	.00	.00	3.44	.74	.75
17	.78	.40	.27	0.00	.16
18	1.14	.59	1.34	.37	.30
19	1.10	.57	1.87	.42	.45
20	.79	.41	2.40	1.06	.44
21	.42	.22	2.40	1.41	.39
22	.19	.10	1.87	.65	.42
23	.06	.03	1.87	.74	.51
24	.01	.00	1.61	.21	.42
25	.34	.18	--	--	--
26	.56	.29	--	--	--
27	.71	.37	--	--	--
28	.68	.35	--	--	--
29	.70	.36	--	--	--
30	.36	.19	--	--	--
31	.21	.11	--	--	--
32	.07	.04	--	--	--
33	.16	.08	--	--	--
34	.28	.15	--	--	--
35	.41	.21	--	--	--
36	.46	.24	--	--	--
37	.43	.22	--	--	--
38	.35	.18	--	--	--
39	.27	.14	--	--	--
40	0.00	0.00	--	--	--

CONFIGURATION NUMBER 21

RUN NUMBER 21   RUN NUMBER 65

SOURCE DENSITY - NEUTRAL   SOURCE AT SPECIFIC GRAVITY OF
                                                LNG AT BOILOFF

SAMPLE POINT	NONDIMENSIONAL CONCENTRATION COEFFICIENT,K	MEAN CONCENTRATION PERCENT	PEAK PERCENT	CONCENTRATION MEAN PERCENT	RMS PERCENT
1	5.53	2.77	17.12	11.00	3.99
2	5.78	2.90	12.45	4.73	3.35
3	6.29	3.15	15.38	10.91	2.43
4	4.64	2.32	12.91	10.10	1.40
5	4.14	2.08	11.76	9.11	1.14
6	.74	.37	11.06	8.11	.91
7	.09	.05	11.99	8.18	1.23
8	0.00	0.00	8.93	5.52	1.89
9	1.30	.65	.81	.18	.11
10	1.76	.88	1.87	.16	.32
11	1.94	.97	1.87	.59	.45
12	2.04	1.02	4.21	2.13	.96
13	1.47	.74	5.23	3.61	.89
14	.74	.37	5.48	3.86	.81
15	.10	.05	4.97	3.05	.91
16	.00	.00	3.70	2.20	.71
17	.91	.45	.27	0.00	.16
18	1.10	.55	0.00	0.00	0.00
19	1.36	.68	1.34	.04	.35
20	1.34	.67	2.40	.86	.58
21	1.05	.53	1.61	.57	.47
22	.49	.25	1.87	.66	.47
23	.14	.07	1.87	.99	.36
24	.02	.01	2.13	.68	.50
25	.44	.22	--	--	--
26	.53	.26	--	--	--
27	.65	.33	--	--	--
28	.72	.36	--	--	--
29	.67	.33	--	--	--
30	.44	.22	--	--	--
31	.20	.10	--	--	--
32	.05	.03	--	--	--
33	.14	.07	--	--	--
34	.26	.13	--	--	--
35	.33	.16	--	--	--
36	.40	.20	--	--	--
37	.42	.21	--	--	--
38	.33	.16	--	--	--
39	.19	.09	--	--	--
40	0.00	0.00	--	--	--

CONFIGURATION NUMBER 22

	RUN NUMBER 22			RUN NUMBER 66	
	SOURCE DENSITY - NEUTRAL			SOURCE AT SPECIFIC GRAVITY OF LNG AT BOILOFF	
SAMPLE POINT	NONDIMENSIONAL CONCENTRATION COEFFICIENT,K	MEAN CONCENTRATION PERCENT	PEAK PERCENT	CONCENTRATION MEAN PERCENT	RMS PERCENT
1	9.45	4.74	21.23	18.37	1.54
2	5.04	2.53	19.45	16.23	1.76
3	2.04	1.02	20.89	17.48	1.54
4	.85	.42	16.90	13.67	1.81
5	.06	.03	12.22	9.65	1.58
6	.00	.00	10.59	8.21	1.28
7	0.00	0.00	11.30	7.75	1.46
8	0.00	0.00	10.36	6.61	1.58
9	2.01	1.01	4.21	2.04	.71
10	2.39	1.20	5.23	2.69	1.05
11	1.80	.90	4.21	2.17	.79
12	.89	.45	4.97	2.50	.92
13	.22	.11	3.18	1.13	.66
14	.02	.01	2.66	.74	.70
15	.00	.00	3.18	1.29	.55
16	0.00	0.00	2.92	1.19	.59
17	1.15	.58	1.07	.50	.20
18	1.41	.71	2.40	.81	.50
19	1.39	.70	2.66	1.15	.50
20	.91	.46	3.44	2.19	.53
21	.43	.21	2.92	1.50	.64
22	.07	.04	2.92	1.46	.59
23	.01	.00	1.87	1.01	.46
24	0.00	0.00	1.34	.33	.42
25	.52	.26	--	--	--
26	.65	.33	--	--	--
27	.68	.34	--	--	--
28	.66	.33	--	--	--
29	.63	.32	--	--	--
30	.56	.28	--	--	--
31	.05	.02	--	--	--
32	.01	.00	--	--	--
33	.21	.10	--	--	--
34	.32	.16	--	--	--
35	.35	.17	--	--	--
36	.34	.17	--	--	--
37	.29	.15	--	--	--
38	.19	.10	--	--	--
39	.09	.04	--	--	--
40	0.00	0.00	--	--	--

CONFIGURATION NUMBER   1

RUN NUMBER 23   RUN NUMBER 67

SOURCE DENSITY - NEUTRAL   SOURCE AT SPECIFIC GRAVITY OF
                                          LNG AT BOILOFF

SAMPLE POINT	NONDIMENSIONAL CONCENTRATION COEFFICIENT,K	MEAN CONCENTRATION PERCENT	PEAK PERCENT	CONCENTRATION MEAN PERCENT	RMS PERCENT
1	25.60	7.33	24.46	20.74	2.32
2	8.19	2.35	22.50	18.31	2.65
3	.30	.09	17.76	10.13	4.66
4	.00	.00	6.48	.49	1.15
5	0.00	0.00	1.07	.76	.10
6	0.00	0.00	.27	0.00	.12
7	0.00	0.00	0.00	0.00	0.00
8	0.00	0.00	.27	.08	.11
9	9.92	2.84	14.04	11.28	1.43
10	3.80	1.09	13.82	10.60	1.73
11	.71	.20	12.22	6.77	2.58
12	.02	.00	8.69	2.68	2.33
13	0.00	0.00	3.18	1.53	.32
14	0.00	0.00	.54	.33	.16
15	0.00	0.00	.81	.36	.16
16	0.00	0.00	0.00	0.00	0.00
17	5.01	1.43	9.17	6.96	1.21
18	2.32	.66	8.44	5.97	1.32
19	.74	.21	7.22	4.11	1.41
20	.06	.02	5.23	1.41	1.35
21	0.00	0.00	1.34	0.00	.55
22	0.00	0.00	.81	.36	.09
23	0.00	0.00	0.00	0.00	0.00
24	0.00	0.00	.27	0.00	.08
25	2.01	.58	4.97	3.96	.57
26	1.18	.34	5.23	3.67	.57
27	0.00	0.00	4.97	3.65	.60
28	.02	.01	4.72	2.55	.69
29	.13	.04	4.72	2.65	1.02
30	0.00	0.00	4.97	1.92	1.08
31	0.00	0.00	2.13	.25	.43
32	0.00	0.00	.27	0.00	.19
33	.94	.27	2.66	1.94	.38
34	.63	.18	3.70	2.24	.52
35	.33	.10	3.70	1.82	.77
36	.14	.04	2.66	1.47	.68
37	.03	.01	2.92	1.65	.63
38	.00	.00	1.61	.59	.42
39	0.00	0.00	1.07	.34	.22
40	0.00	0.00	.27	0.00	.21

CONFIGURATION NUMBER 2

| RUN NUMBER 24 | | | RUN NUMBER 68 | |
| SOURCE DENSITY - NEUTRAL | | | SOURCE AT SPECIFIC GRAVITY OF LNG AT BOILOFF | |

SAMPLE POINT	NONDIMENSIONAL CONCENTRATION COEFFICIENT, K	MEAN CONCENTRATION PERCENT	PEAK PERCENT	CONCENTRATION MEAN PERCENT	RMS PERCENT
1	2.88	.85	5.98	.92	.74
2	1.46	.43	16.47	3.20	2.23
3	.25	.07	20.48	7.18	3.99
4	.00	.00	16.69	4.91	3.74
5	.00	.00	5.73	1.28	.45
6	.00	.00	1.07	.74	.20
7	0.00	0.00	1.07	.46	.16
8	0.00	0.00	1.07	.50	.13
9	1.98	.58	1.07	.01	.24
10	1.57	.46	2.92	.71	.42
11	.79	.23	3.18	1.10	.61
12	.18	.05	7.71	2.22	.87
13	.01	.00	3.95	.58	.96
14	.00	.00	.54	0.00	.38
15	0.00	0.00	.27	.11	.15
16	0.00	0.00	.27	0.00	.18
17	1.55	.46	1.87	.96	.14
18	1.31	.39	1.34	.82	.19
19	.86	.25	1.61	.79	.31
20	.33	.10	2.66	1.19	.38
21	.05	.02	2.40	1.23	.40
22	.00	.00	2.66	1.26	.48
23	.00	.00	1.61	.83	.26
24	.00	.00	1.07	.33	.15
25	1.05	.31	1.34	.92	.17
26	.89	.26	1.07	.65	.15
27	.65	.19	1.07	.74	.15
28	.35	.10	1.07	.64	.14
29	.48	.14	1.07	.63	.20
30	.03	.01	1.87	1.30	.22
31	.00	.00	1.34	.61	.22
32	.00	.00	1.07	.64	.20
33	.66	.20	--	--	--
34	.57	.17	--	--	--
35	.42	.12	--	--	--
36	.25	.07	--	--	--
37	.11	.03	--	--	--
38	.03	.01	--	--	--
39	.01	.00	--	--	--
40	.00	.00	--	--	--

CONFIGURATION NUMBER 3

RUN NUMBER 25   RUN NUMBER 69

SOURCE DENSITY - NEUTRAL   SOURCE AT SPECIFIC GRAVITY OF
                                                        LNG AT BOILOFF

SAMPLE POINT	NONDIMENSIONAL CONCENTRATION COEFFICIENT,K	MEAN CONCENTRATION PERCENT	PEAK PERCENT	CONCENTRATION MEAN PERCENT	RMS PERCENT
1	13.74	4.03	19.86	12.10	4.69
2	12.30	3.60	19.86	10.58	4.04
3	3.99	1.17	17.76	10.85	3.62
4	.15	.04	11.53	4.93	3.24
5	.00	.00	5.48	0.00	1.05
6	.00	.00	.27	0.00	.11
7	0.00	0.00	.27	0.00	.11
8	0.00	0.00	.54	.18	.14
9	4.62	1.35	9.65	4.21	1.99
10	4.69	1.37	8.20	4.24	1.81
11	3.22	.94	8.20	3.75	1.94
12	.75	.22	7.47	3.75	1.58
13	.06	.02	6.73	2.68	1.50
14	.00	.00	6.23	2.27	1.22
15	0.00	0.00	1.61	0.00	.28
16	0.00	0.00	.27	0.00	.13
17	0.00	0.00	5.48	2.69	1.36
18	2.49	.73	6.98	3.13	1.47
19	0.00	0.00	4.47	2.53	.97
20	.71	.21	4.72	2.32	.84
21	.13	.04	3.18	1.55	.76
22	.01	.00	4.21	1.21	.95
23	0.00	0.00	2.13	.38	.50
24	0.00	0.00	.81	0.00	.18
25	1.16	.34	2.13	1.30	.31
26	1.10	.32	2.66	1.65	.38
27	.84	.25	2.13	1.16	.35
28	.44	.13	2.13	1.07	.31
29	.57	.17	2.13	1.27	.37
30	.05	.01	2.40	1.61	.38
31	.01	.00	2.13	1.18	.35
32	0.00	0.00	1.34	.24	.33
33	.65	.19	--	--	--
34	.56	.16	--	--	--
35	.40	.12	--	--	--
36	.24	.07	--	--	--
37	.12	.03	--	--	--
38	.05	.01	--	--	--
39	.01	.00	--	--	--
40	0.00	0.00	--	--	--

CONFIGURATION NUMBER   4

RUN NUMBER 26

RUN NUMBER 70

SOURCE DENSITY - NEUTRAL

SOURCE AT SPECIFIC GRAVITY OF
LNG AT BOILOFF

SAMPLE POINT	NONDIMENSIONAL CONCENTRATION COEFFICIENT,K	MEAN CONCENTRATION PERCENT	PEAK PERCENT	CONCENTRATION MEAN PERCENT	RMS PERCENT
1	3.69	1.05	20.07	8.30	4.01
2	3.24	.93	16.47	6.77	3.78
3	2.83	.81	16.04	7.54	3.39
4	.82	.23	11.76	5.29	2.63
5	.11	.03	7.47	1.79	1.99
6	.00	.00	.27	0.00	.19
7	0.00	0.00	0.00	0.00	0.00
8	0.00	0.00	0.00	0.00	0.00
9	1.65	.47	6.48	2.89	1.24
10	1.54	.44	6.73	2.97	1.53
11	1.54	.44	7.47	2.57	1.29
12	1.25	.36	7.47	3.36	1.30
13	.49	.14	4.72	2.22	1.22
14	.09	.03	3.44	.07	.75
15	.01	.00	1.61	0.00	.19
16	.00	.00	0.00	0.00	0.00
17	1.09	.31	3.44	1.25	.39
18	1.04	.30	2.92	1.20	.45
19	1.03	.29	2.66	1.32	.48
20	.91	.26	2.66	1.20	.46
21	.59	.17	2.66	1.27	.45
22	.17	.05	2.13	.92	.43
23	.04	.01	1.61	.50	.34
24	.01	.00	1.34	.53	.22
25	.69	.20	1.07	.66	.15
26	.63	.18	1.87	.83	.22
27	.61	.17	1.34	.46	.27
28	.60	.17	1.87	.90	.35
29	.57	.16	2.13	.94	.46
30	.30	.09	1.61	.72	.41
31	.11	.03	1.61	.67	.35
32	.03	.01	.81	.28	.21
33	.45	.13	--	--	--
34	.42	.12	--	--	--
35	.39	.11	--	--	--
36	.38	.11	--	--	--
37	.35	.10	--	--	--
38	.26	.08	--	--	--
39	.14	.04	--	--	--
40	.00	.00	--	--	--

CONFIGURATION NUMBER 5

RUN NUMBER 27	RUN NUMBER 71
SOURCE DENSITY - NEUTRAL	SOURCE AT SPECIFIC GRAVITY OF LNG AT BOILOFF

SAMPLE POINT	NONDIMENSIONAL CONCENTRATION COEFFICIENT, K	MEAN CONCENTRATION PERCENT	PEAK PERCENT	CONCENTRATION MEAN PERCENT	RMS PERCENT
1	1.95	.54	3.44	.85	.43
2	1.53	.43	7.71	1.14	1.26
3	.68	.19	11.53	3.27	2.05
4	.09	.03	10.59	3.32	1.90
5	.00	.00	6.48	.53	1.47
6	0.00	0.00	0.00	0.00	0.00
7	0.00	0.00	0.00	0.00	0.00
8	0.00	0.00	0.00	0.00	0.00
9	1.41	.39	1.34	.50	.19
10	1.28	.36	2.92	1.37	.37
11	.97	.27	2.13	1.00	.35
12	.35	.10	3.18	1.54	.46
13	.06	.02	3.70	1.64	.72
14	.00	.00	2.40	.77	.48
15	0.00	0.00	2.13	.74	.21
16	0.00	0.00	.54	.30	.16
17	1.19	.33	1.87	1.04	.16
18	1.10	.31	2.40	1.10	.32
19	.92	.26	2.92	1.54	.24
20	.43	.12	2.13	1.25	.30
21	.13	.04	2.92	1.88	.35
22	.02	.00	3.44	2.03	.43
23	.00	.00	1.34	.49	.20
24	0.00	0.00	1.07	.58	.15
25	.82	.23	1.87	1.53	.18
26	.77	.21	.81	0.00	.12
27	.64	.18	1.34	.96	.11
28	.40	.11	.81	.36	.11
29	.53	.15	.27	0.00	.22
30	.04	.01	1.07	.65	.18
31	.01	.00	.54	0.00	.22
32	.00	.00	1.07	.32	.17
33	.54	.15	--	--	--
34	.52	.14	--	--	--
35	.45	.12	--	--	--
36	.28	.08	--	--	--
37	.13	.04	--	--	--
38	.04	.01	--	--	--
39	.01	.00	--	--	--
40	0.00	0.00	--	--	--

CONFIGURATION NUMBER 6

RUN NUMBER 28   RUN NUMBER 72

SOURCE DENSITY - NEUTRAL   SOURCE AT SPECIFIC GRAVITY OF
                                                    LNG AT BOILOFF

SAMPLE POINT	NONDIMENSIONAL CONCENTRATION COEFFICIENT,K	MEAN CONCENTRATION PERCENT	PEAK PERCENT	CONCENTRATION MEAN PERCENT	RMS PERCENT
1	.64	.18	1.34	.73	.15
2	.76	.22	4.97	1.29	.66
3	2.03	.59	8.93	2.93	1.85
4	1.75	.50	16.47	8.37	2.95
5	.02	.01	14.27	9.51	2.75
6	.00	.00	14.04	3.16	4.72
7	.00	.00	1.87	.27	.14
8	0.00	0.00	.27	0.00	.14
9	.58	.17	.81	.20	.10
10	.77	.22	2.13	0.00	.30
11	1.33	.38	3.95	.99	.82
12	1.06	.31	7.71	3.93	1.69
13	.12	.04	8.93	5.39	1.56
14	.01	.00	7.47	3.51	2.11
15	.00	.00	4.97	.55	.84
16	.00	.00	.81	.41	.17
17	.51	.15	1.07	.69	.11
18	.56	.16	2.13	.66	.28
19	.76	.22	2.40	.99	.38
20	.76	.22	3.44	1.58	.65
21	.31	.09	4.21	2.55	.75
22	.02	.01	5.23	3.02	1.10
23	.00	.00	4.21	.96	1.07
24	.00	.00	.81	.27	.10
25	.43	.12	.81	.51	.09
26	.42	.12	1.61	.19	.18
27	.44	.13	1.07	.60	.18
28	.43	.12	1.87	.96	.24
29	.43	.12	2.40	1.76	.28
30	.11	.03	2.40	1.41	.36
31	.01	.00	1.87	.77	.42
32	0.00	0.00	1.61	.50	.27
33	.35	.10	--	--	--
34	.32	.09	--	--	--
35	.31	.09	--	--	--
36	.28	.08	--	--	--
37	.19	.05	--	--	--
38	.09	.03	--	--	--
39	.03	.01	--	--	--
40	.00	.00	--	--	--

CONFIGURATION NUMBER 7

	RUN NUMBER 29			RUN NUMBER 73	
	SOURCE DENSITY - NEUTRAL			SOURCE AT SPECIFIC GRAVITY OF LNG AT BOILOFF	
SAMPLE POINT	NONDIMENSIONAL CONCENTRATION COEFFICIENT,K	MEAN CONCENTRATION PERCENT	PEAK PERCENT	CONCENTRATION MEAN PERCENT	RMS PERCENT
1	10.87	3.23	12.91	8.49	2.07
2	10.17	3.02	12.22	8.33	1.99
3	3.99	1.18	16.69	12.97	2.18
4	.08	.02	18.40	12.38	4.10
5	0.00	0.00	10.83	1.60	2.81
6	0.00	0.00	0.00	0.00	0.00
7	0.00	0.00	.54	.20	.11
8	0.00	0.00	0.00	0.00	0.00
9	.91	.27	.54	.40	.08
10	1.33	.39	1.34	0.00	.35
11	2.48	.74	3.70	.95	.79
12	1.57	.47	7.96	4.50	1.31
13	.03	.01	9.41	6.71	1.95
14	0.00	0.00	9.17	1.77	2.53
15	0.00	0.00	.81	.56	.08
16	.00	.00	.54	.21	.11
17	.78	.23	1.07	.42	.13
18	.88	.26	2.40	.43	.44
19	1.27	.38	3.18	1.07	.63
20	.83	.25	4.21	2.61	.69
21	.13	.04	5.48	3.32	1.47
22	.00	.00	5.98	2.59	2.20
23	0.00	0.00	5.23	.41	1.25
24	.00	.00	.27	.02	.12
25	.54	.16	.27	0.00	.13
26	.55	.16	1.61	.57	.33
27	.57	.17	1.87	.69	.39
28	.47	.14	2.13	1.30	.41
29	.54	.16	2.92	1.76	.51
30	.09	.03	2.13	.84	.64
31	.01	.00	2.40	.62	.54
32	.00	.00	.54	0.00	.12
33	.42	.12	1.34	.98	.16
34	.39	.12	.81	.01	.20
35	.36	.11	1.07	.24	.18
36	.29	.09	.81	.28	.20
37	.21	.06	.54	0.00	.21
38	.09	.03	.27	0.00	.22
39	.03	.01	.27	0.00	.21
40	0.00	0.00	.54	0.00	.23

CONFIGURATION NUMBER 8

	RUN NUMBER 30			RUN NUMBER 74	
	SOURCE DENSITY - NEUTRAL			SOURCE AT SPECIFIC GRAVITY OF LNG AT BOILOFF	

SAMPLE POINT	NONDIMENSIONAL CONCENTRATION COEFFICIENT,K	MEAN CONCENTRATION PERCENT	PEAK PERCENT	CONCENTRATION MEAN PERCENT	RMS PERCENT
1	24.78	7.13	22.30	19.69	1.40
2	11.78	3.39	20.89	16.73	2.43
3	.67	.19	17.12	9.60	4.01
4	.00	.00	6.98	1.03	1.97
5	0.00	0.00	0.00	0.00	0.00
6	0.00	0.00	0.00	0.00	0.00
7	0.00	0.00	0.00	0.00	0.00
8	0.00	0.00	0.00	0.00	0.00
9	7.98	2.27	9.41	6.57	1.42
10	7.75	2.23	10.36	6.46	1.40
11	5.45	1.57	11.06	7.87	1.67
12	.88	.25	11.30	6.49	2.72
13	.02	.00	4.21	.51	.76
14	0.00	0.00	.54	.13	.11
15	0.00	0.00	0.00	0.00	0.00
16	.00	.00	0.00	0.00	0.00
17	1.09	.31	2.13	1.44	.21
18	1.51	.43	3.95	1.07	.49
19	2.66	.76	3.70	1.56	.67
20	2.81	.81	6.98	3.51	1.13
21	.37	.11	6.98	3.86	1.71
22	.00	.00	4.21	.64	.57
23	0.00	0.00	.54	.41	.10
24	0.00	0.00	.81	.61	.11
25	.67	.19	1.07	.55	.17
26	.70	.20	.81	.19	.22
27	.93	.27	1.61	.48	.36
28	1.17	.34	2.40	1.30	.47
29	1.07	.31	3.18	1.84	.68
30	.23	.07	3.95	1.70	1.06
31	.02	.01	3.18	.68	.51
32	.00	.00	.54	.12	.20
33	.51	.15	1.07	.70	.12
34	.49	.14	1.07	.09	.29
35	.52	.15	.81	.15	.23
36	.61	.17	1.34	.54	.22
37	.56	.16	1.34	.42	.25
38	.37	.11	1.61	.87	.30
39	.14	.04	1.61	.63	.34
40	0.00	0.00	1.61	.55	.32

CONFIGURATION NUMBER 10

RUN NUMBER 32   RUN NUMBER 76

SOURCE DENSITY - NEUTRAL   SOURCE AT SPECIFIC GRAVITY OF
                                           LNG AT BOILOFF

SAMPLE POINT	NONDIMENSIONAL CONCENTRATION COEFFICIENT,K	MEAN CONCENTRATION PERCENT	PEAK PERCENT	CONCENTRATION MEAN PERCENT	RMS PERCENT
1	2.58	.73	5.73	.77	.50
2	2.13	.60	10.12	2.76	1.82
3	.72	.20	20.27	8.03	3.87
4	.02	.01	17.97	8.03	3.70
5	.00	.00	14.27	.80	2.85
6	0.00	0.00	1.07	.65	.20
7	.00	.00	.54	.12	.12
8	.00	.00	.54	.10	.15
9	1.90	.54	1.34	.34	.17
10	1.65	.47	3.18	.89	.40
11	1.31	.37	4.47	1.04	.89
12	.42	.12	6.48	2.75	1.27
13	.03	.01	8.93	2.62	1.85
14	.00	.00	2.40	.01	.48
15	.00	.00	.27	.04	.08
16	.00	.00	0.00	0.00	0.00
17	1.54	.44	.54	.01	.14
18	1.29	.37	1.61	.44	.29
19	1.04	.30	1.61	.63	.32
20	.59	.17	2.92	1.25	.46
21	.12	.04	4.21	2.23	.75
22	.01	.00	2.13	.06	.65
23	.00	.00	1.87	.08	.39
24	.00	.00	.81	0.00	.27
25	1.08	.31	--	--	--
26	.92	.26	--	--	--
27	.77	.22	--	--	--
28	.54	.15	--	--	--
29	.63	.18	--	--	--
30	.07	.02	--	--	--
31	.01	.00	--	--	--
32	.00	.00	--	--	--
33	.75	.21	--	--	--
34	.68	.19	--	--	--
35	.58	.17	--	--	--
36	.42	.12	--	--	--
37	.23	.07	--	--	--
38	.09	.02	--	--	--
39	.02	.01	--	--	--
40	.00	.00	--	--	--

CONFIGURATION NUMBER 11

RUN NUMBER 33   RUN NUMBER 77

SOURCE DENSITY - NEUTRAL   SOURCE AT SPECIFIC GRAVITY OF
                                              LNG AT BOILOFF

SAMPLE POINT	NONDIMENSIONAL CONCENTRATION COEFFICIENT,K	MEAN CONCENTRATION PERCENT	PEAK PERCENT	CONCENTRATION MEAN PERCENT	RMS PERCENT
1	1.82	.51	9.41	2.88	2.02
2	.50	.14	15.60	6.10	2.86
3	.05	.01	18.19	3.74	2.79
4	.10	.03	10.59	2.51	2.21
5	.00	.00	7.22	1.13	1.25
6	0.00	0.00	.27	0.00	.16
7	0.00	0.00	.81	.60	.07
8	.00	.00	.81	.48	.12
9	1.23	.35	2.66	1.19	.45
10	.53	.15	3.95	1.62	.71
11	.33	.09	2.92	1.17	.32
12	.15	.04	1.34	.51	.19
13	.01	.00	1.61	.49	.35
14	.00	.00	2.40	.15	.60
15	0.00	0.00	1.87	0.00	.29
16	.00	.00	0.00	0.00	0.00
17	1.18	.33	.54	0.00	.14
18	.87	.25	.81	0.00	.25
19	.62	.18	.81	.13	.23
20	.41	.12	1.34	.35	.21
21	.18	.05	1.87	1.16	.19
22	.05	.01	2.40	1.20	.32
23	.01	.00	1.87	.69	.31
24	.00	.00	1.34	.65	.12
25	.81	.23	--	--	--
26	.65	.19	--	--	--
27	.55	.16	--	--	--
28	.45	.13	--	--	--
29	.48	.14	--	--	--
30	.21	.06	--	--	--
31	.07	.02	--	--	--
32	.02	.01	--	--	--
33	.54	.15	--	--	--
34	.47	.13	--	--	--
35	.41	.11	--	--	--
36	.35	.10	--	--	--
37	.29	.08	--	--	--
38	.22	.06	--	--	--
39	.12	.03	--	--	--
40	0.00	0.00	--	--	--

CONFIGURATION NUMBER 12

RUN NUMBER 34   RUN NUMBER 78

SOURCE DENSITY - NEUTRAL   SOURCE AT SPECIFIC GRAVITY OF
                                                        LNG AT BOILOFF

SAMPLE POINT	NONDIMENSIONAL CONCENTRATION COEFFICIENT,K	MEAN CONCENTRATION PERCENT	PEAK PERCENT	CONCENTRATION MEAN PERCENT	RMS PERCENT
1	2.78	.86	11.99	1.72	1.56
2	1.76	.54	19.65	5.85	3.62
3	.44	.14	20.68	10.55	4.24
4	.03	.01	15.82	3.03	3.51
5	0.00	0.00	.81	.55	.13
6	0.00	0.00	.54	.19	.19
7	0.00	0.00	.27	0.00	.12
8	.00	.00	.27	0.00	.14
9	1.86	.58	1.34	.27	.19
10	1.71	.53	2.13	0.00	.36
11	1.33	.41	1.87	.58	.50
12	.58	.18	4.47	2.06	.83
13	.13	.04	3.70	1.38	.96
14	.01	.00	1.34	0.00	.42
15	0.00	0.00	0.00	0.00	0.00
16	0.00	0.00	0.00	0.00	0.00
17	1.20	.37	.27	0.00	.14
18	1.25	.39	1.07	.28	.33
19	1.28	.40	1.34	.49	.30
20	.97	.30	1.87	.85	.27
21	.38	.12	2.40	1.23	.43
22	.07	.02	2.13	1.06	.56
23	.00	.00	2.40	.66	.38
24	0.00	0.00	.81	.49	.19
25	.79	.25	--	--	--
26	.78	.24	--	--	--
27	.77	.24	--	--	--
28	.73	.23	--	--	--
29	.72	.22	--	--	--
30	.23	.07	--	--	--
31	.06	.02	--	--	--
32	.01	.00	--	--	--
33	.77	.24	--	--	--
34	.56	.17	--	--	--
35	.55	.17	--	--	--
36	.52	.16	--	--	--
37	.44	.14	--	--	--
38	.26	.08	--	--	--
39	.10	.03	--	--	--
40	0.00	0.00	--	--	--

CONFIGURATION NUMBER 13

RUN NUMBER 35   RUN NUMBER 79

SOURCE DENSITY - NEUTRAL   SOURCE AT SPECIFIC GRAVITY OF
                                                          LNG AT BOILOFF

SAMPLE POINT	NONDIMENSIONAL CONCENTRATION COEFFICIENT,K	MEAN CONCENTRATION PERCENT	PEAK PERCENT	CONCENTRATION MEAN PERCENT	RMS PERCENT
1	2.32	.68	5.48	1.30	.76
2	4.54	1.33	17.97	7.95	4.50
3	6.51	1.91	17.97	12.75	3.28
4	.68	.20	13.37	6.05	3.42
5	.02	.01	4.21	.15	.70
6	0.00	0.00	0.00	0.00	0.00
7	0.00	0.00	0.00	0.00	0.00
8	.00	.00	.27	0.00	.13
9	1.32	.39	3.70	.74	.62
10	1.64	.48	7.22	2.67	1.67
11	2.28	.67	7.71	4.36	1.54
12	1.14	.33	9.65	4.30	1.94
13	.24	.07	7.96	2.30	2.30
14	.02	.00	3.44	0.00	1.05
15	0.00	0.00	.54	0.00	.24
16	0.00	0.00	0.00	0.00	0.00
17	.98	.29	1.87	.84	.32
18	1.07	.31	3.70	1.76	.59
19	1.21	.35	5.48	2.81	1.10
20	.81	.24	5.23	2.99	1.08
21	.31	.09	4.72	2.33	1.03
22	.04	.01	2.92	.84	.66
23	.00	.00	.81	.22	.17
24	0.00	0.00	1.07	.30	.30
25	.65	.19	--	--	--
26	.67	.20	--	--	--
27	.57	.17	--	--	--
28	.39	.11	--	--	--
29	.45	.13	--	--	--
30	.07	.02	--	--	--
31	.01	.00	--	--	--
32	.00	.00	--	--	--
33	.46	.13	--	--	--
34	.42	.12	--	--	--
35	.34	.10	--	--	--
36	.25	.07	--	--	--
37	.15	.04	--	--	--
38	.06	.02	--	--	--
39	.02	.01	--	--	--
40	0.00	0.00	--	--	--

CONFIGURATION NUMBER 14

	RUN NUMBER 36			RUN NUMBER 80	
	SOURCE DENSITY - NEUTRAL			SOURCE AT SPECIFIC GRAVITY OF LNG AT BOILOFF	

SAMPLE POINT	NONDIMENSIONAL CONCENTRATION COEFFICIENT,K	MEAN CONCENTRATION PERCENT	PEAK PERCENT	CONCENTRATION MEAN PERCENT	RMS PERCENT
1	2.46	.72	4.97	1.02	.82
2	3.22	.94	16.47	6.80	4.11
3	5.51	1.61	19.03	11.09	3.58
4	1.31	.38	15.60	6.15	4.04
5	.07	.02	8.20	.58	1.12
6	.00	.00	.81	.34	.19
7	.00	.00	.54	.51	.09
8	.00	.00	.54	.29	.11
9	1.29	.38	4.47	1.11	.76
10	1.35	.39	7.22	3.43	1.34
11	1.80	.53	7.96	3.76	1.79
12	1.80	.53	6.73	3.80	1.41
13	.50	.15	9.17	4.15	1.96
14	.08	.02	6.48	2.79	1.06
15	.00	.00	1.61	1.12	.15
16	.00	.00	1.07	.84	.11
17	.97	.28	1.61	.39	.34
18	.94	.27	1.61	.54	.44
19	1.06	.31	2.66	1.14	.64
20	1.13	.33	4.21	2.30	.90
21	.64	.19	3.70	1.54	.89
22	.16	.05	3.95	1.08	.95
23	.02	.01	2.92	.88	.51
24	.00	.00	.54	.04	.15
25	.68	.20	--	--	--
26	.61	.18	--	--	--
27	.62	.18	--	--	--
28	.61	.18	--	--	--
29	.60	.18	--	--	--
30	.29	.09	--	--	--
31	.09	.03	--	--	--
32	.02	.01	--	--	--
33	.00	.00	--	--	--
34	.46	.13	--	--	--
35	.45	.13	--	--	--
36	.41	.12	--	--	--
37	.36	.10	--	--	--
38	.24	.07	--	--	--
39	.12	.03	--	--	--
40	.00	.00	--	--	--

CONFIGURATION NUMBER 15

	RUN NUMBER 37			RUN NUMBER 81	
	SOURCE DENSITY - NEUTRAL			SOURCE AT SPECIFIC GRAVITY OF LNG AT BOILOFF	
SAMPLE POINT	NONDIMENSIONAL CONCENTRATION COEFFICIENT,K	MEAN CONCENTRATION PERCENT	PEAK PERCENT	CONCENTRATION MEAN PERCENT	RMS PERCENT
1	2.84	.81	8.69	2.30	1.18
2	1.49	.43	13.59	5.31	2.31
3	.41	.12	15.60	7.15	2.61
4	.02	.01	6.98	1.30	1.56
5	.00	.00	1.07	.49	.25
6	0.00	0.00	.54	0.00	.29
7	0.00	0.00	.27	0.00	.12
8	.01	.00	.27	0.00	.11
9	2.28	.65	2.13	.88	.25
10	1.76	.50	4.21	2.12	.59
11	.84	.24	4.72	2.80	.73
12	.09	.03	4.72	1.29	1.03
13	.01	.00	4.47	1.11	.51
14	.00	.00	1.34	.36	.18
15	0.00	0.00	.81	.44	.09
16	.00	.00	.81	.50	.14
17	1.85	.53	1.61	.84	.24
18	1.59	.45	2.66	1.37	.52
19	1.01	.29	3.44	2.08	.46
20	.13	.04	2.66	1.26	.52
21	.02	.01	2.66	1.30	.41
22	.00	.00	1.87	.77	.40
23	.00	.00	1.07	.51	.16
24	.00	.00	1.07	.43	.18
25	1.31	.37	--	--	--
26	1.19	.34	--	--	--
27	.82	.23	--	--	--
28	.24	.07	--	--	--
29	.42	.12	--	--	--
30	.02	.01	--	--	--
31	.00	.00	--	--	--
32	.00	.00	--	--	--
33	.00	.00	--	--	--
34	.83	.24	--	--	--
35	.60	.17	--	--	--
36	.26	.07	--	--	--
37	.10	.03	--	--	--
38	.03	.01	--	--	--
39	.01	.00	--	--	--
40	0.00	0.00	--	--	--

CONFIGURATION NUMBER 16

RUN NUMBER 38   RUN NUMBER 82

SOURCE DENSITY - NEUTRAL   SOURCE AT SPECIFIC GRAVITY OF
                                                        LNG AT BOILOFF

SAMPLE POINT	NONDIMENSIONAL CONCENTRATION COEFFICIENT,K	MEAN CONCENTRATION PERCENT	PEAK PERCENT	CONCENTRATION MEAN PERCENT	RMS PERCENT
1	1.51	.42	5.48	1.00	.66
2	3.04	.86	11.06	2.69	1.97
3	7.16	2.01	16.90	8.72	3.21
4	1.81	.51	16.90	9.77	4.15
5	0.00	0.00	11.06	2.48	2.59
6	0.00	0.00	2.13	0.00	.42
7	0.00	0.00	.27	.06	.12
8	.00	.00	.81	.40	.14
9	.76	.21	1.07	.26	.18
10	.85	.24	4.47	1.50	.45
11	1.48	.42	6.23	2.28	1.37
12	2.43	.68	8.44	4.23	1.52
13	.56	.15	7.96	3.10	1.81
14	.03	.01	6.73	.77	1.29
15	0.00	0.00	4.47	.11	.62
16	.00	.00	.27	0.00	.11
17	.71	.20	1.34	.19	.22
18	.73	.21	2.40	.62	.49
19	1.09	.31	3.95	1.52	.90
20	1.28	.36	3.44	2.23	.60
21	.51	.14	4.21	2.61	.64
22	.07	.02	3.95	1.62	.99
23	.00	.00	2.13	.13	.44
24	.00	.00	0.00	0.00	0.00
25	.50	.14	--	--	--
26	.51	.14	--	--	--
27	.59	.17	--	--	--
28	.73	.20	--	--	--
29	.66	.19	--	--	--
30	.19	.05	--	--	--
31	.02	.01	--	--	--
32	.00	.00	--	--	--
33	.00	.00	--	--	--
34	.43	.12	--	--	--
35	.43	.12	--	--	--
36	.46	.13	--	--	--
37	.34	.10	--	--	--
38	.17	.05	--	--	--
39	.04	.01	--	--	--
40	0.00	0.00	--	--	--

CONFIGURATION NUMBER 17

	RUN NUMBER 39			RUN NUMBER 83	
	SOURCE DENSITY - NEUTRAL			SOURCE AT SPECIFIC GRAVITY OF LNG AT BOILOFF	
SAMPLE POINT	NONDIMENSIONAL CONCENTRATION COEFFICIENT,K	MEAN CONCENTRATION PERCENT	PEAK PERCENT	CONCENTRATION MEAN PERCENT	RMS PERCENT
1	2.40	.69	4.21	1.13	.62
2	5.84	1.69	16.47	8.19	4.34
3	5.30	1.53	18.61	14.25	2.71
4	.13	.04	14.94	6.44	4.50
5	.00	.00	8.44	1.27	1.40
6	0.00	0.00	1.07	.42	.19
7	0.00	0.00	.54	.25	.20
8	.00	.00	.27	0.00	.28
9	1.70	.49	1.87	.66	.34
10	1.94	.56	4.21	1.56	.55
11	2.81	.81	5.98	3.01	1.24
12	1.14	.33	8.93	5.69	1.44
13	.08	.02	7.71	4.36	1.68
14	.00	.00	5.73	1.50	1.23
15	0.00	0.00	1.87	.55	.26
16	.00	.00	.81	.28	.22
17	.75	.22	1.07	.71	.09
18	.87	.25	2.66	.81	.28
19	1.23	.35	2.92	1.02	.60
20	1.31	.38	5.98	2.60	1.06
21	.31	.09	5.73	3.62	1.10
22	.02	.01	4.97	1.70	1.57
23	0.00	0.00	2.92	.96	.53
24	0.00	0.00	1.07	.84	.18
25	.55	.16	1.61	.98	.15
26	.58	.17	1.61	.85	.30
27	.70	.20	2.66	1.53	.37
28	.63	.18	1.61	.98	.36
29	.70	.20	2.13	1.33	.38
30	.07	.02	2.40	1.40	.50
31	.00	.00	1.87	.36	.55
32	.00	.00	1.61	.12	.42
33	0.00	0.00	--	--	--
34	.44	.13	--	--	--
35	.46	.13	--	--	--
36	.40	.12	--	--	--
37	.24	.07	--	--	--
38	.09	.03	--	--	--
39	.02	.00	--	--	--
40	0.00	0.00	--	--	--

CONFIGURATION NUMBER 18

RUN NUMBER 40   RUN NUMBER 84

SOURCE DENSITY - NEUTRAL   SOURCE AT SPECIFIC GRAVITY OF
                                              LNG AT BOILOFF

SAMPLE POINT	NONDIMENSIONAL CONCENTRATION COEFFICIENT,K	MEAN CONCENTRATION PERCENT	PEAK PERCENT	CONCENTRATION MEAN PERCENT	RMS PERCENT
1	5.86	1.72	21.70	12.38	4.54
2	4.11	1.21	16.90	9.52	2.41
3	3.68	1.08	17.97	10.21	3.10
4	1.13	.33	11.99	5.83	2.37
5	.15	.04	4.72	1.28	.93
6	.01	.00	.81	0.00	.25
7	.00	.00	.27	0.00	.16
8	.00	.00	0.00	0.00	0.00
9	1.90	.56	3.44	1.25	.51
10	1.54	.45	4.97	2.42	.69
11	1.30	.38	3.44	1.99	.58
12	1.06	.31	3.44	1.74	.67
13	.45	.13	2.40	.56	.67
14	.11	.03	2.13	.87	.48
15	.01	.00	1.34	.85	.25
16	.00	.00	1.07	.49	.33
17	1.33	.39	3.44	1.68	.49
18	1.10	.32	3.95	2.10	.62
19	.96	.28	3.18	2.01	.40
20	.83	.24	2.66	1.73	.36
21	.55	.16	1.34	.38	.43
22	.22	.07	2.40	1.38	.36
23	.05	.02	1.07	.76	.12
24	.01	.00	1.34	.82	.12
25	.87	.25	--	--	--
26	.72	.21	--	--	--
27	.61	.18	--	--	--
28	.55	.16	--	--	--
29	.58	.17	--	--	--
30	.35	.10	--	--	--
31	.20	.06	--	--	--
32	.07	.02	--	--	--
33	.00	.00	--	--	--
34	.54	.16	--	--	--
35	.45	.13	--	--	--
36	.41	.12	--	--	--
37	.33	.10	--	--	--
38	.30	.09	--	--	--
39	.22	.07	--	--	--
40	.00	.00	--	--	--

CONFIGURATION NUMBER 19

RUN NUMBER 41   RUN NUMBER 85

SOURCE DENSITY - NEUTRAL   SOURCE AT SPECIFIC GRAVITY OF
                                              LNG AT BOILOFF

SAMPLE POINT	NONDIMENSIONAL CONCENTRATION COEFFICIENT,K	MEAN CONCENTRATION PERCENT	PEAK PERCENT	CONCENTRATION MEAN PERCENT	RMS PERCENT
1	3.98	1.15	18.40	6.44	3.99
2	2.70	.78	11.99	5.85	2.53
3	2.50	.73	14.94	7.60	2.86
4	1.28	.37	12.45	5.42	2.58
5	.30	.09	7.22	2.67	1.42
6	.02	.01	1.61	0.00	.46
7	0.00	0.00	.27	.04	.13
8	.00	.00	0.00	0.00	0.00
9	1.81	.53	2.40	.99	.42
10	1.48	.43	3.18	1.73	.57
11	1.34	.39	3.95	1.89	.50
12	1.01	.29	3.70	2.13	.49
13	.48	.14	3.44	1.96	.66
14	.13	.04	1.87	.45	.56
15	.01	.00	1.07	.04	.34
16	.00	.00	.81	.06	.33
17	1.31	.38	1.87	.95	.29
18	1.14	.33	2.13	1.49	.32
19	.98	.28	1.87	1.19	.31
20	.88	.25	2.13	1.17	.35
21	.56	.16	2.13	.93	.39
22	.21	.06	2.13	.85	.40
23	.04	.01	.81	.12	.21
24	.01	.00	.54	.05	.19
25	.87	.25	--	--	--
26	.79	.23	--	--	--
27	.72	.21	--	--	--
28	.66	.19	--	--	--
29	.69	.20	--	--	--
30	.35	.10	--	--	--
31	.13	.04	--	--	--
32	.04	.01	--	--	--
33	.00	.00	--	--	--
34	.57	.16	--	--	--
35	.52	.15	--	--	--
36	.48	.14	--	--	--
37	.46	.13	--	--	--
38	.35	.10	--	--	--
39	.19	.05	--	--	--
40	0.00	0.00	--	--	--

CONFIGURATION NUMBER 20

	RUN NUMBER 42			RUN NUMBER 86	
	SOURCE DENSITY - NEUTRAL			SOURCE AT SPECIFIC GRAVITY OF LNG AT BOILOFF	

SAMPLE POINT	NONDIMENSIONAL CONCENTRATION COEFFICIENT,K	MEAN CONCENTRATION PERCENT	PEAK PERCENT	CONCENTRATION MEAN PERCENT	RMS PERCENT
1	3.38	.97	6.73	.87	.68
2	2.91	.83	5.23	1.54	1.06
3	.95	.27	13.82	3.83	1.81
4	.76	.22	9.88	3.56	1.60
5	.45	.13	2.40	0.00	.87
6	.03	.01	2.13	.39	.47
7	0.00	0.00	.54	.16	.15
8	0.00	0.00	.27	.17	.11
9	2.34	.67	.81	.13	.22
10	2.06	.59	1.87	.52	.39
11	1.61	.46	2.92	.90	.38
12	1.05	.30	2.92	1.66	.36
13	.42	.12	2.66	1.35	.62
14	.09	.03	2.66	1.12	.57
15	.00	.00	1.61	.61	.30
16	0.00	0.00	1.61	.81	.33
17	1.86	.53	1.07	.45	.12
18	1.77	.51	1.07	.33	.20
19	1.50	.43	1.34	.47	.19
20	1.18	.34	1.34	.74	.20
21	.56	.16	2.13	1.45	.22
22	.14	.04	1.87	.67	.46
23	.03	.01	1.61	.83	.35
24	.00	.00	1.87	.91	.26
25	1.22	.35	--	--	--
26	1.23	.35	--	--	--
27	1.11	.32	--	--	--
28	.99	.28	--	--	--
29	1.02	.29	--	--	--
30	.36	.10	--	--	--
31	.09	.03	--	--	--
32	.02	.01	--	--	--
33	.83	.24	--	--	--
34	.81	.23	--	--	--
35	.78	.22	--	--	--
36	.71	.20	--	--	--
37	.63	.18	--	--	--
38	.44	.13	--	--	--
39	.20	.06	--	--	--
40	0.00	0.00	--	--	--

CONFIGURATION NUMBER 21

RUN NUMBER 43   RUN NUMBER 87

SOURCE DENSITY — NEUTRAL   SOURCE AT SPECIFIC GRAVITY OF
                                         LNG AT BOILOFF

SAMPLE POINT	NONDIMENSIONAL CONCENTRATION COEFFICIENT,K	MEAN CONCENTRATION PERCENT	PEAK PERCENT	CONCENTRATION MEAN PERCENT	RMS PERCENT
1	9.62	2.75	16.47	5.21	3.53
2	7.95	2.27	10.12	3.69	2.08
3	6.39	1.83	14.49	7.78	2.62
4	3.22	.92	13.59	9.06	1.75
5	2.02	.58	8.93	4.92	2.26
6	.07	.02	6.98	2.91	2.11
7	.01	.00	4.97	.55	.90
8	.00	.00	0.00	0.00	0.00
9	.84	.24	.27	0.00	.12
10	1.06	.30	1.87	.66	.27
11	1.95	.56	1.87	.99	.33
12	2.37	.68	4.72	2.87	.56
13	1.51	.43	3.18	1.57	.66
14	.44	.12	4.47	3.24	.61
15	.03	.01	3.44	1.61	.54
16	.00	.00	1.61	.87	.18
17	.67	.19	1.07	.53	.12
18	.79	.23	1.87	.81	.25
19	1.23	.35	1.61	.93	.25
20	1.54	.44	2.13	1.24	.28
21	1.05	.30	3.95	2.57	.46
22	.35	.10	2.66	1.11	.40
23	.06	.02	1.34	.27	.38
24	.01	.00	.54	0.00	.21
25	.42	.12	--	--	--
26	.42	.12	--	--	--
27	.55	.16	--	--	--
28	.69	.20	--	--	--
29	.63	.18	--	--	--
30	.51	.15	--	--	--
31	.17	.05	--	--	--
32	.04	.01	--	--	--
33	.32	.09	--	--	--
34	.32	.09	--	--	--
35	.34	.10	--	--	--
36	.40	.11	--	--	--
37	.44	.13	--	--	--
38	.38	.11	--	--	--
39	.24	.07	--	--	--
40	0.00	0.00	--	--	--

CONFIGURATION NUMBER 22

RUN NUMBER 44   RUN NUMBER 88

SOURCE DENSITY - NEUTRAL   SOURCE AT SPECIFIC GRAVITY OF
                                             LNG AT BOILOFF

SAMPLE POINT	NONDIMENSIONAL CONCENTRATION COEFFICIENT,K	MEAN CONCENTRATION PERCENT	PEAK PERCENT	CONCENTRATION MEAN PERCENT	RMS PERCENT
1	14.67	4.25	24.85	16.84	3.74
2	6.48	1.88	20.68	14.29	2.86
3	1.73	.50	19.65	13.93	3.10
4	.30	.09	13.37	6.85	2.85
5	.07	.02	8.20	3.15	1.77
6	.04	.01	1.87	.81	.24
7	.03	.01	.81	.70	.07
8	.02	.01	.54	.32	.11
9	4.53	1.31	3.70	2.15	.48
10	4.07	1.18	4.72	3.04	.64
11	2.42	.70	3.70	2.24	.57
12	.64	.19	4.21	1.83	.67
13	.11	.03	2.66	1.38	.43
14	.04	.01	1.34	.52	.25
15	.03	.01	.81	.47	.12
16	.02	.01	1.07	.78	.16
17	1.21	.35	.81	.45	.11
18	1.51	.44	2.13	.61	.41
19	2.01	.58	2.13	.86	.39
20	1.32	.38	2.66	1.50	.48
21	.31	.09	3.70	2.17	.67
22	.06	.02	2.40	1.14	.44
23	.03	.01	1.07	.49	.15
24	.02	.01	.27	.12	.11
25	.70	.20	--	--	--
26	.74	.22	--	--	--
27	.90	.26	--	--	--
28	.85	.25	--	--	--
29	.90	.26	--	--	--
30	.17	.05	--	--	--
31	.05	.01	--	--	--
32	.04	.01	--	--	--
33	.02	.01	--	--	--
34	.50	.15	--	--	--
35	.54	.16	--	--	--
36	.52	.15	--	--	--
37	.40	.12	--	--	--
38	.21	.06	--	--	--
39	.09	.03	--	--	--
40	.02	.01	--	--	--